ENERGY DISSIPATION CHARACTERISTICS OF CLUSTERED RUBBER CYLINDERS

by

Dean L. Sicking
Assistant Research Engineer

Michael F. Thompson
Research Assistant

and

Hayes E. Ross, Jr.
Research Engineer

Research Report 453-1F

on

Research Study No. 2-8-87-453
Low-Maintenance Crash Cushion

Sponsored by

Texas State Department of Highways and Public Transportation

in cooperation with

The U. S. Department of Transportation
Federal Highway Administration

February 1989

Texas Transportation Institute
Texas A&M University
College Station, Texas

TECHNICAL REPORT STANDARD TITLE PAGE

1. Report No.	2. Government Accession No.	3. Recipient's Catalog No.
FHWA/TX-89/453-1F		

4. Title and Subtitle	5. Report Date
ENERGY DISSIPATION CHARACTERISTICS OF CLUSTERED RUBBER CYLINDERS	February 1989
	6. Performing Organization Code

7. Author's:	8. Performing Organization Report No.
Dean L. Sicking, Michael F. Thompson, and Hayes E. Ross, Jr.	Research Report 453-1F

9. Performing Organization Name and Address	10. Work Unit No.
Texas Transportation Institute The Texas A&M University System College Station, Texas 77843-3135	11. Contract or Grant No. Study No. 2-8-87-453
	13. Type of Report and Period Covered Final - September 1986 August 1988
12. Sponsoring Agency Name and Address Texas State Department of Highways and Public Transportation; Transportation Planning Division P. O. Box 5051 Austin, Texas 78763	14. Sponsoring Agency Code

15. Supplementary Notes

Research performed in cooperation with DOT, FHWA.
Research Study Title: Low-Maintenance Crash Cushion

16. Abstract

Crash cushions have proven to be one of the most cost-beneficial life-saving devices on our nation's highways. However, all of the widely used designs utilize sacrificial, energy-absorbing materials. A significant maintenance effort, with associated costs, is necessary to restore these cushions after an impact.

The purpose of the present research was to develop a low-maintenance crash cushion utilizing reusable rubber elements. An extensive laboratory study was made to evaluate various rubber compounds and shapes in terms of energy-absorbing characteristics, durability, sensitivity to the environment, and cost. Of the materials examined, it was found that a natural rubber--20% EPDM blend--offered the greatest promise. A full-scale prototype crash cushion was then constructed consisting of a cluster of hollow circular cylinders formed from the above material. The prototype was subjected to a series of vehicular crash tests. Due to unexpected failures in the rubber cylinders, it was not possible to completely qualify the cushion in terms of recommended impact performance criteria. The failures were attributed to the mandrell wrapping process by which the cylinders were constructed. It was concluded that these problems could be solved by constructing the cylinders from a compression mold process. It was further concluded that a low-maintenance rubber crash cushion is feasible and could reduce life-cycle costs in excess of 60 percent for high accident locations. Further research is recommended to complete the work reported herein.

17. Key Words	18. Distribution Statement
Crash Cushion, Full-Scale Crash Test, Scale Model Impact Test	No restrictions. This document is available to the public through the National Technical Information Service 5285 Port Royal Road Springfield, Virginia 22161

19. Security Classif. (of this report)	20. Security Classif. (of this page)	21. No. of Pages	22. Price
Unclassified	Unclassified	112	

Form DOT F 1700.7 (8-69)

METRIC (SI*) CONVERSION FACTORS

APPROXIMATE CONVERSIONS TO SI UNITS

Symbol	When You Know	Multiply By	To Find	Symbol
LENGTH				
in	inches	2.54	millimetres	mm
ft	feet	0.3048	metres	m
yd	yards	0.914	metres	m
mi	miles	1.61	kilometres	km
AREA				
in²	square inches	645.2	millimetres squared	mm²
ft²	square feet	0.0929	metres squared	m²
yd²	square yards	0.836	metres squared	m²
mi²	square miles	2.59	kilometres squared	km²
ac	acres	0.395	hectares	ha
MASS (weight)				
oz	ounces	28.35	grams	g
lb	pounds	0.454	kilograms	kg
T	short tons (2000 lb)	0.907	megagrams	Mg
VOLUME				
fl oz	fluid ounces	29.57	millilitres	mL
gal	gallons	3.785	litres	L
ft³	cubic feet	0.0328	metres cubed	m³
yd³	cubic yards	0.0765	metres cubed	m³

NOTE: Volumes greater than 1000 L shall be shown in m³.

TEMPERATURE (exact)

°F	Fahrenheit temperature	5/9 (after subtracting 32)	Celsius temperature	°C

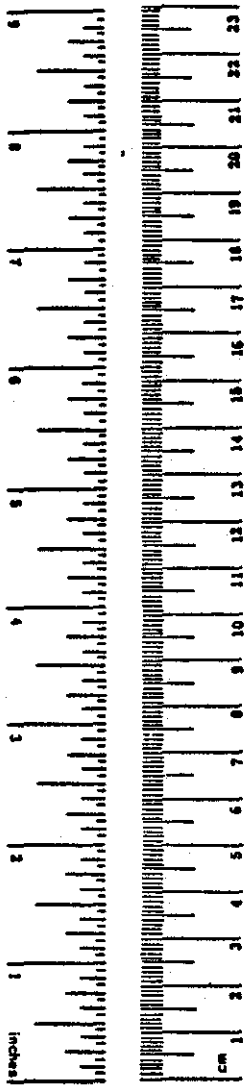

APPROXIMATE CONVERSIONS TO SI UNITS

Symbol	When You Know	Multiply By	To Find	Symbol
LENGTH				
mm	millimetres	0.039	inches	in
m	metres	3.28	feet	ft
m	metres	1.09	yards	yd
km	kilometres	0.621	miles	mi
AREA				
mm²	millimetres squared	0.0016	square inches	in²
m²	metres squared	10.764	square feet	ft²
km²	kilometres squared	0.39	square miles	mi²
ha	hectores (10 000 m²)	2.53	acres	ac
MASS (weight)				
g	grams	0.0353	ounces	oz
kg	kilograms	2.205	pounds	lb
Mg	megagrams (1 000 kg)	1.103	short tons	T
VOLUME				
mL	millilitres	0.034	fluid ounces	fl oz
L	litres	0.264	gallons	gal
m³	metres cubed	35.315	cubic feet	ft³
m³	metres cubed	1.308	cubic yards	yd³

TEMPERATURE (exact)

°C	Celsius temperature	9/5 (then add 32)	Fahrenheit temperature	°F

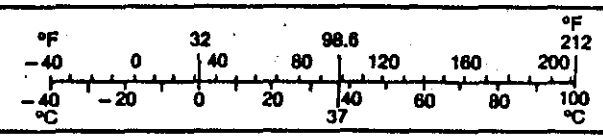

These factors conform to the requirement of FHWA Order 5190.1A.

* SI is the symbol for the International System of Measurements

DISCLAIMER

The contents of this report reflect the views of the authors who are responsible for the opinions, findings, and conclusions presented herein. The comments do not necessarily reflect the official views or policies of the Texas State Department of Highways and Public Transportation or the Federal Highway Administration. This report does not constitute a standard, specification, or regulation.

KEY WORDS

Crash Cushion, Full-Scale Crash Test, Scale Model Impact Test

ACKNOWLEDGMENTS

This research study was conducted under a cooperative program between the Texas Transportation Institute (TTI), the Texas State Department of Highways and Public Transportation (SDHPT), and the Federal Highway Administration (FHWA).

IMPLEMENTATION STATEMENT

Further development of low-maintenance crash cushions is recommended before implementation into SDHPT standard specifications.

ABSTRACT

Crash cushions have proven to be one of the most cost-beneficial life-saving devices on our nation's highways. However, all of the widely used designs utilize sacrificial, energy-absorbing materials. A significant maintenance effort, with associated costs, is necessary to restore these cushions after an impact.

The purpose of the present research was to develop a low-maintenance crash cushion utilizing reusable rubber elements. An extensive laboratory study was made to evaluate various rubber compounds and shapes in terms of energy-absorbing characteristics, durability, sensitivity to the environment, and cost. Of the materials examined, it was found that a natural rubber--20% EPDM blend--offered the greatest promise. A full-scale prototype crash cushion was then constructed consisting of a cluster of hollow circular cylinders formed from the above material. The prototype was subjected to a series of vehicular crash tests. Due to unexpected failures in the rubber cylinders, it was not possible to completely qualify the cushion in terms of recommended impact performance criteria. The failures were attributed to the mandrell wrapping process by which the cylinders were constructed. It was concluded that these problems could be solved by constructing the cylinders from a compression mold process. It was further concluded that a low-maintenance rubber crash cushion is feasible and could reduce life-cycle costs in excess of 60 percent for high accident locations. Further research is recommended to complete the work reported herein.

TABLE OF CONTENTS

LIST OF FIGURES

FIGURE

LIST OF FIGURES (CONTINUED)

FIGURE

LIST OF FIGURES (CONTINUED)

FIGURE

LIST OF TABLES

INTRODUCTION

Highway crash cushions are widely used on major urban freeways across Texas and most other states. These devices have proven to be some of the most cost-beneficial safety features in use today. However, costs associated with the installation and maintenance of crash cushions can be very significant. Maintenance costs are of particular concern if the cushion is impacted frequently and/or if the cushion requires frequent inspection. Further, maintenance activities on heavily traveled streets and freeways interrupt traffic, thereby increasing accident risk and endangering both motorists and repair crews.

Most conventional crash cushions, such as steel drum (1) and sand barrel cushions (2), incorporate sacrificial elements for attenuating head-on impacts. Although these systems are relatively inexpensive initially, the entire installation is frequently destroyed after relatively minor accidents. Systems that were designed to be less costly to repair, such as water-filled cushions, have become very costly to construct, and repair costs have frequently exceeded original expectations. As a result, crash cushion repair costs remain relatively high.

A low-maintenance attenuator was recently developed to shield the end of concrete safety-shaped barriers and other narrow rigid objects (3). This system utilizes rubber cylinders as an energy-absorbing medium. Full-scale crash tests of the cushion indicated that the device could safely attenuate high-speed, head-on impacts without any damage to the rubber energy-absorbing cells. Extension of this technology to conventional cushions should lead to a major reduction in the maintenance costs associated with such devices. Therefore, a study was undertaken to determine the feasibility of adapting rubber cell attenuating elements to conventional, clustered crash cushions.

RESEARCH APPROACH

Extensive testing of rubber energy-absorbing components described in reference 3 has indicated that such elements can be effectively used in crash cushion design. However, this research also indicated that heavy rubber components were generally necessary to absorb significant amounts of impact energy and that the cost of these heavy rubber elements is significant. Since most conventional cushions incorporate many such elements, the cost of this type crash cushion utilizing these heavy rubber attenuating elements may be excessive. Therefore, a major objective of this research was to identify methods for improving the efficiency of rubber attenuating cells.

Perhaps the most appealing method for improving the performance of rubber attenuating cells is to change the rubber compound used in the elements. Therefore, a major search was launched into identifying a compound that would exhibit better energy dissipation performance than the 80-durometer natural rubber compound used in the previous study. Desirable properties for a rubber compound identified in reference 3 included low temperature sensitivity, high stiffness, high damping, and good durability. Numerous rubber companies were contacted and a number of different compounds were obtained. Each compound was then subjected to a series of scale model static and dynamic tests at various temperatures to identify the most promising material.

Another method for improving the energy dissipation characteristics of rubber crash cushion components is to modify the shape of the elements. Therefore, an effort was made to evaluate various shapes of attenuation elements. Although a great effort was expended to solicit alternate element shapes for testing, only square and circular cylinders could be obtained. These scale model elements were then subjected to a series of static and dynamic tests in an effort to determine the most appropriate shape for use in a conventional crash cushion.

The final step in the analysis of rubber attenuation elements involved an evaluation of the effects of clustering on energy dissipations. Clustering of attenuating elements was believed to offer some geometric constraint to inhibit the collapse of each individual element. Therefore, it was important to quantify these effects for each element shape under consideration. Scale-model static tests and full-scale dynamic tests were

conducted to evaluate the performance of square and round cylinders when confined in a cluster.

Results of all of these static and dynamic tests were then used to develop candidate crash cushion designs. Full-scale dynamic tests were conducted to evaluate the performance of these designs.

MATERIALS

Rubber materials can be defined as "materials which display the property of long-range reversible elasticity." Long-range reversible elasticity can be thought of as the ability to sustain large strains under an applied load without appreciable damage and return to its original shape once the load is removed (i.e., like a rubber band). Using this definition, the terms rubber and elastomer can be used interchangeably.

Rubber can be broadly divided into two categories--natural and synthetic. The raw ingredient for natural rubber is latex, a fluid produced by the latex vessels of the Hevea brasiliensis tree. The molecular formula for natural rubber is $(C_5H_8)_{20,000}$. The structural formula for the natural rubber monomer is (C_5H_8), and is shown schematically as:

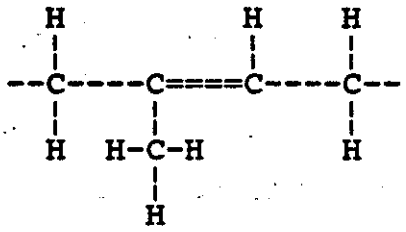

This monomer is repeated many thousands of times to form a polymer chain or macromolecule. These chains become entangled and form very viscous fluids--viscous enough to exhibit properties of an elastic solid. Vulcanization is a chemical process used to cross-link polymer chains with sulfur, giving the material a memory of its original shape by preventing flowing of the chains. This development makes practical the use of natural rubber for many applications.

Variation in world production of natural rubber and the desire to obtain independent sources of rubber during World War II created a need for synthetic rubber. After gaining the technical ability to produce synthetic polymers having desirable physical properties, the only historical restraint on its commercial development was its cost. Synthetic rubber is now a major alternative to natural rubber in a variety of applications.

Natural and synthetic rubber polymers are processed with additional ingredients to form rubber compounds--a process referred to as compounding. Compounding ingredients include processing aids, vulcanization agents, accelerators, antidegradents, fillers, plasticizers, and softeners. Blending two or more different rubber polymers in the

compound is also common. A wide variety of material properties can be achieved by altering specific ingredients and processing methods used to produce a particular rubber compound.

Although many manufacturing processes are used in the manufacture of small components, most large rubber parts are manufactured through either compression molding or mandrel wrapping. Compression molding involves precision mold that is used to apply pressure to an unshaped rubber piece and form it into the desired shape. The alternative method involves wrapping a rubber compound in thin layers around a steel mandrell forming a cylinder. Successive layers add additional thickness to the cylindrical product. The manufacturing technique used in forming a rubber product can affect its properties and behavior. Compression molding generally produces a homogenous product with only irregular perfections. Initial costs associated with compression molding are very high due to the high cost of precision molds. Although mandrell wrapping usually produces less homogenous products with the potential for delamination failure, initial costs of the procedure are relatively low. Therefore, although most rubber products are manufactured through compression molding, special samples and test specimens are frequently made through mandrel wrapping.

Numerous companies specializing in rubber compounding were solicited in an effort to develop rubber compounds for this research. A list of properties appropriate for rubber crash cushion elements was developed and discussed with each participating firm (see Table 1). Several of the companies then developed candidate compounds for use in rubber crash cushion components. Due to the possible commercial value of these compounds, specific compounding processes and ingredients used were considered proprietary.

Compounds Studied

Base polymers used in each of the compounds studied are listed in Table 2, along with abbreviations used in the remainder of the report to identify the individual compounds. Properties of each of the base elastomers represented are discussed below. Since considerable variation of properties can exist within a particular compound classification, comparisons made throughout the remainder of this research are primarily intended to identify the specific compound among those studied which is most suitable to be used for rubber crash cushion elements.

Table 1. Desirable Characteristics for Rubber Cushion Elements

Item	Characteristic
1.	Property changes over temperature range of -30°F to 150°F as small as possible: a) 50% change in stiffness and dampening maximum b) Nonbrittle behavior at lower temperature
2.	Useful life of 10 or more years: a) 10% change in stiffness maximum over useful life b) Ozone resistant c) Ultraviolet light resistant d) Low water absorption
3.	Stiffness/weight ratio: as high as possible given other constraints.
4.	Nonelastic recovery behavior: slow return from deformed shape to undeformed shape.
5.	High tear resistance.
6.	Low cost of compound comparable to other general use rubber compounds.

Table 2. Rubber Compounds Investigated

Item	Base Elastomer	Abbreviation	Supplier
1.	Natural Rubber	NR	Regal International, Inc.
2.	Natural Rubber/ Butadiene	NR/BD	Regal International, Inc.
3.	Natural Rubber/ Ethylene-Propylene	NR/EPDM	Regal International, Inc.
4.	Natural Rubber/ Butyl	NR/BU	Regal International, Inc.
5.	Butyl	BU	Applied Rubber Technology
6.	Natural Rubber/ 20% Ethylene-Prop.	NR/20%EPDM	Applied Rubber Technology
7.	Neoprene	NEO	Regal International, Inc.
8.	Not named	LTV	LTV Energy Products Co.

Natural Rubber (NR) has been used commercially since the mid-nineteenth century, when the vulcanization process was discovered. In present compounding technology, additives are included to give natural rubber improved physical properties and ultraviolet light resistance. About 70 percent of all natural rubber produced is used in automotive tires, usually composing the carcass and sidewalls (2). General properties of natural rubber include high strength, fatigue resistance, and durability.

Butadiene (BD) comprises about one-half of all synthetic rubber usage and is approximately equal to that of natural rubber (3). Butadiene has been produced commercially since World War II. The raw ingredient for this monomer is a by-product of oil refining and, therefore, provides a relatively inexpensive alternative to natural rubber. Popularity of this synthetic rubber is due to its relatively low cost and properties that, in many cases, can match natural rubber.

Ethylene-propylene (EPDM) went into commercial production in 1963, and since that time its usage has grown faster than any other elastomers. Properties of EPDM include excellent ozone resistance and high extension. EPDM has found commercial uses in many applications such as dock bumpers, tire sidewalls, radiator hoses, seals, sheeting for roofing, and vibration isolators.

Butyl (BU) rubber was introduced in 1942 and used during World War II by the U.S. Government. Butyl polymers are widely used around the world, accounting for one-third of all synthetic rubber production. Butyl has beneficial properties of low gas permeability, high hysteresis, high tearing strength, heat resistance, resistance to chemical attack, and ozone resistance. The vibration damping property of butyl makes it a common rubber for shock absorption devices and, therefore, could have some application to highway crash cushion development.

Neoprene (NEO) has been in wide use since 1931 when chemists from DuPont Company announced development of the polychloroprene polymer (3). Neoprene was first used as an alternative to natural rubber due to its superior resistance to swelling in oil. Subsequent improvements in compounding have given neoprene a wide range of applications where ozone resistance and weathering durability are desired.

The LTV Energy Products Company provided samples of an unnamed product for this research that will be referred to simply as LTV. The LTV rubber compound investigated was developed for the aviation industry in locations subject to temperature

extremes and as a vibration isolator in transporting sensitive military cargo such as nuclear war heads (4). Due to the proprietary nature of this elastomer, little literature is available documenting its properties.

COMPOUND SELECTION

Energy dissipation characteristics of each material was evaluated through static and dynamic testing of scale model rubber cylinders. Each cylinder was 4.8 in. long with a 4.8 in. outer diameter and 0.45 in. wall thickness. Static and dynamic testing was first used to evaluate basic energy dissipation properties of each material at room temperatures. The scale model cylinders were then subjected to similar testing over a wide range of temperature conditions to evaluate thermal effects on energy dissipation characteristics.

Energy Dissipation

High speed dynamic compression testing was conducted for each of the materials under consideration. The cylinders were compressed at a speed of 65 ft/sec. while load and deflection data were sampled every 0.02 ms. Although several problems were initially encountered during this effort, each was eventually resolved as described in detail in reference 4. Total energy dissipation for each material was recorded as shown in Table 3. Recall that the overall objective of this effort was to identify materials with increased energy dissipation. Based on this evaluation, the NR/20% EPDM compound showed the most potential for improving the performance of rubber crash cushion components. Note that the natural rubber material used in the narrow hazard crash cushion, shown as item 5 in Table 3, was found to have only 50 percent of the energy dissipation of the NR/20% EPDM compound.

Temperature Sensitivity

The temperature sensitivity of each material's energy dissipation properties was evaluated through static and dynamic testing at -10°, 34°, 70°, and 114°F. Static testing of each material is summarized in Table 4. The temperature range was selected based on temperature extremes that can be expected in Texas. Note that if the rubber material is black, its surface temperature during sunny weather will likely be significantly higher than ambient temperatures. In an effort to quantify the effects of solar heating, thermocouples were placed at several locations through the thickness of a rubber cylinder. Temperature readings during sunny days indicated that rubber surface temperatures can be 40° or more above ambient conditions. However, these high surface temperatures were not transmitted throughout the cylinder, and material temperatures

Table 3. Energy Dissipation of Rubber Compound

Item	Material	Dynamic Energy (in-lb)	Percent of Largest
1.	NR/20%EPDM	1920	100
2.	BU	1200	63
3.	LTV	1190	62
4.	NR/BD	1020	53
5.	NR	990	51
6.	NR/EPDM	910	47

Table 4. Temperature Effects on Static Test Results

Sample	Durom.	Wall Th. (in)	Temp. (°F)	Defl. (in)	Energy (in-lb)
BU 1	80	0.296	-10	4.1	358
BU 1	80	0.296	34	4.1	265
BU 1	80	0.296	70	4.1	186
BU 1	80	0.296	114	4.1	139
BU 2	60	0.31	-10	4.1	128
BU 2	60	0.31	34	4.1	112
BU 2	60	0.31	70	4.1	98
BU 2	60	0.31	114	4.1	83
BU 3	60	0.472	-10	3.85	324
BU 3	60	0.472	34	3.85	216
BU 3	60	0.472	70	3.85	205
BU 3	60	0.472	114	3.85	188
BU 4	80	0.6	-10	3.6	2089
BU 4	80	0.6	34	3.6	1162
BU 4	80	0.6	70	3.6	901
BU 4	80	0.6	114	3.6	577
BU 5	60	0.609	-10	3.6	644
BU 5	60	0.609	34	3.6	472
BU 5	60	0.609	70	3.6	382
BU 5	60	0.609	114	3.6	341
BU 6	80	0.467	-10	3.85	1120
BU 6	80	0.467	34	3.85	622
BU 6	80	0.467	70	3.85	459
BU 6	80	0.467	114	3.85	346
BU 7	80	1.18	34	2.7	4270
BU 7	80	1.18	70	2.7	3374
BU 7	80	1.18	114	2.7	2310
BU 8	60	1.17	-10	2.7	2110
BU 8	60	1.17	34	2.7	1556
BU 8	60	1.17	70	2.7	1345
BU 8	60	1.17	114	2.7	1235
NEO 2	70	0.305	70	4.1	145
NEO 3	70	0.3047	70	4.1	121
NEO 4	70	0.3077	34	4.1	156
NEO 4	70	0.3077	70	4.1	146

Table 4. Temperature Effects on Static Test Results (continued)

Sample	Durom.	Wall Th. (in)	Temp. (°F)	Defl. (in)	Energy (in-lb)
NEO 5	70	0.314	-10	4.1	199
NEO 5	70	0.314	34	4.1	149
NEO 5	70	0.314	70	4.1	136
NEO 5	70	0.314	114	4.1	129
NEO 6	70	0.313	-10	4.1	189
NEO 6	70	0.313	34	4.1	150
NEO 6	70	0.313	70	4.1	135
NEO 6	70	0.313	114	4.1	126
NEO 7	70	0.6107	-10	3.6	1517
NEO 7	70	0.6107	34	3.6	756
NEO 7	70	0.6107	70	3.6	576
NEO 7	70	0.6107	114	3.6	533
NEO 8	70	1.1987	34	2.7	2465
NEO 8	70	1.1987	70	2.7	2073
NEO 8	70	1.1987	114	2.7	1850
NR 5 S	80	0.4839	34	3.85	1856
NR 7 S	80	0.4796	-10	3.85	2730
NR 7 S	80	0.4796	34	3.85	1822
NR 7 S	80	0.4796	70	3.85	1645
NR 7 S	80	0.4796	114	3.85	1364
NR 8 S	80	0.4828	-10	3.85	3170
NR 8 S	80	0.4828	34	3.85	1985
NR 8 S	80	0.4828	70	3.85	1845
NR 8 S	80	0.4828	114	3.85	1495
NR 9 S	80	0.4751	-10	3.85	2885
NR 9 S	80	0.4751	34	3.85	1750
NR 9 S	80	0.4751	70	3.85	1691
NR 9 S	80	0.4751	114	3.85	1335
NR 12 S	80	0.4816	34	3.85	1661
NR 17 S	80	0.6248	34	3.6	2870
NR 17 S	80	0.6248	70	3.6	2796
NR 17 S	80	0.6248	114	3.6	2305
NR 18 S	80	0.6229	-10	3.6	4900
NR 18 S	80	0.6229	34	3.6	2985
NR 18 S	80	0.6229	70	3.6	2930
NR 18 S	80	0.6229	114	3.6	2195

Table 4. Temperature Effects on Static Test Results (continued)

Sample	Durom.	Wall Th. (in)	Temp. (°F)	Defl. (in)	Energy (in-lb)
NR 19 S	80	0.6241	34	3.6	4005
NR 19 S	80	0.6241	70	3.6	2890
NR 19 S	80	0.6241	114	3.6	2510
NR 2 C	80	0.445	-10	3.85	901
NR 2 C	80	0.445	34	3.85	550
NR 2 C	80	0.445	70	3.85	473
NR 2 C	80	0.445	114	3.85	422
NR 23 S	80	0.623	34	3.6	3675
NR 3 C	80	0.559	-10	3.6	1594
NR 3 C	80	0.559	34	3.6	1055
NR 3 C	80	0.559	70	3.6	966
NR 3 C	80	0.559	114	3.6	772
NR 4 C	50	0.295	-10	4.1	302
NR 4 C	50	0.295	34	4.1	48
NR 4 C	50	0.295	70	4.1	49
NR 4 C	50	0.295	114	4.1	48
NR 5 C	80	0.306	-10	4.1	365
NR 5 C	80	0.306	34	4.1	291
NR 5 C	80	0.306	70	4.1	253
NR 5 C	80	0.306	114	4.1	218
NR 6 C	80	0.451	-10	3.85	854
NR 6 C	80	0.451	34	3.85	582
NR 6 C	80	0.451	70	3.85	485
NR 6 C	80	0.451	114	3.85	430
NR 7 C	50	0.5962	-10	3.6	568
NR 7 C	50	0.5962	34	3.6	213
NR 7 C	50	0.5962	70	3.6	209
NR 7 C	50	0.5962	114	3.6	204
NR/BD 1	--	0.4555	-10	3.85	1034
NR/BD 1	--	0.4555	34	3.85	776
NR/BD 1	--	0.4555	70	3.85	505
NR/BD 1	--	0.4555	114	3.85	522
NR/BD 2	--	0.4555	-10	3.85	1118
NR/BD 2	--	0.4555	34	3.85	807
NR/BD 2	--	0.4555	70	3.85	670
NR/BD 2	--	0.4555	114	3.85	548

Table 4. Temperature Effects on Static Test Results (continued)

Sample	Durom.	Wall Th. (in)	Temp. (°F)	Defl. (in)	Energy (in-lb)
NR/BU 1	--	0.301	-10	4.1	429
NR/BU 1	--	0.301	34	4.1	300
NR/BU 1	--	0.301	70	4.1	270
NR/BU 1	--	0.301	114	4.1	224
NR/BU 2	--	0.3063	-10	4.1	451
NR/BU 2	--	0.3063	34	4.1	303
NR/BU 2	--	0.3063	70	4.1	295
NR/BU 2	--	0.3063	114	4.1	242
NR/EPDM	--	0.4545	-10	3.85	1172
NR/EPDM	--	0.4545	34	3.85	640
NR/EPDM	--	0.4545	70	3.85	583
NR/EPDM	--	0.4545	114	3.85	436
NR/EPDM	--	0.4567	-10	3.85	1322
NR/EPDM	--	0.4567	34	3.85	732
NR/EPDM	--	0.4567	34	3.85	824
NR/EPDM	--	0.4567	114	3.85	454

dropped to near ambient condition even a short distance away from the surface exposed to direct sunlight. Therefore, since the majority of the rubber cylinder would have a temperature close to ambient, it was concluded that an upper temperature extreme of 114°F would be adequate for thick rubber cylinders used along the roadside. Since a crash cushion must be designed to perform over such a wide range of temperatures, it is important to obtain a material with as little thermal sensitivity as possible.

A series of dynamic tests was conducted at each of the above temperatures in an effort to identify the temperature sensitivity of the energy dissipation for the rubber compounds. All scale model dynamic test results are reported in reference 4. The relative temperature sensitivity of each compound was evaluated with a temperature performance index. This index is defined as the ratio between the dynamic energy dissipation of a sample at 114°F and -10°F. Temperature performance indices for each material are listed in Table 5. Note that the LTV material had the lowest index of the rubber compounds tested and, therefore, exhibited the least sensitivity to temperature changes.

Summary

As described above, the NR/20% EPDM compound exhibited the highest overall energy dissipation capacity, while the LTV material was found to be the least sensitive to temperature changes. Material suppliers were then queried to identify the cost differential between the two compounds. The proprietary LTV material was found to be very expensive, more than 4 times the cost of the NR/20% EPDM compound. Therefore, the NR/20% EPDM material was selected for further evaluation.

Scale model samples of the NR/20% EPDM compound were manufactured through a mandrell wrapping process. As mentioned previously, this process does not yield as homogenous a product as does compression molding. In an effort to evaluate the durability of the mandrell wrapped cylinders, a series of high speed compression tests was conducted on a single NR/20% EPDM sample. The static force-deflection characteristics of the sample were first recorded, and then it was impacted 20 times at 75 ft/sec. As shown in Figure 1, the static force-deflection characteristics of the sample were not changed significantly. It was therefore concluded that the mandrell wrapping process was sufficiently reliable for the manufacture of full-scale test specimens.

Table 5. Temperature Performance Indices

Item	Material	Energy $-10^{\circ}F$ (in-lb)	Energy $114^{\circ}F$ (in-lb)	Index
1.	LTV	1819	1282	1.45
2.	NR	2866	864	3.32
3.	NR/20%EPDM	4703	1325	3.55
4.	NR/BU	3277	856	3.83
5.	NR/BD	2861	679	4.21
6.	NR/EPDM	3655	789	4.63
7.	BU	6338	593	10.69

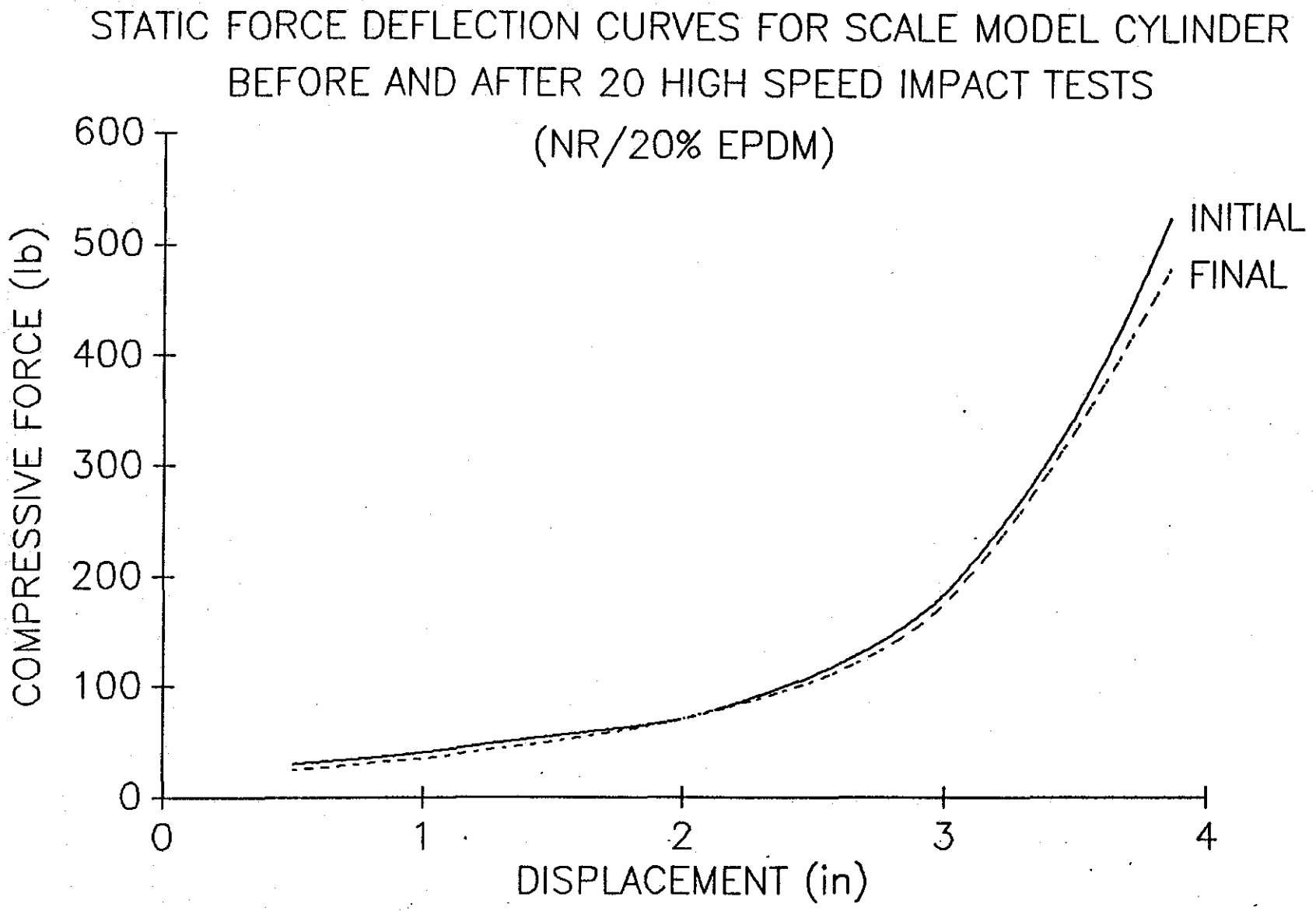

FIGURE 1. Change in Static Compression Properties During Durability Testing

SHAPE EVALUATION

The effects of the geometric shape of crash cushion cells was also evaluated in an effort to maximize energy dissipation properties. An optimal shape should efficiently dissipate energy and be suitable for use in a multi-element crash cushion arrangement. While several shapes were considered conceptually, practical constraints limited the laboratory study to circular and square cylinders. The effects of bore stiffeners and clustering of elements were also investigated for each shape.

The circular cylinder is probably the most widely used shape for rubber attenuation elements. During impact the walls of the cylinder deflect outward and compression forces are relatively constant over a large range of cylinder collapse. Due to symmetry, the circular shape is insensitive to the angle of impact. This characteristic is very important for crash cushion elements, since errant vehicles can impact from any angle.

Square cylinder deformation is dependant on the angle of impact. When the impact is parallel to two of the sides, high buckling forces develop in the walls before the cylinder begins to deform. As the walls continue to buckle, the buckling forces are significantly reduced. During side impacts, however, significant bending moments develop in the cylinder walls and force deflection characteristics are greatly changed. Sequential photographs of static compression tests of circular and square cylinders are shown in Figure 2.

The primary objective of this phase of the research was to identify differences in the energy dissipation characteristics of these two geometric shapes. Circular and square laboratory elements composed of identical natural rubber compounds with a length of 4.8 in., a diameter of 4.8 in., and a wall thickness of 0.45 in. were used to compare static and dynamic energy dissipation of the two shapes. Static force versus displacement relationships for the two cylinders are shown in Figure 3. The square cylinder initially exhibits a very high stiffness before its two walls parallel to the applied force begin to buckle. As shown in the figure, the circular cylinder has a much lower initial stiffness, but it continues to stiffen throughout its deflection. However, the square cylinder still absorbed much more energy than did the circular shape. During static testing the square cylinder dissipated an average of 1690 in-lb compared to a 485 in-lb. average for the circular cylinder.

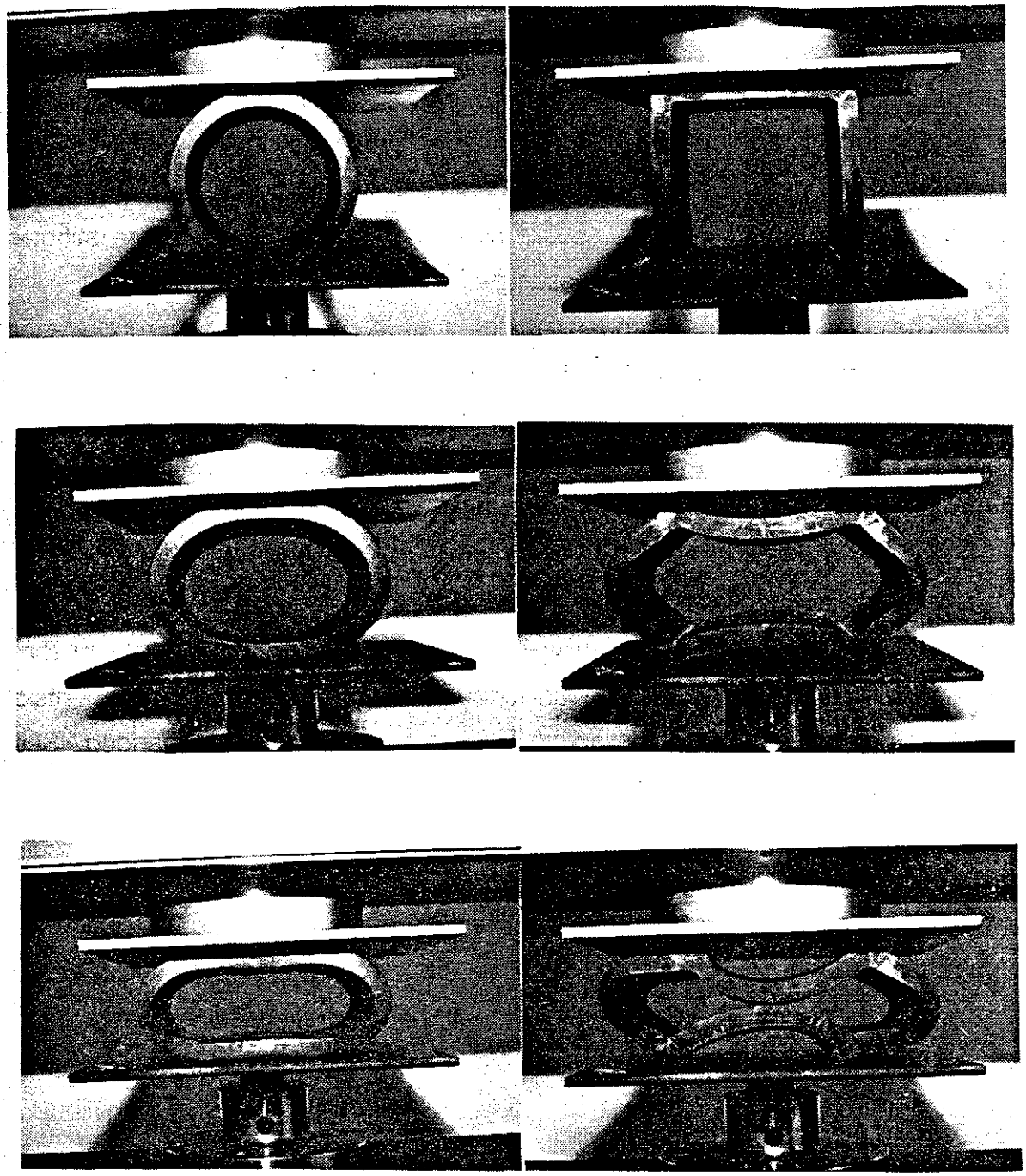

FIGURE 2. Sequential Photographs of Static Tests of Circular and Square Cylinders

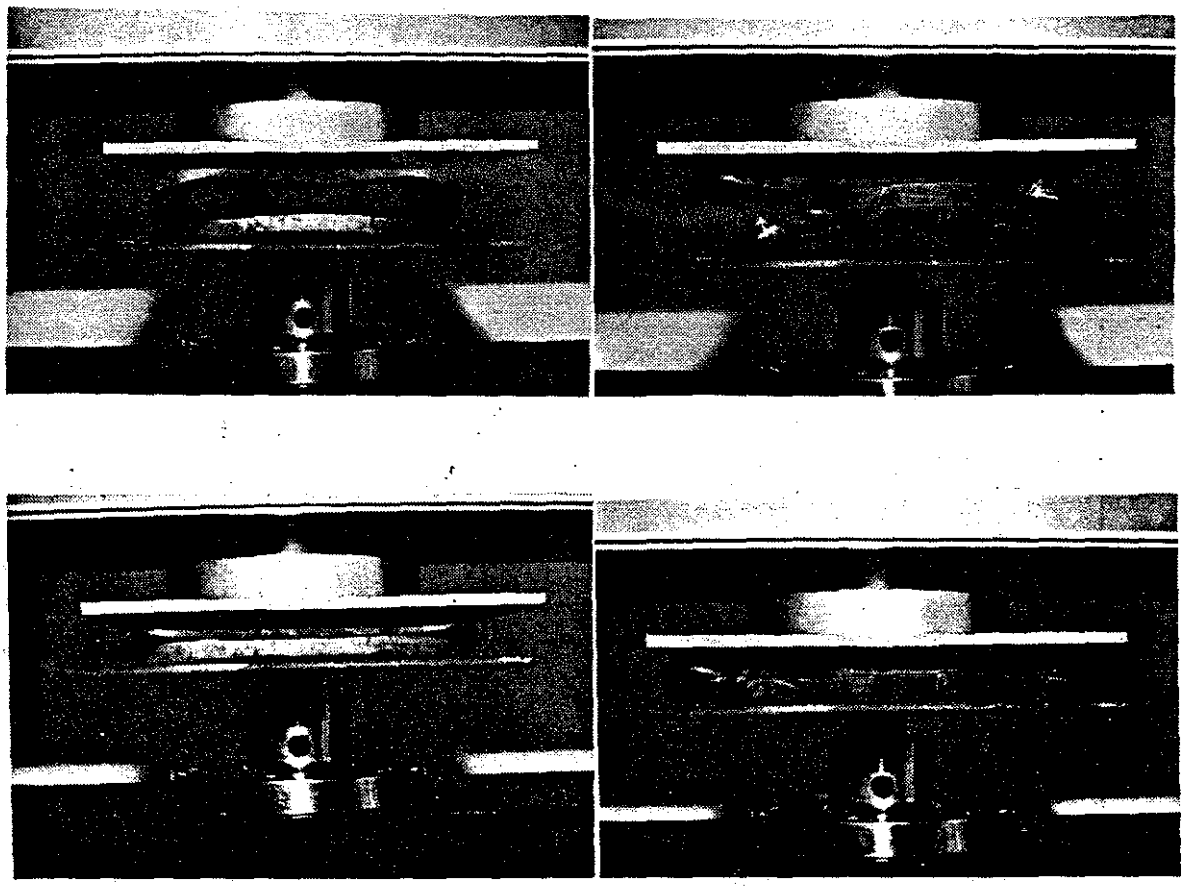

FIGURE 2. Sequential Photographs of Static Tests of Circular and Square Cylinders (continued)

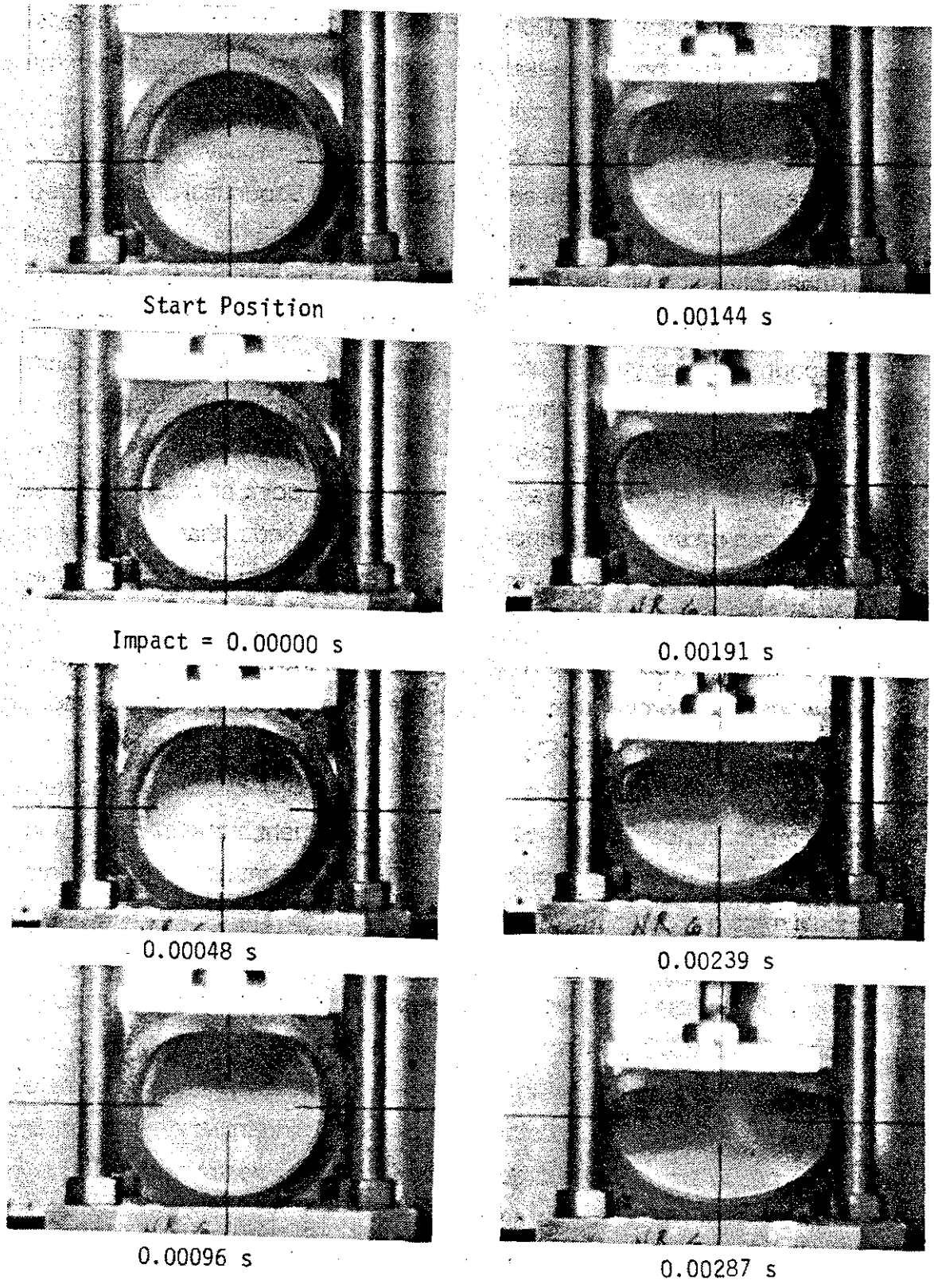

FIGURE 4. Sequential Photographs of Dynamic Test of Circular Cylinder

The impact behavior of these geometric shapes was investigated through high speed dynamic compression tests. During preliminary dynamic testing, compressive load transducers were placed below the test specimens. These load transducers measured little or no force under the round cylinders until the elements were over 75 percent collapsed. High speed films were then taken of both circular and square cylinder compression tests to help explain these low force levels. Sequential photographs of a 44 ft/sec dynamic test of a circular cylinder are shown in Figure 4. Several important behavioral characteristics of the circular shape may be observed in the sequential photographs. During static testing, the deflected shape of the circular cross section is symmetric about two axes (parallel and perpendicular to the direction of applied force). Note that during dynamic testing, the deflected shape is symmetric about only one axis (parallel to the direction of the applied force). This reduced symmetry is due to the delayed response of the cylinder wall farthest from the point of impact. For example, more deflection can be seen in the upper portion of the cylinder than the lower portion at a time of 0.00191 seconds. Energy transferred due to momentum transfer to the rubber material is affected by this manner of deformation.

Another important observation is the tendency for the bottom portion of the cylinder to deflect toward the incoming ram. This can be seen by comparing deflected shapes between times of 0.00000 and 0.00478 seconds. Although the photographs do not clearly indicate the behavior of the interior of the sample, the edge of the cylinder nearest the camera has lifted its support plate. A DYNA3D finite element model of this test indicated that this effect is more pronounced at the edge of the element and that the center of the cylinder would remain in contact with the support plate. Nevertheless, these photographs give a clear indication that the forces under the cylinder during dynamic testing are much lower than would normally be expected. Force-deflection curves for the circular cylinder, measured both at the top and bottom of the element, are shown in Figure 5. This figure shows the magnitude of the delay in the reactive force at the bottom. This behavior indicates that a cushion comprised of rows of circular cylinders will tend to collapse row by row from front to back and that large forces will not be transmitted to a backup structure until the cushion is fully collapsed.

Sequential photographs of a dynamic compression test of a square cylinder are shown in Figure 6. The square cylinder shown is 4.8 in. long, 4.8 in. wide, and has a 0.45

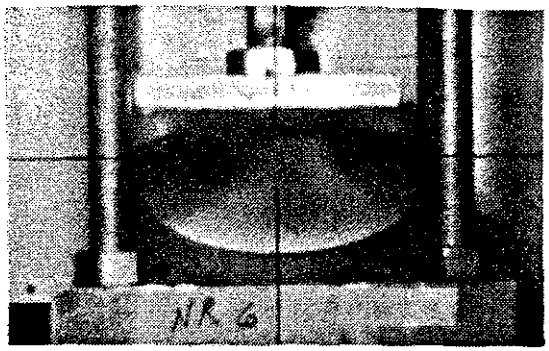

0.00335 s

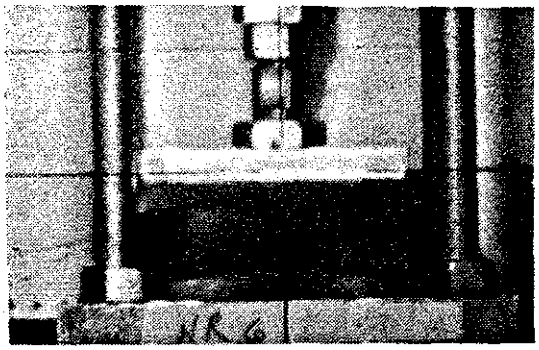

0.000526 s

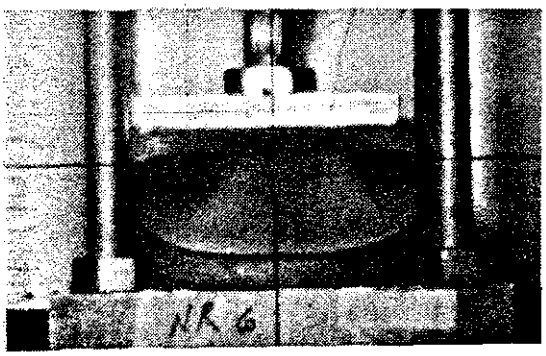

0.00383 s

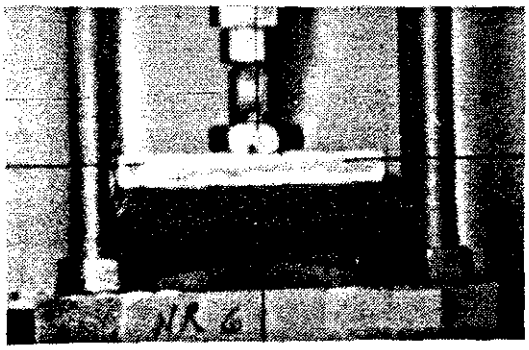

0.00574 s

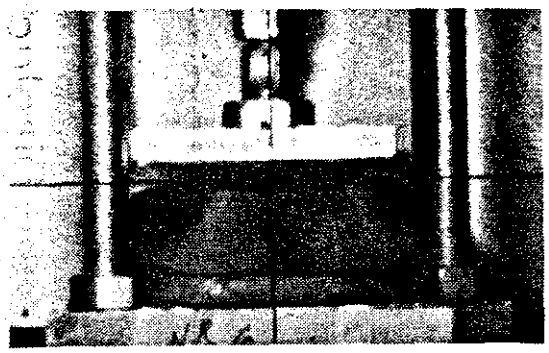

0.00431 s

0.00622 s

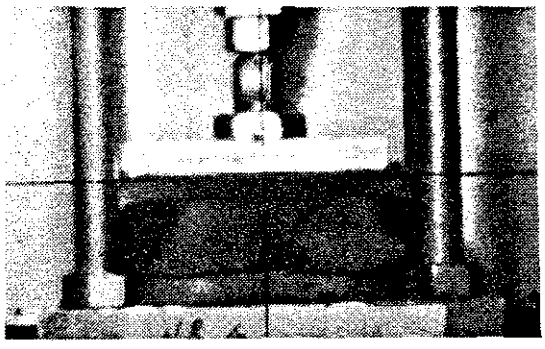

0.00478 s

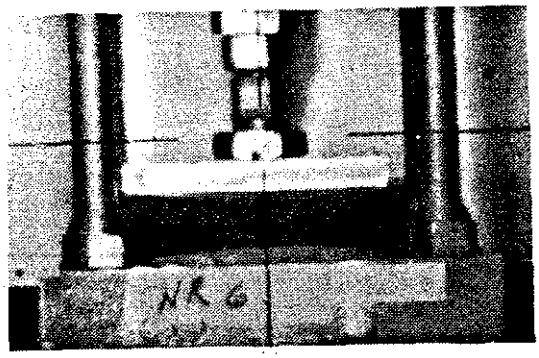

0.00670 s

FIGURE 4. Sequential Photographs of Dynamic Test of Circular Cylinder (continued)

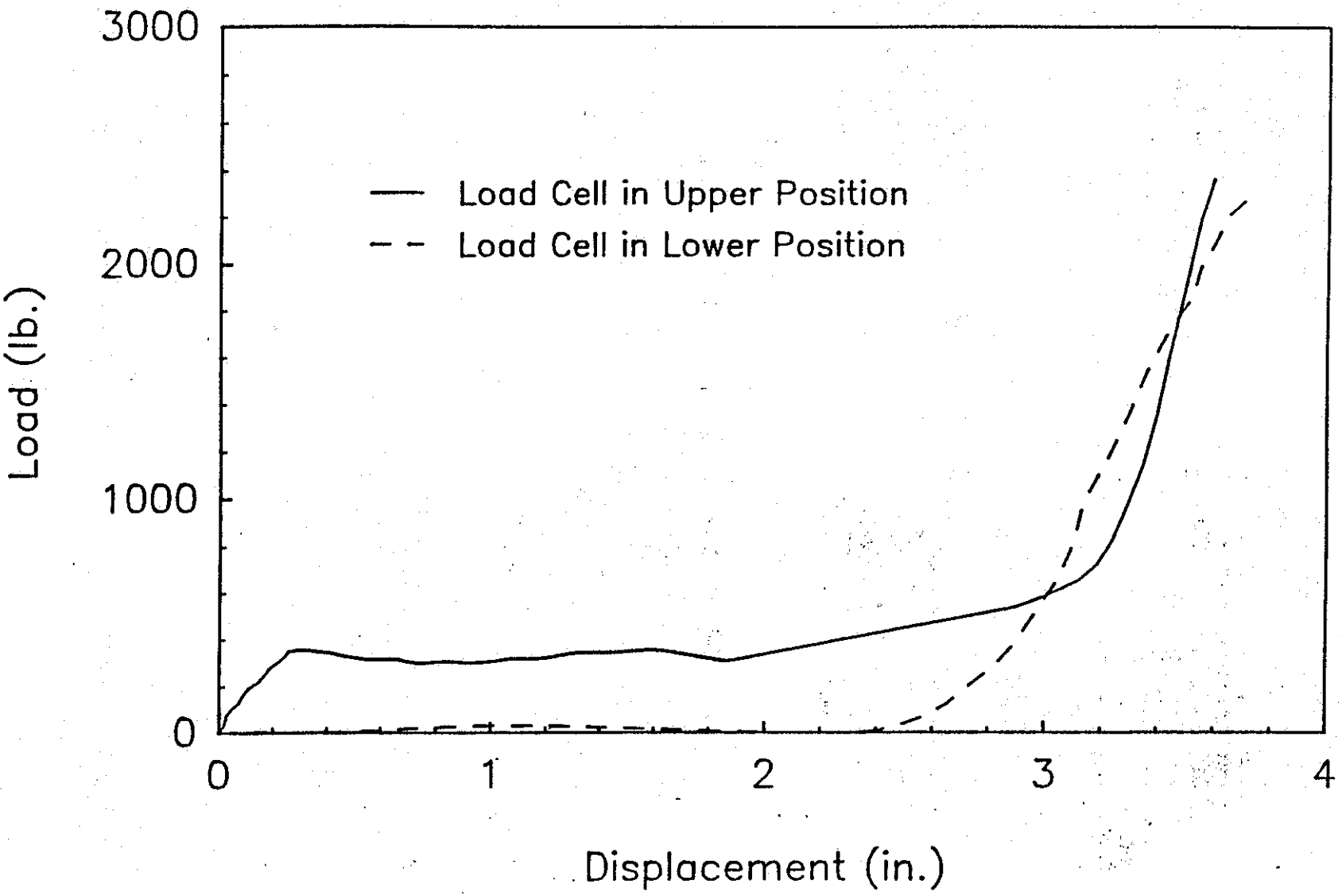

FIGURE 5. Force vs Deflection From Dynamic Test of Circular Cylinder

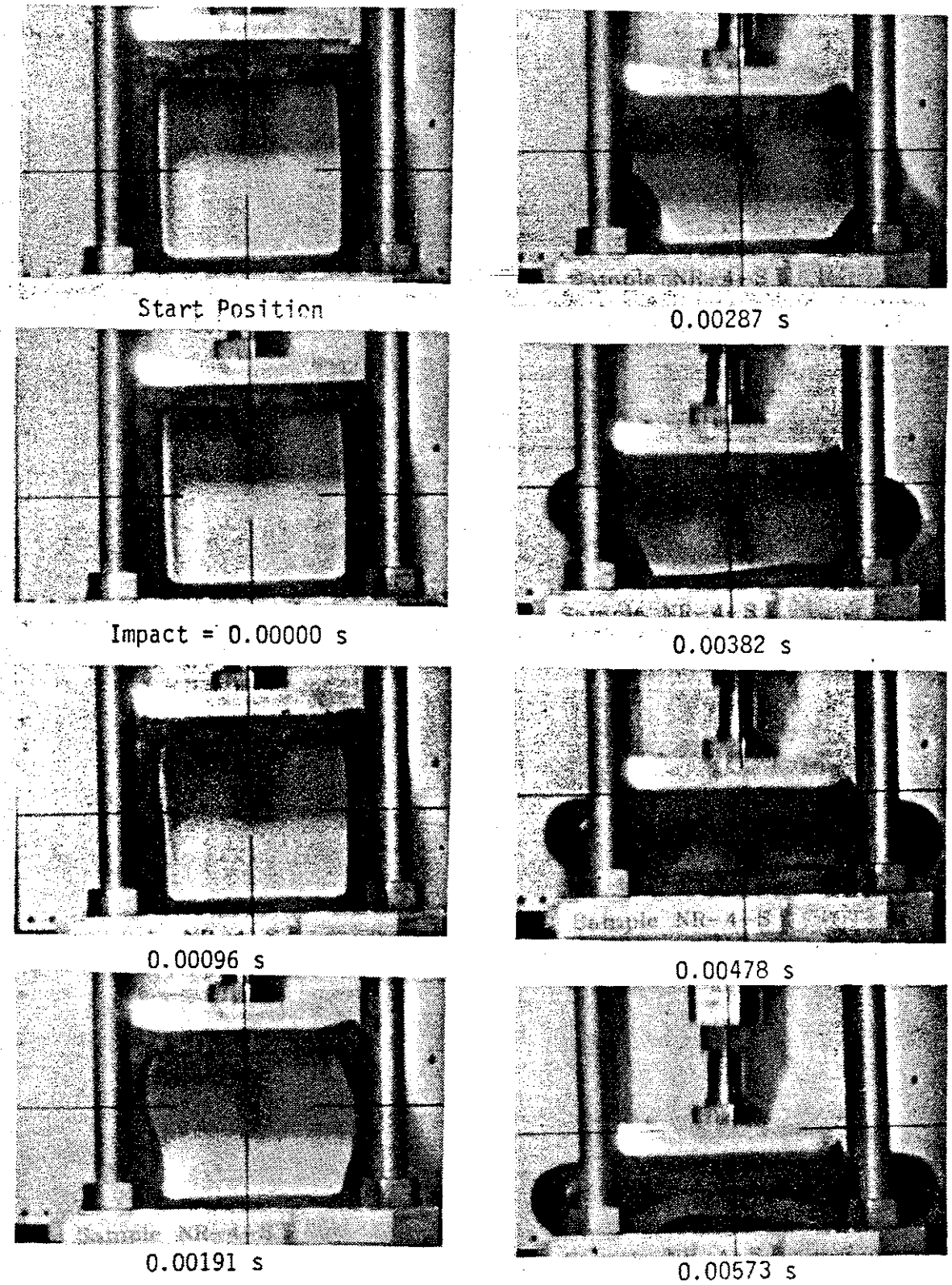

FIGURE 6. Sequential Photographs of Dynamic Test of Square Cylinder

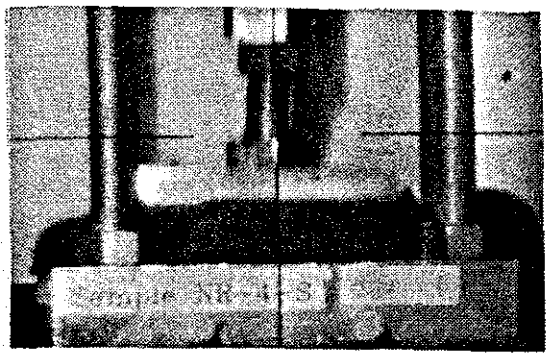

0.00669 s

0.01051 s

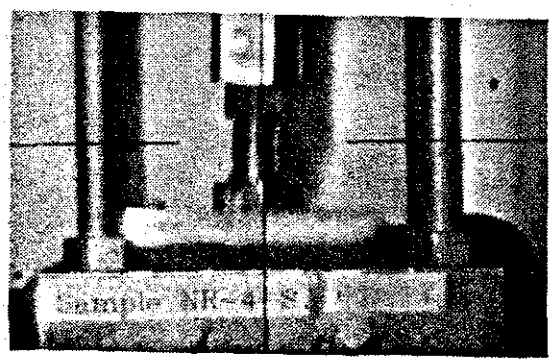

0.00764 s

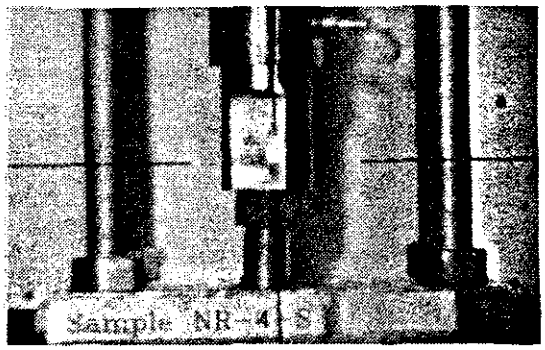

0.001147 s

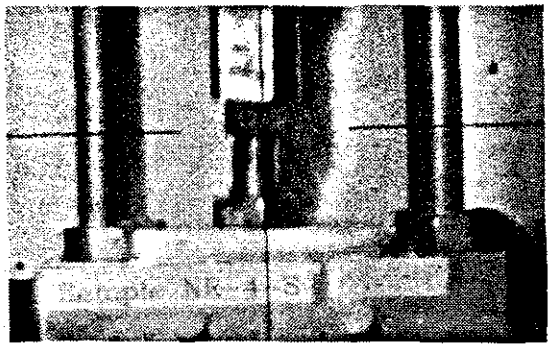

0.00860 s

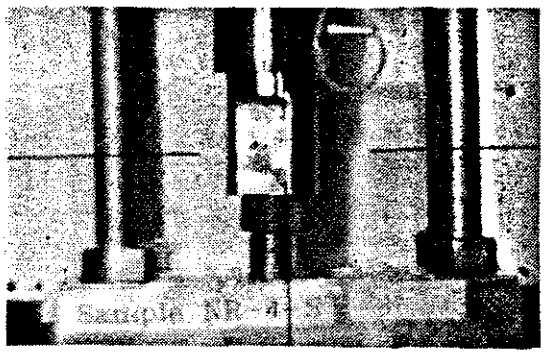

0.01242 s

0.00955 s

0.01338 s

FIGURE 6. Sequential Photogrpahs of Dynamic Test of Square Cylinder (continued)

in. wall thickness. The velocity of the impacting ram was again 44 ft/sec. Unlike the circular shape, the square cylinder immediately transmits applied impact forces to the bottom of the element. As shown in Figure 6, the walls of the element behave as columns; and as a result, the element is very stiff until the walls buckle. It is also interesting to observe the buckled shape of the square cylinder. At times of 0.00191 and 0.00287 seconds the left wall seems to be buckling into a second order shape; but by 0.00478 seconds, it has returned to a first order shape.

Transmission of impacting force to the bottom of the square cylinder is also noted in dynamic tests when the load cell is positioned to measure force on the bottom of the element. Figure 7 shows the difference in force recorded on top and bottom of the square cylinder. As mentioned previously, force transmission is important in determining the order of collapse of elements in a clustered crash cushion.

As shown in Figure 8, the square shape does dissipate much more impact energy than the circular shape and, therefore, makes a more efficient energy-absorbing element. However, the square cylinders also proved to be much more difficult to restore to their original shape than the circular cylinders.

The effects of geometric stiffeners was also investigated to evaluate their effects on both square and circular elements. The circular shape exhibited relatively low energy dissipation capacity and, therefore, web stiffeners across the bore, perpendicular to the primary direction of impact, were studied as a means of improving its performance. Bore stiffeners in an X shape were also studied as a means of stabilizing the square shape for angular impacts. Rubber web stiffeners were glued into a number of scale model cylinders, as shown in Figure 9. These stiffeners were installed by the manufacturer of the test specimens. The relatively thin web stiffener in the circular cylinder increased the static energy required to collapse the element by 110 percent, as shown in Figure 10. However, the bond developed between rubber stiffener and the cylinder proved to be a weak point that failed during some static and all dynamic tests. In fact, no meaningful tests of reinforced square cylinders were completed before the failure of the stiffener bonds. The high cost of mold construction precluded the production of cylinders molded with stiffeners that would not fail during testing. Therefore, although this feature appears to show promise for future research, use of rubber web stiffeners was not considered for the remainder of this study.

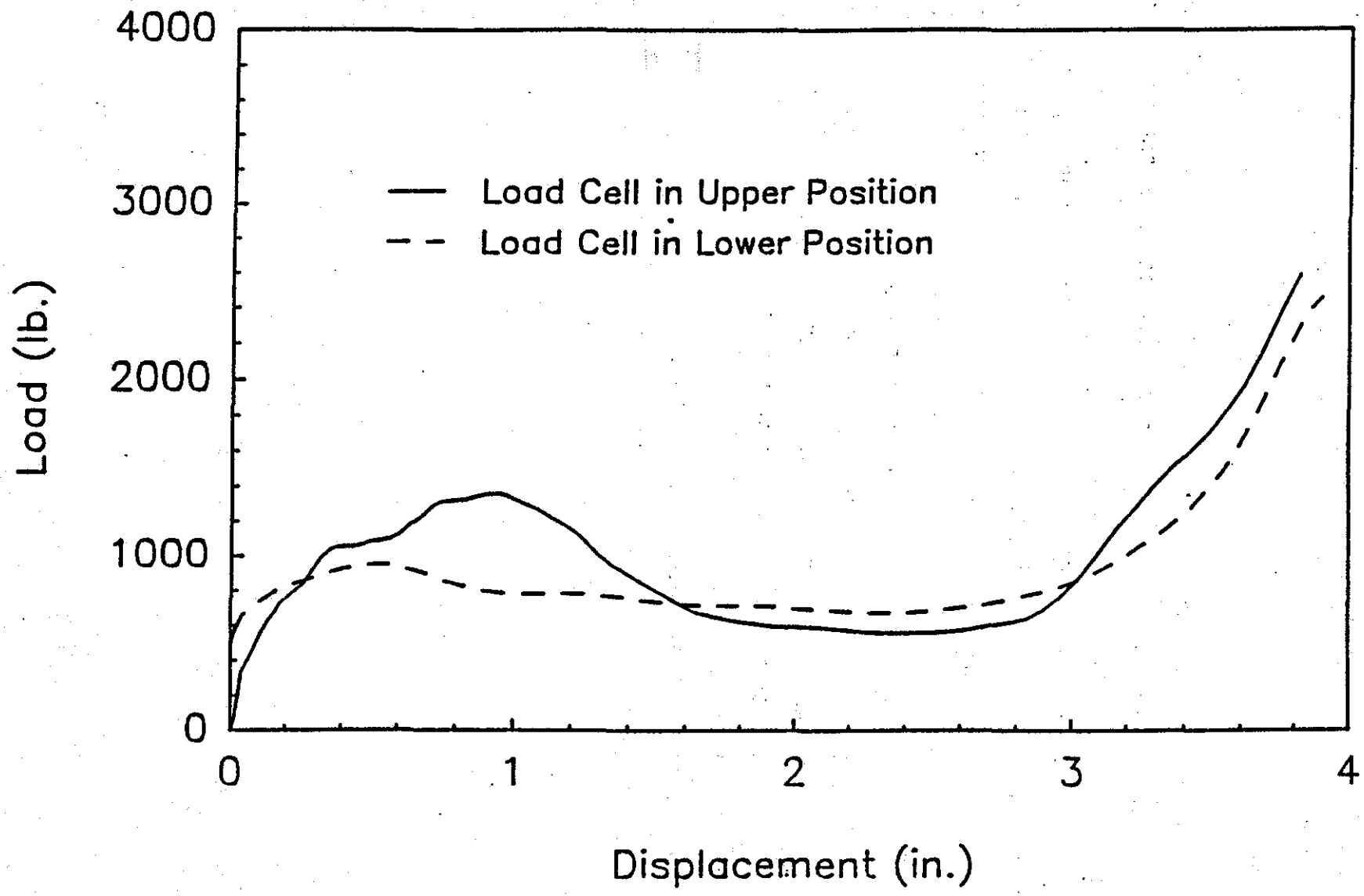

FIGURE 7. Force vs Deflection from Dynamic Test of Square Cylinder

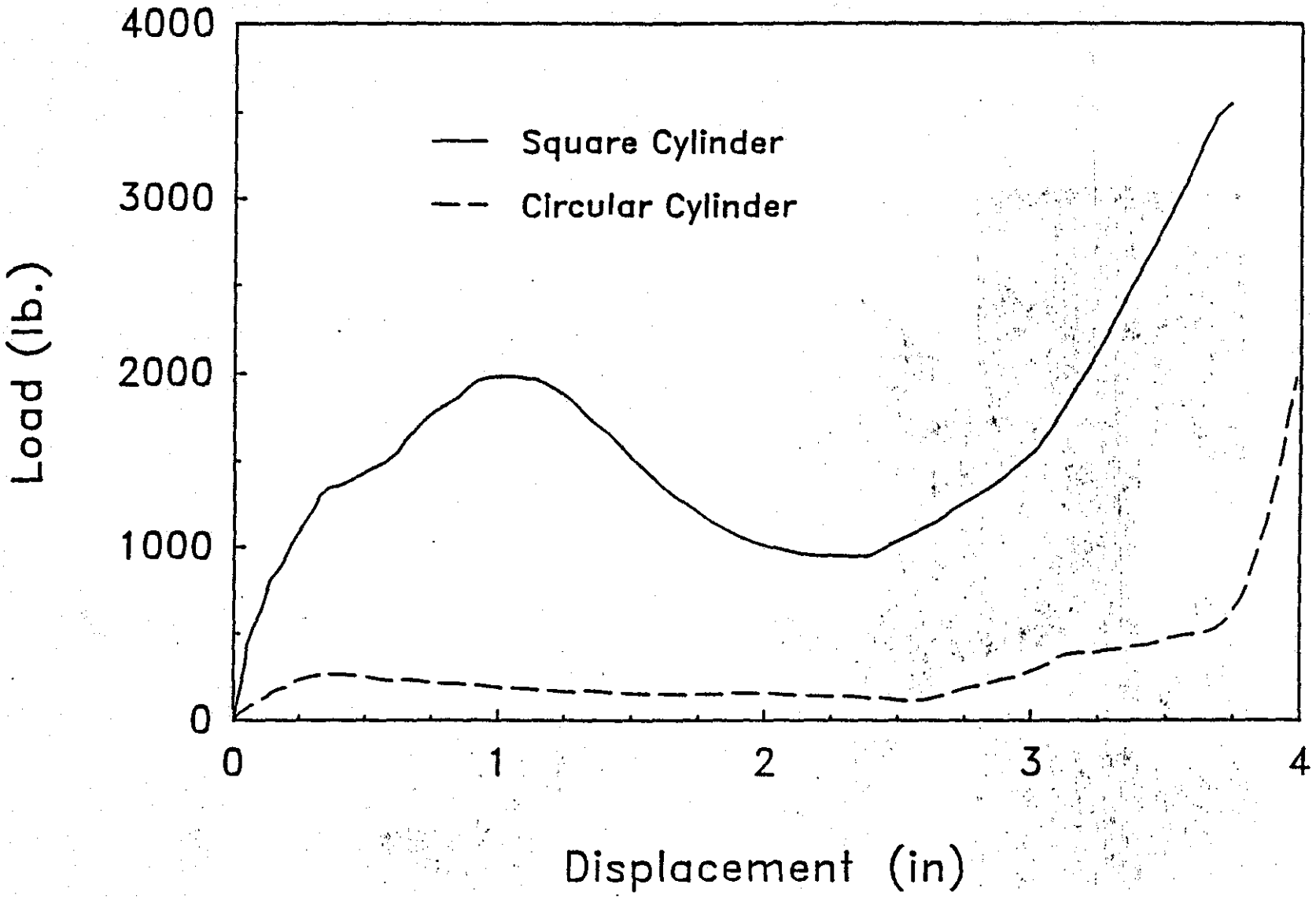

FIGURE 8. Dynamic Energy Dissipation of Circular and Square Cylinders

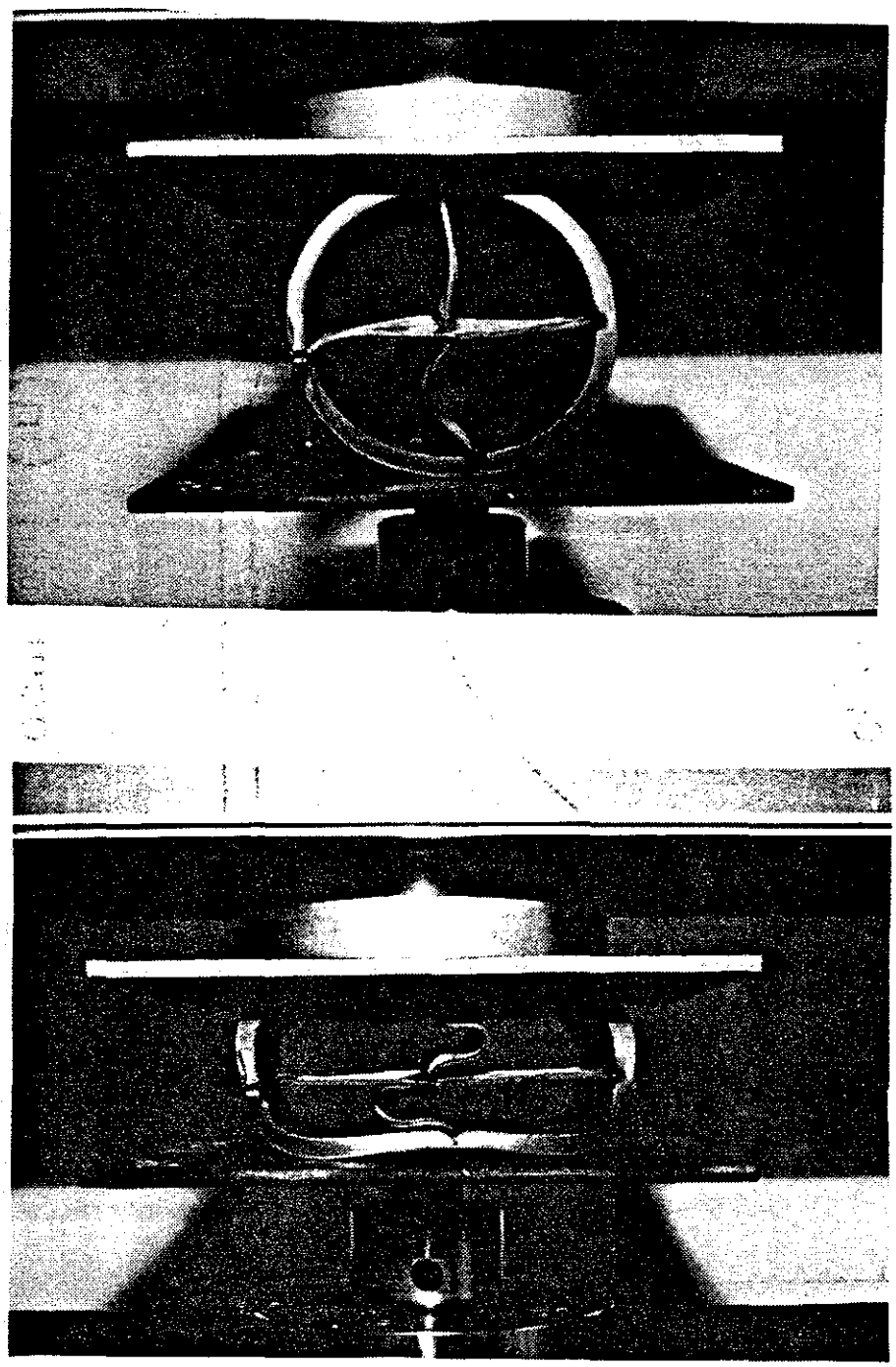

FIGURE 9. Circular Cylinder With Rubber Stiffener

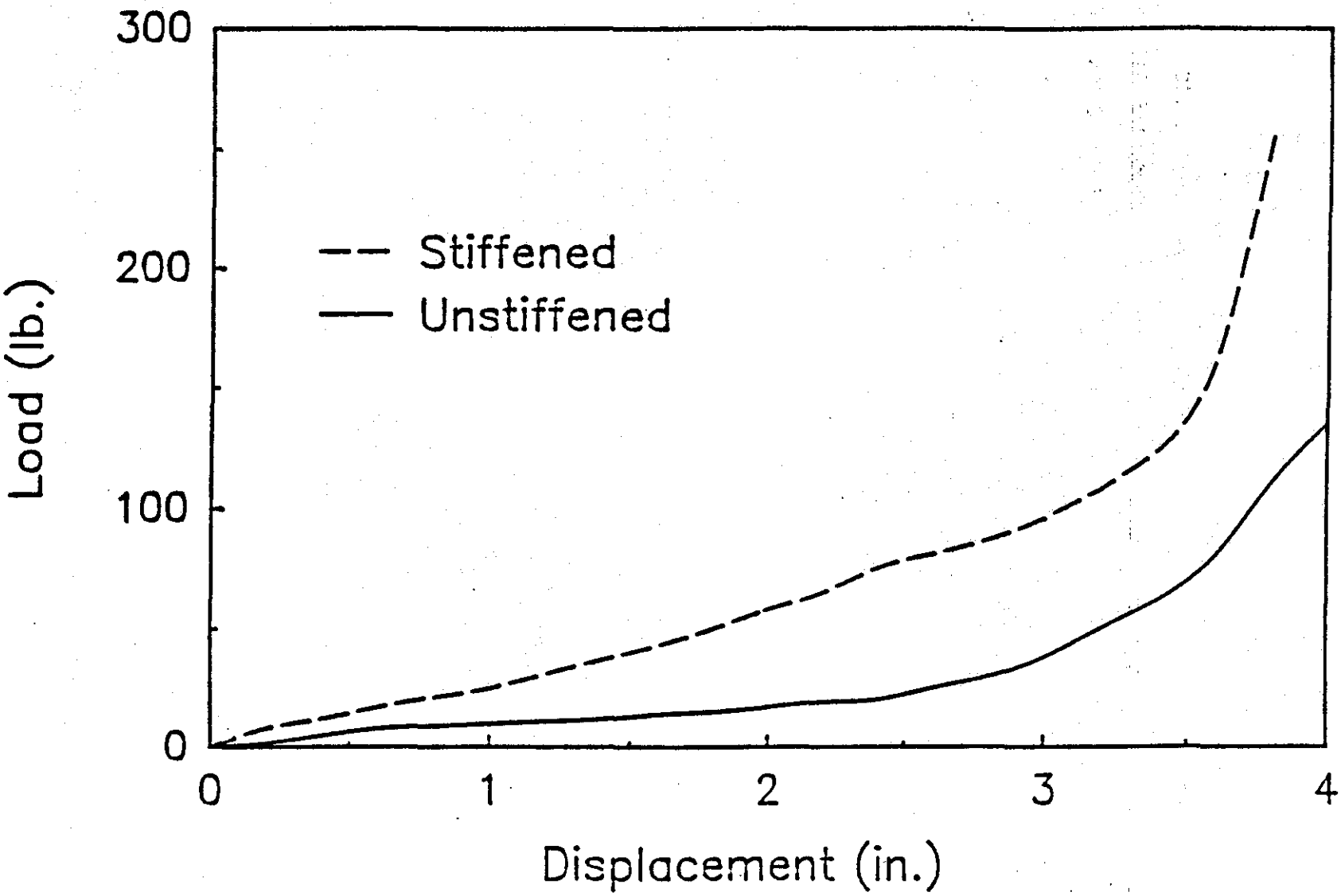

FIGURE 10. Energy Dissipation of Circular Cylinder With Rubber Web Stiffener

The effects of rigid stiffeners were also investigated, as shown in Figure 11. The energy dissipated during static testing was increased approximately 100 percent by the rigid stiffener. The deflected shape of the cylinder was changed considerably, as indicated by the buckled wall on the left side of the cylinder shown in Figure 11. Note that although a rigid plate was used in this testing, the concept under consideration for use in crash cushion designs involved steel cable tension bands placed inside the rubber cylinders, as shown in Figure 12. These test results indicated that this method for improving element energy dissipation merited further consideration. However, limitations on dynamic test equipment prevented impact testing of scale model cylinders with rigid stiffeners. Further, there was some concern regarding the potential for rigid stiffeners causing serious damage to the rubber cells during severe impacts. Therefore, further investigation of this concept was to be delayed until late in the full-scale testing program.

The effects of clustering rubber elements on energy dissipation characteristics was then studied as a final comparison between the two different shapes. Preliminary testing involved static compression of three clustered cylinders of each shape. Sequential photographs of these tests are shown in Figure 13. Notice that the deflected shapes of the rubber cylinders are not significantly different than observed in single element testing. As a result, the total energy dissipation of the three cylinders was only slightly greater than three times that of a single element. However, as shown in Figure 13, the square cylinders buckled as a unit and dissipated much less than three times the energy dissipated by a single element. In fact, the energy dissipation of the clustered circular elements was approximately equal to that of the clustered square elements. Subsequent testing of five- and seven-cell clusters exhibited similar performance for both of the two shapes.

Although the circular shape did not perform as well when tested individually, its performance in clusters was deemed to be equal to that of the square shape. Further, the circular shape is not sensitive to the direction of impact and its energy dissipation characteristics can be improved by relatively simple bore reinforcement. Therefore, the circular cylindrical energy-absorbing cell was selected as the most appropriate for use in a conventional crash cushion design.

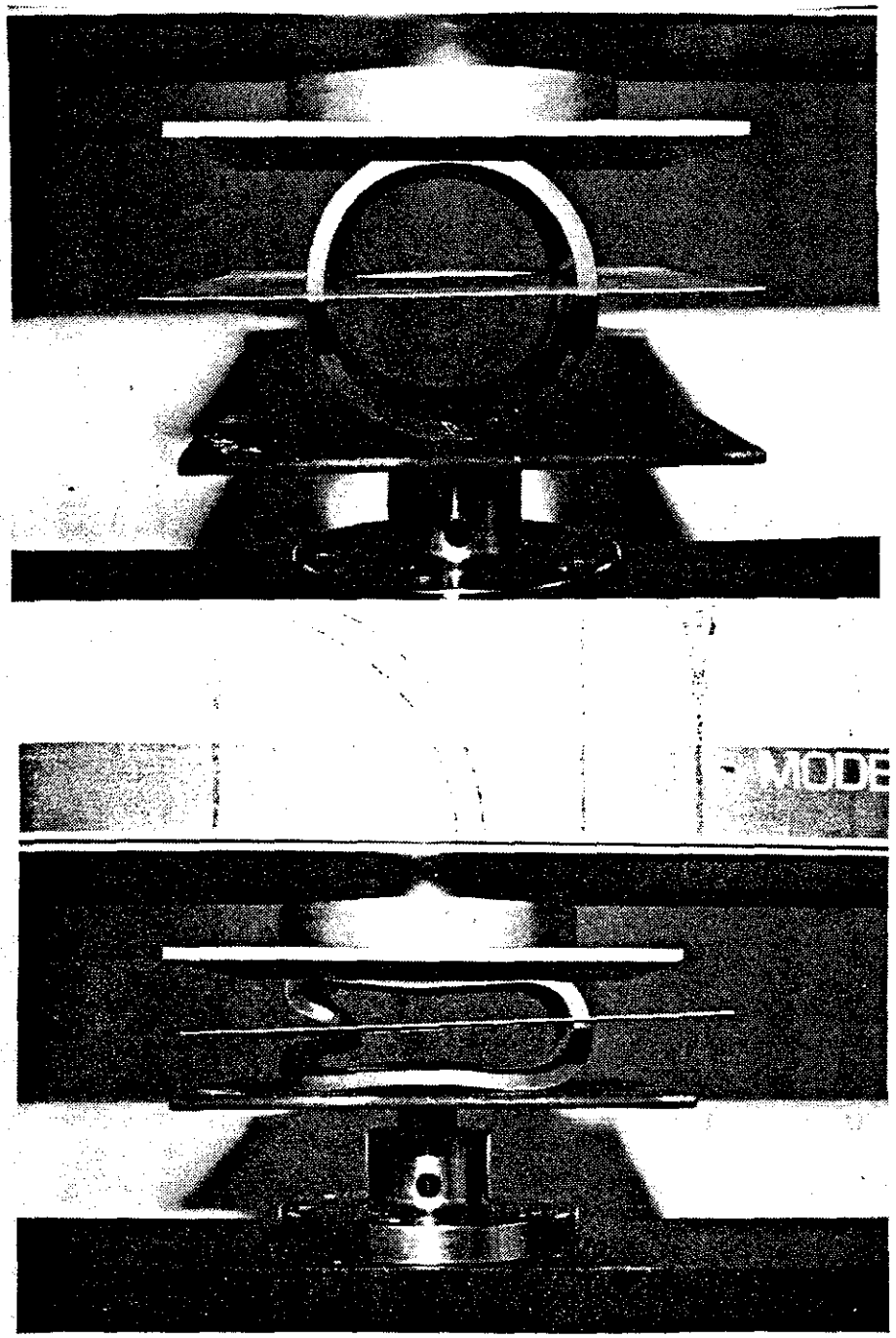

FIGURE 11. Circular Cylinder With Rigid Stiffener

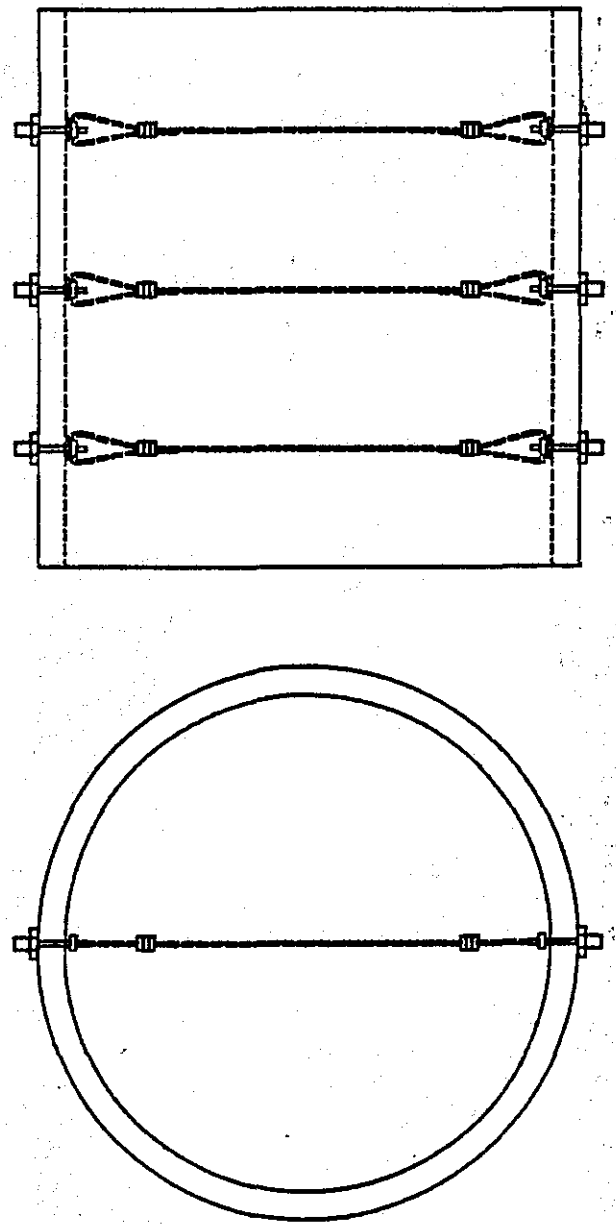

FIGURE 12. Rigid Element Stiffener Concept

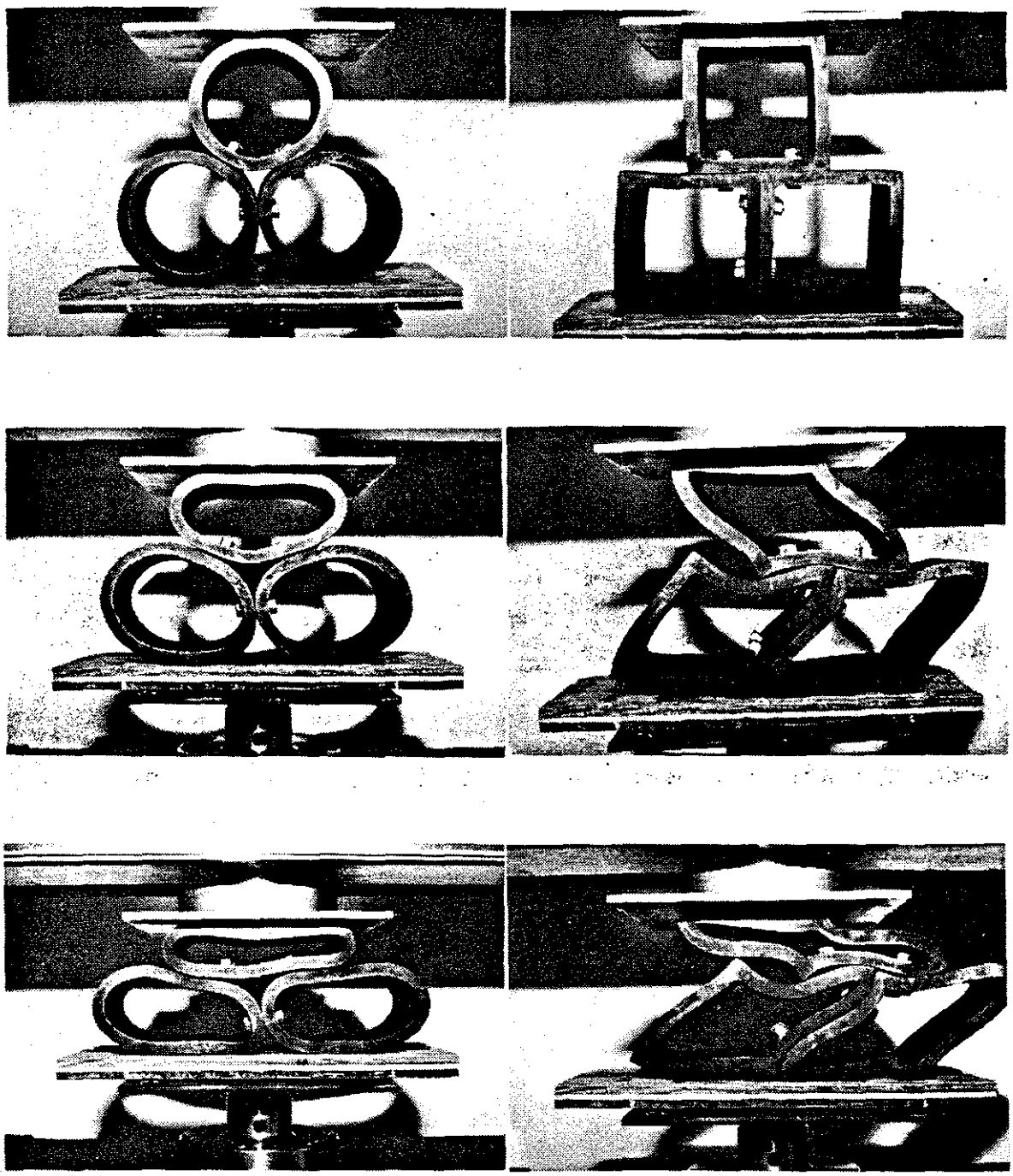

FIGURE 13. Sequential Photogrpahs from Static Tests of Clustered Cylinders

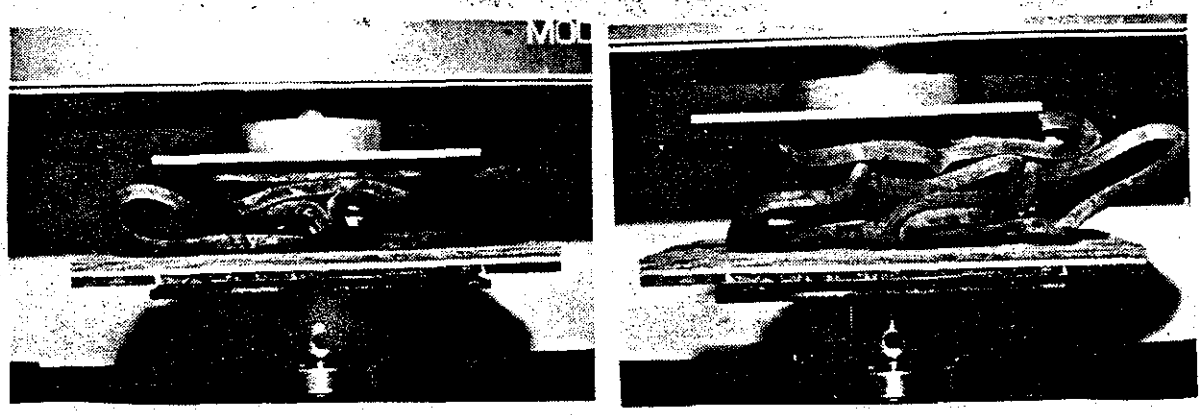

FIGURE 13. Sequential Photographs from Static Tests of Clustered Cylinders (continued)

FULL-SCALE ELEMENT TESTS

Dynamic testing of full-scale cylinders was then undertaken in an effort to verify results of some of the scale model studies. The effects of clustering several elements was of primary interest. This testing involved a 5,245 lb cart that was directed into rubber cylinder specimens in front of a rigid backstop, as shown in Figure 14. The maximum impact speed that could be generated with the cart was 30 mph. Accelerometers attached to the cart were used to collect force deflection data and high speed films were used to verify electronically determined impact speeds. Full-scale element tests were conducted first on single elements and then on five-element clusters. Preliminary testing involved rubber attenuating elements used in the development of a narrow hazard crash cushion. Results of this testing were then used to determine appropriate sizes for new elements for a conventional cushion that was in turn tested under similar conditions.

Preliminary Testing

Rubber cylinders incorporated in the narrow hazard crash cushion design (3) were 24 in. long, had a 28 in. outside diameter, and either a 1.75 in. or a 4.5 in. wall thickness. These cylinders were first tested individually to compare scale model predictions with full-scale cylinder performance. The test installation for single element testing is shown in Figure 15. Table 6 summarizes results of these tests and the dynamic energy dissipation for the two test specimens is shown in Figure 16. The measured energy dissipation of the 1.75 in. thick cylinder was 4.2 kip-ft compared to a scale model prediction of 3.0. Predicted energy dissipation for the thick walled cylinder was 24.6 kip-ft, compared to a measured value of 22.0 kip-ft. This level of accuracy for scale model predictions was considered to be quite good and, therefore, further efforts were directed at determining the effects of clustering elements.

Full-scale tests of clustered cells were then conducted on both the thin and the thick walled specimens. The five-element cylinder configuration with connection and leg details is shown in Figure 17. These design details were intended to be evaluated for use on the proposed full-scale crash cushion. A total of 10 cart tests were conducted on the two multi-element cylinder configurations as summarized in Table 7. As shown in this table, the total energy dissipated by the five thin wall cells was 26.1 kip-ft, compared to 4.2 kip-ft for an individual cell. This increase of approximately 25 percent can be

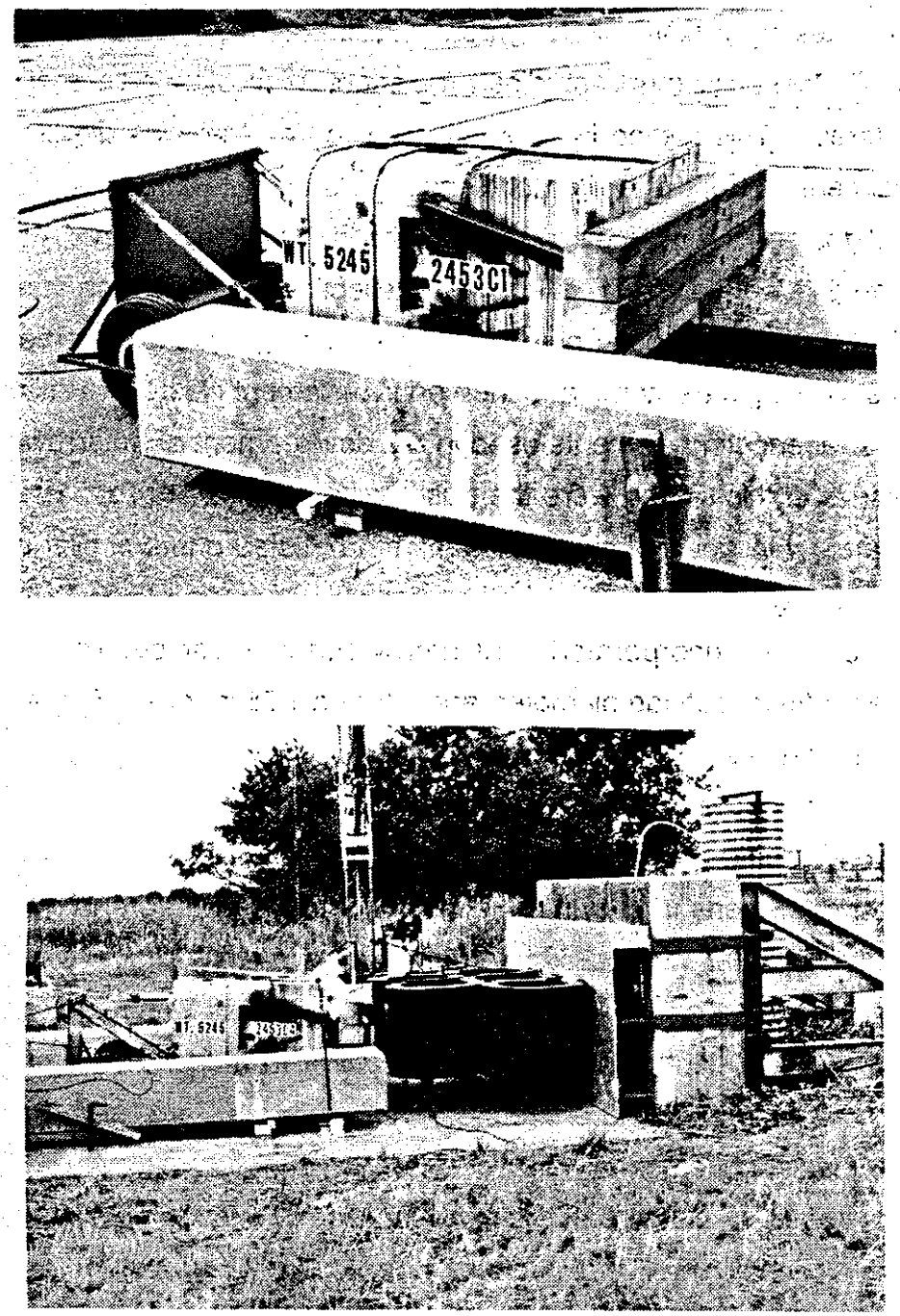

FIGURE 14. Instrumented Cart and Rigid Backstop Used in Full-Scale Dynamic Test

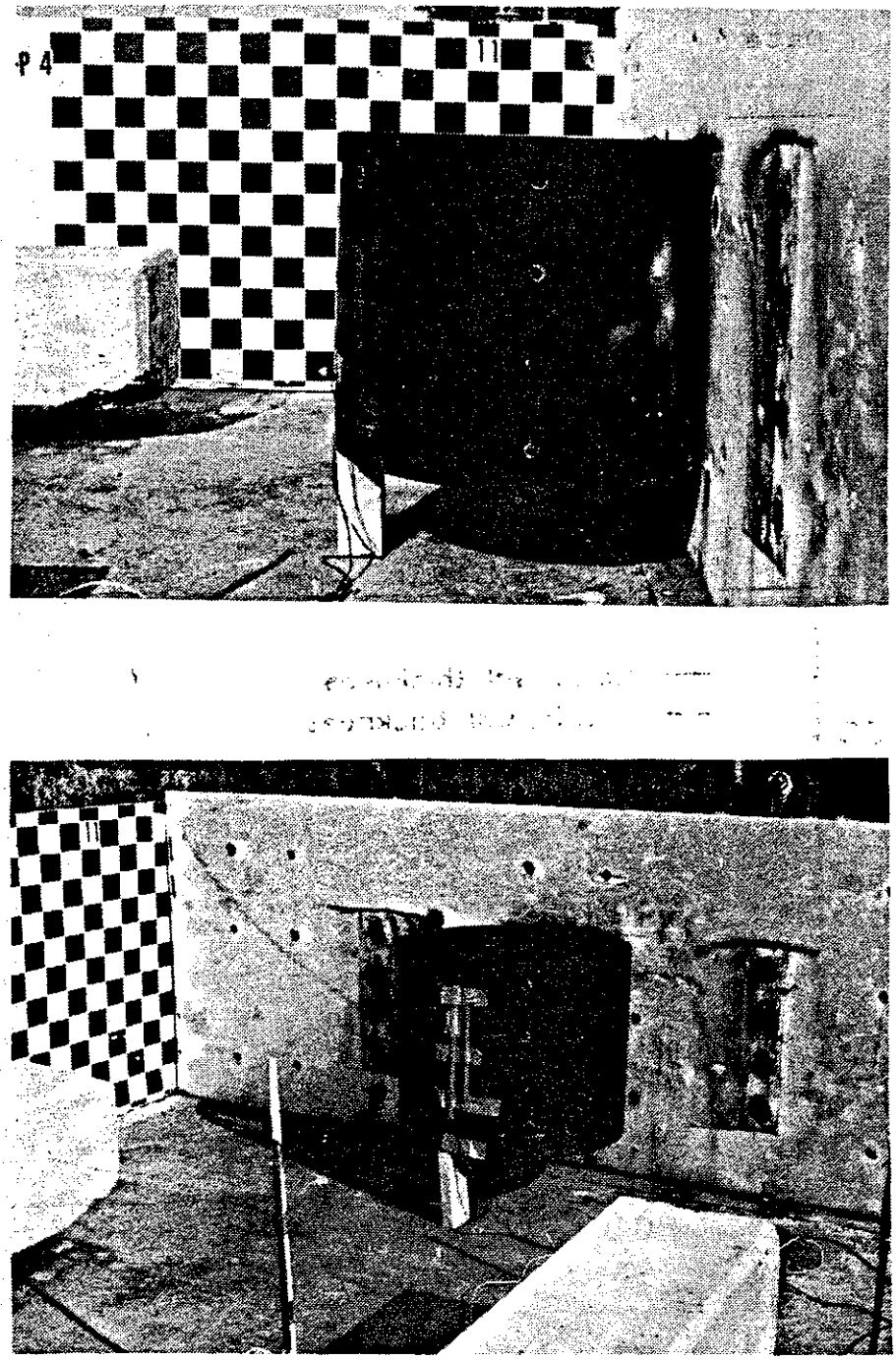

FIGURE 15. Test Installation for Dynamic Tests of Full-Scale Rubber Elements

Table 6. Single Element Cart Tests

Test	Date	Wall Thick. (in)	Wall Temp. Outer/Inner (°F)	Impact Speed (mph)	Energy (k-ft)
1.	9/21/87	1.75	110/85	7.4	4.18
2.	9/21/87	4.50	110/85	14.2	22.0

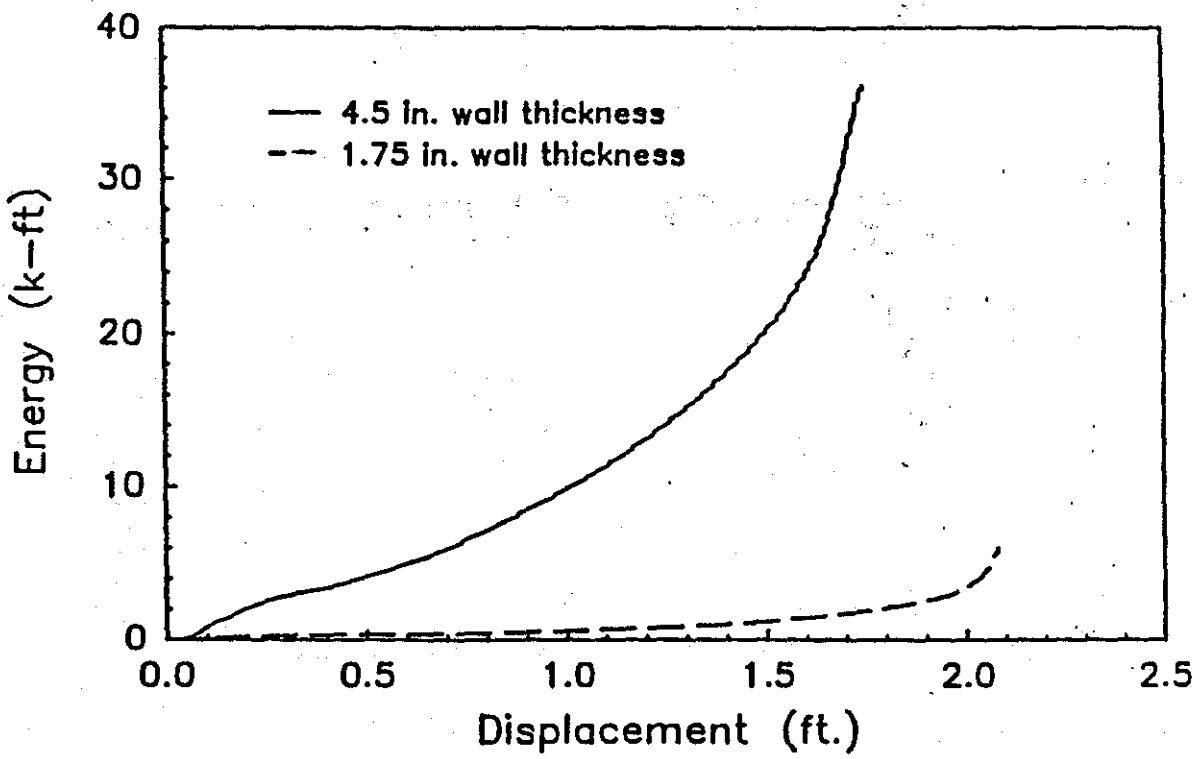

FIGURE 16. Dynamic Energy Dissipation of Full-Scale Rubber Cylinders

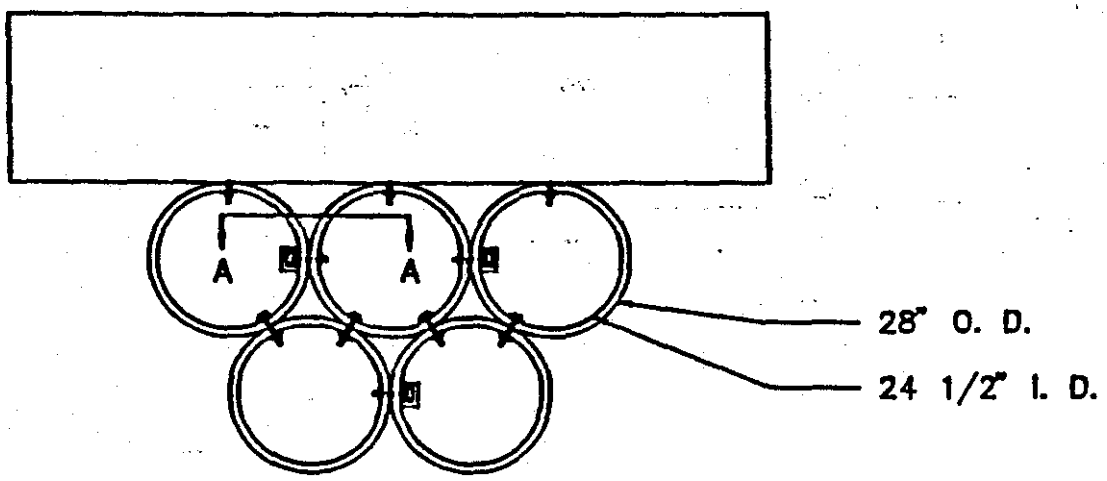

Plan of Crash Cushion

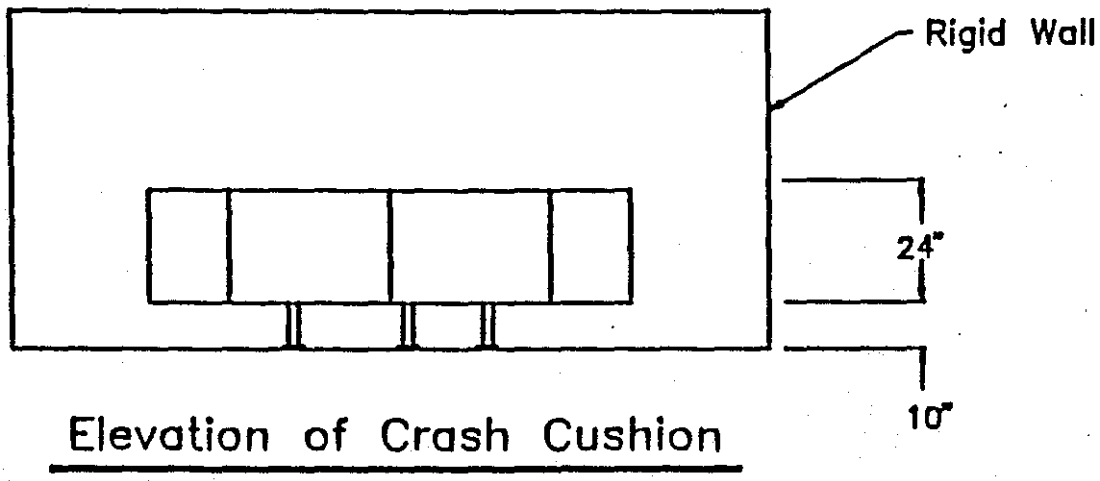

Elevation of Crash Cushion

FIGURE 17. Construction Drawings of Five-Element Rubber Crash Cushion

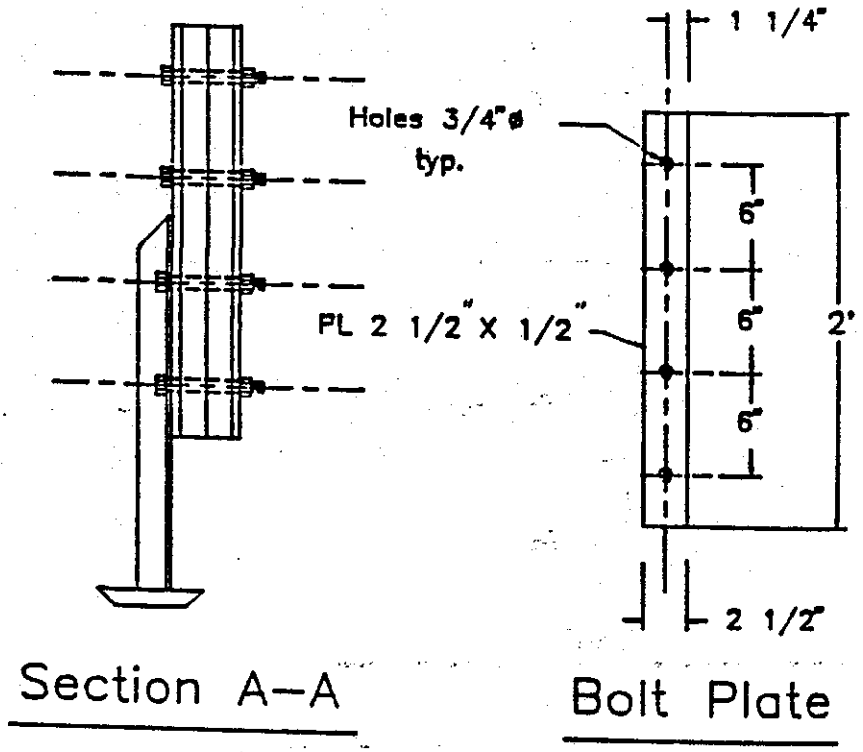

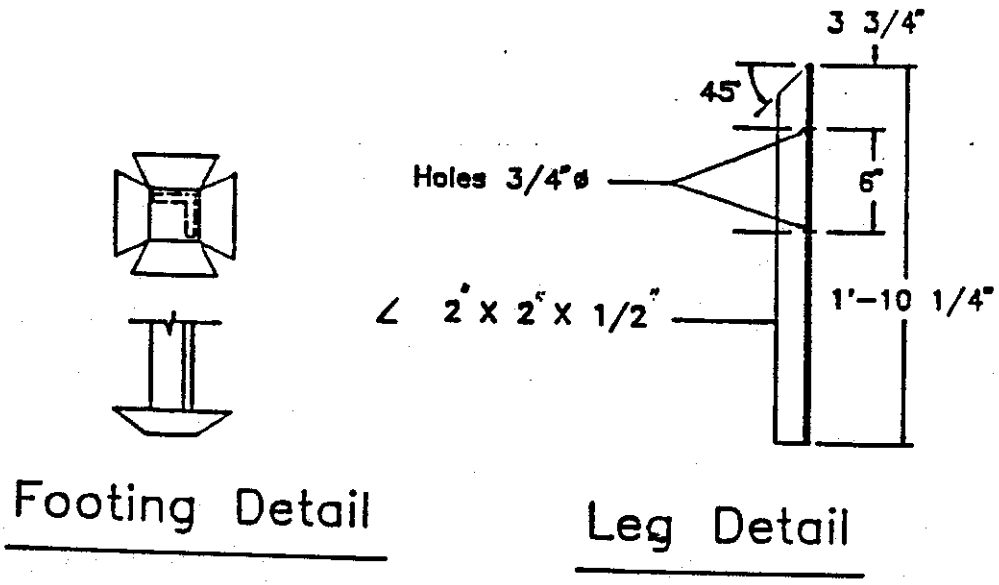

Figure 17. Construction Drawings of Five-Element Rubber Crash Cushion (Continued)

Table 7. Five-Element Cart Tests

Test	Date	Wall Thick. (in)	Wall Temp. Out/In (°F)	Impact Speed (mph)	Exit Speed (mph)	Energy (k-ft)
1.	9/7/87	4.5	110/90	10.4	4.6	-
2.	9/7/87	4.5	110/90	17.6	6.1	-
3.	9/7/87	4.5	110/90	14.9	7.9	-
4.	9/7/87	4.5	110/90	15.1	8.1	-
5.	9/10/87	4.5	120/90	20.0	10.2	-
6.	9/10/87	4.5	120/90	21.4	11.1	-
7.	9/14/87	4.5	120/85	27.8	16.2	137.4
8.	9/16/87	1.75	105/80	7.0	3.4	-
9.	9/16/87	1.75	105/80	9.4	3.4	-
10.	9/16/87	1.75	105/80	14.7	5.7	26.1

attributed to the constraint effects on some of the interior elements. Similarly, the total energy dissipated by the five thick walled elements was 134 kip-ft, or approximately 22 percent more than would be predicted from single element test results. Energy dissipation versus cluster deformation is shown in Figure 18 for both wall thicknesses.

The clustered elements did not return to their original shape after impact and, therefore, some restoration was required, as shown in Figure 19. A special restoration device, shown in Figure 20, was designed for this purpose. One end of the device is attached to a tow vehicle, and the other end was attached to the front cells in the cushion. The two groups of five rubber cylinders were easily restored in less than 30 minutes using this device. None of the rubber cylinders exhibited any signs of damage after the cart tests.

Final Component Testing

Results of the foregoing full-scale element testing were then used to develop a preliminary crash cushion design. This design incorporated 30 in. long, 25 in. I. D. cylinders, with wall thicknesses varying from 1.5 to 3 in. Rubber attenuation cells were then manufactured to these specifications, and one sample of each size was then tested statically. Single specimens were tested statically and a five-cell cluster of 1.5 in. thick samples was tested dynamically. Static and dynamic test results compared reasonably well with predictions based on scale model testing as shown in Table 8. Note that the predicted total dynamic energy dissipation of the 1.5 in. thick wall cylinders was approximately 4,500 ft-lb at 70°F, compared with clustered dynamic test results of 4,376 ft-lb at approximately 95°F. When adjusted for temperature, the predicted value becomes 3,819 ft-lb, or about 15 percent less than the clustered test results. These findings are similar to those from preliminary clustered test results where energy dissipation of each element in a five-cell cluster was found to be 20 to 25 percent greater than results from tests of a single cell. These test results were sufficiently close to predicted values to warrant using scale model test results for design of a prototype crash cushion. When the results of scale model testing of the NR/EPDM material were analyzed in accordance with procedures described in reference 5, the effective modulus and dynamic magnification factors were found to be a function of temperature, as shown in Table 9. This information was used to calculate the energy dissipation characteristics of 28 in. long X 25 in. I. D. rubber cylinders, as shown in Figure 21.

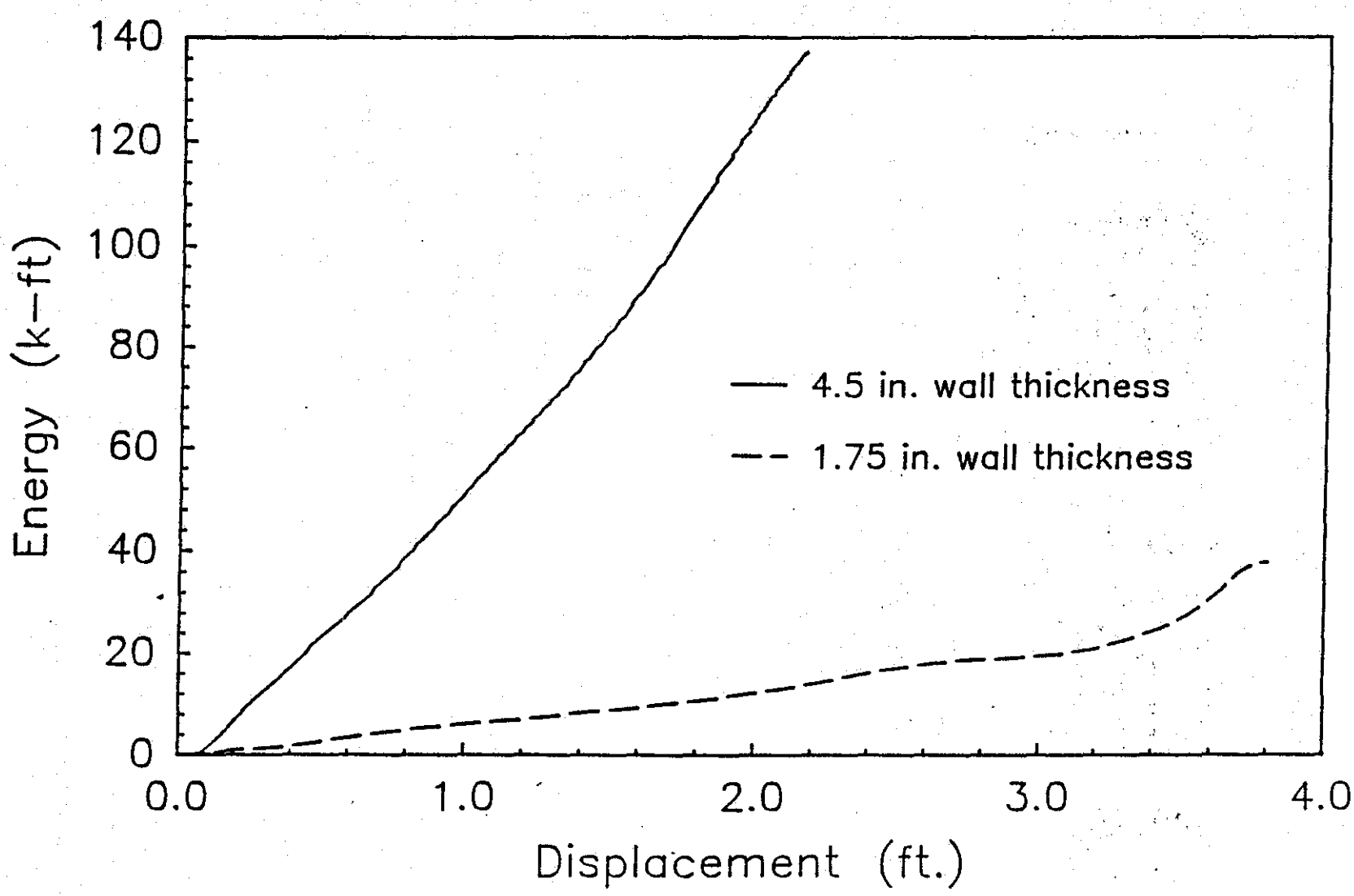

FIGURE 18. Energy Dissipation of 4.5-in. and 1.75-in. Five-Element Cushions

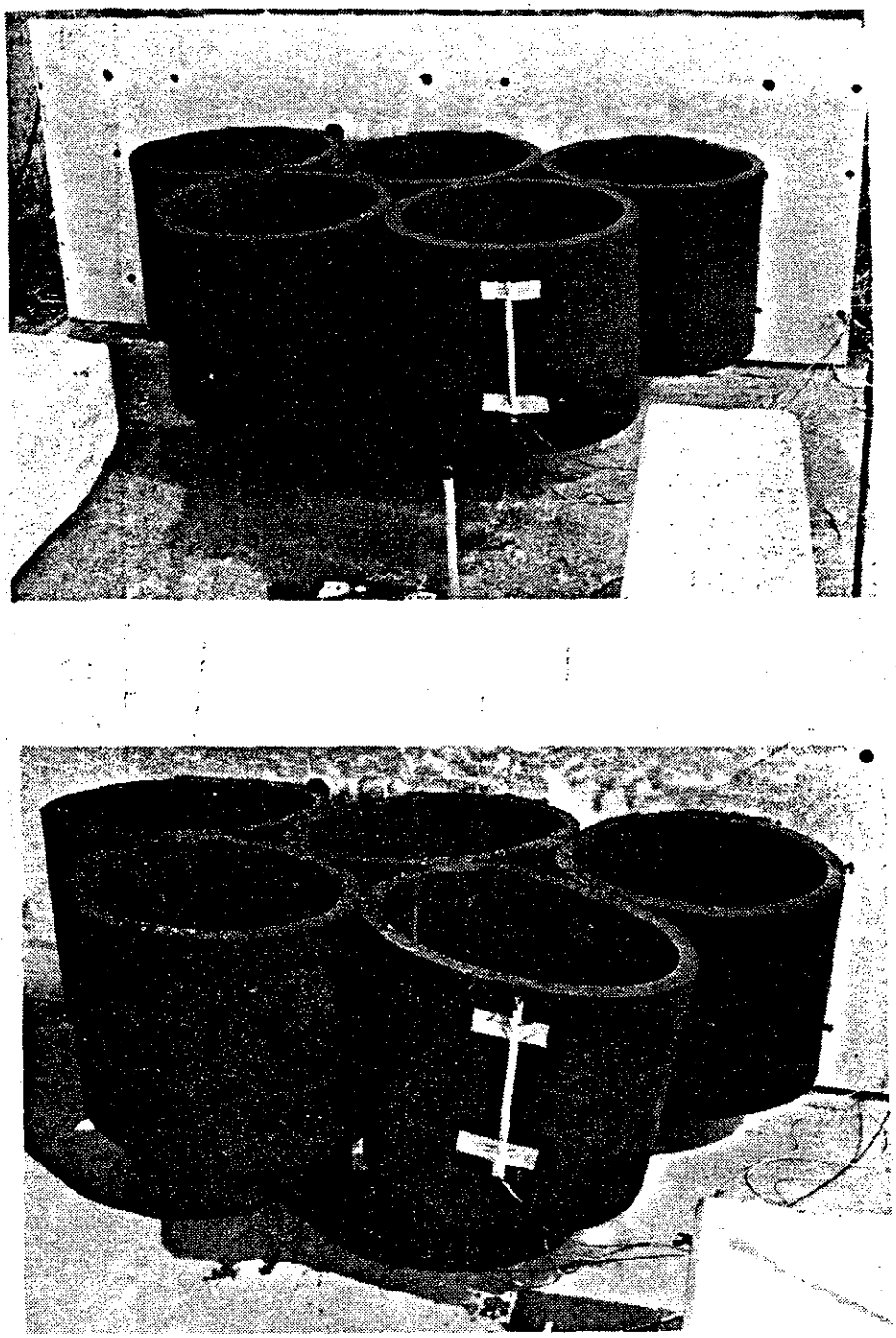

FIGURE 19. Five-Cylinder Cushion Before and After Dynamic Test

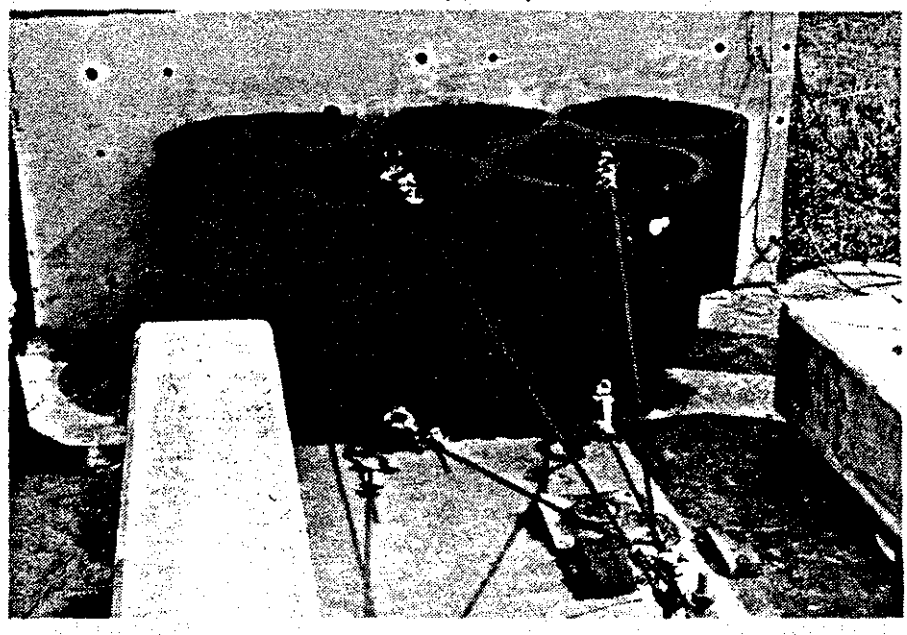

FIGURE 20. Cable Device Used to Restore Rubber Cushion

TABLE 8. PREDICTED AND MEASURED ENERGY DISSIPATION OF 25-IN. I.D., NR/20% EPDM RUBBER CYLINDERS

WALL THICKNESS IN.	STATIC ENERGY, (FT-LB) PREDICTED	STATIC ENERGY, (FT-LB) MEASURED	DYNAMIC ENERGY (FT-LB) PREDICTED	DYNAMIC ENERGY (FT-LB) MEASURED
1.5	1,500	1,560	4,800	4,400
2.25	4,500	5.060	11,500	N/A
3.0	9,300	10,080	23,800	N/A

TABLE 9. EFFECTIVE MODULUS AND DYNAMIC MAGNIFICATION OF (NR/20% EPDM)

TEMPERATURE °F	EFFECTIVE MODULUS, E. (PSI)	DYNAMIC MAGNIFICATION FACTOR, O
-10	5,760	3.2
34	3,280	3.1
70	2,720	2.0
110	2,060	1.9

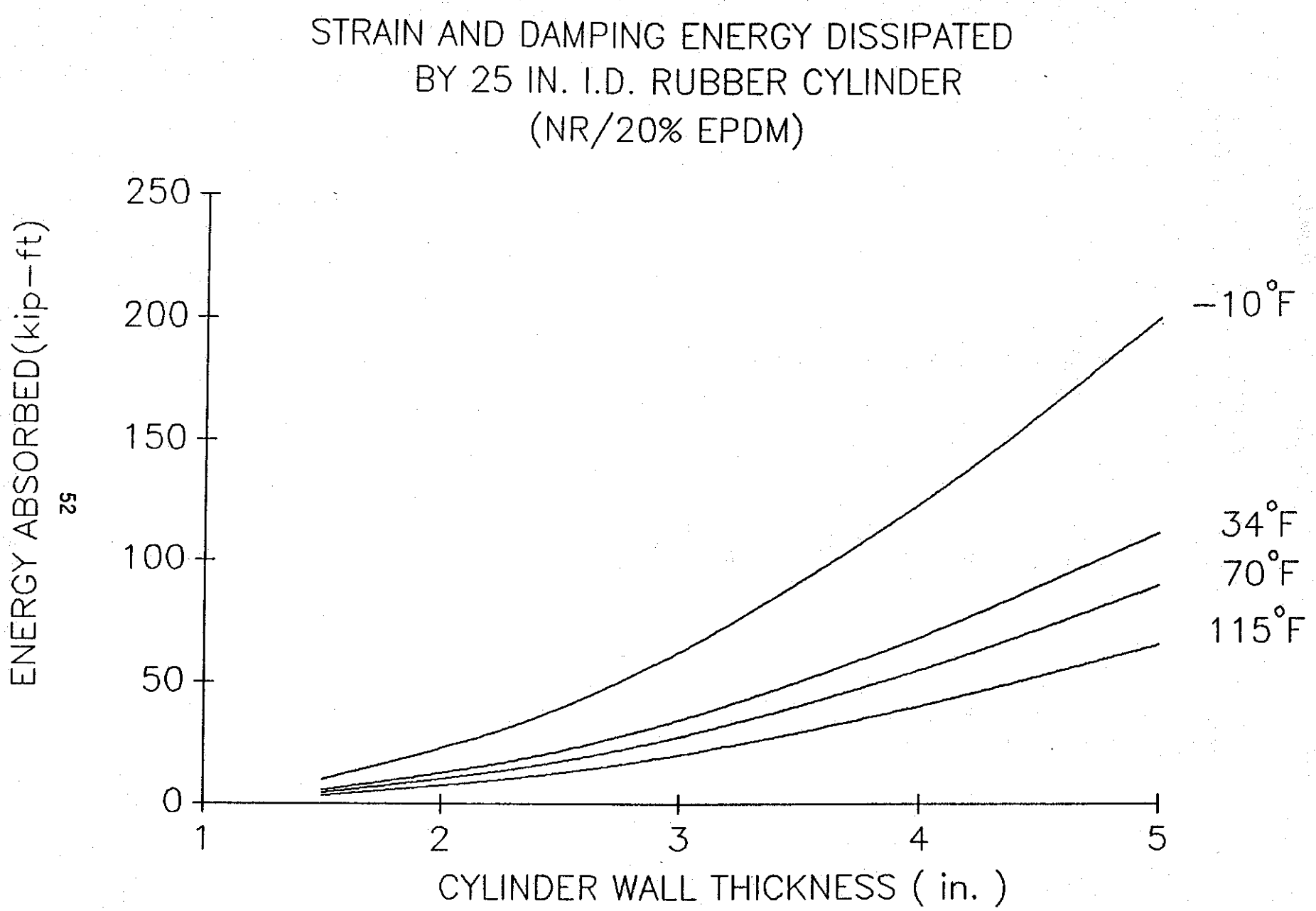

FIGURE 21. Dynamic Energy Dissipation Properties of Large Diameter Rubber Cylinders

TABLE 10. PREDICTED HIGH SPEED CUSHION PERFORMANCE

TEMP. °F	VEHICLE WEIGHT (lb)	IMPACT VELOCITY (mph)	LONGITUDINAL OCCUPANT IMPACT VELOCITY (ft/sec)	STOPPING DISTANCE (ft)
114	4,500	60.0	27.4	18.75
	3,400	60.0	26.1	18.0
	2,200	60.0	28.0	15.8
	1,800	60.0	31.2	14.2
70	4,500	60.0	28.8	18.2
	3,400	60.0	27.5	16.5
	2,200	60.0	28.9	14.2
	1,800	60.0	33.0	13.8
34	4,500	60.0	29.9	17.9
	3,400	60.0	28.6	16.0
	2,200	60.0	30.4	13.9
	1,800	60.0	33.4	13.7
-10	4,500	60.0	28.6	14.4
	3,400	60.0	31.9	13.9
	2,200	60.0	35.7	11.9
	1,800	60.0	34.8	11.5

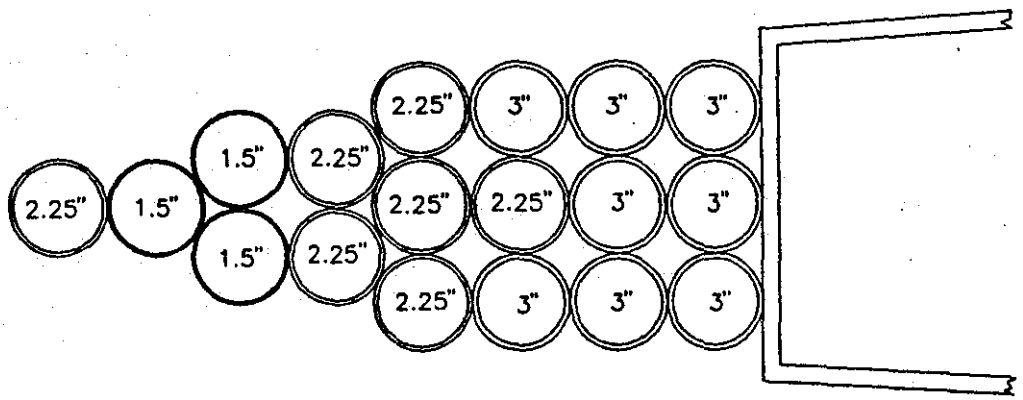

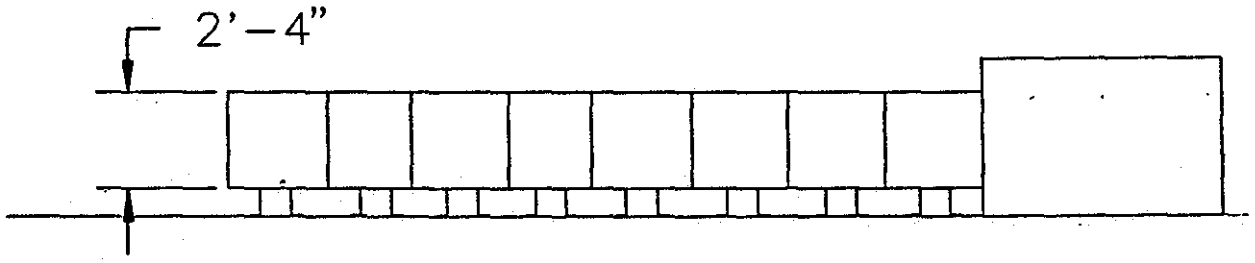

Material Type: Natural Rubber/20% EPDM blend

Cylinder Characteristics:

1.5" – 123 lb
2.25" – 190 lb
3.0" – 261 lb

Total Rubber Weight: 3787 lb

Designed for temperature between −10°F and 115°F

Texas Transportation Institute	LOW PERFORMANCE RUBBER CRASH CUSHION

FIGURE 22. Low Speed Crash Cushion Design

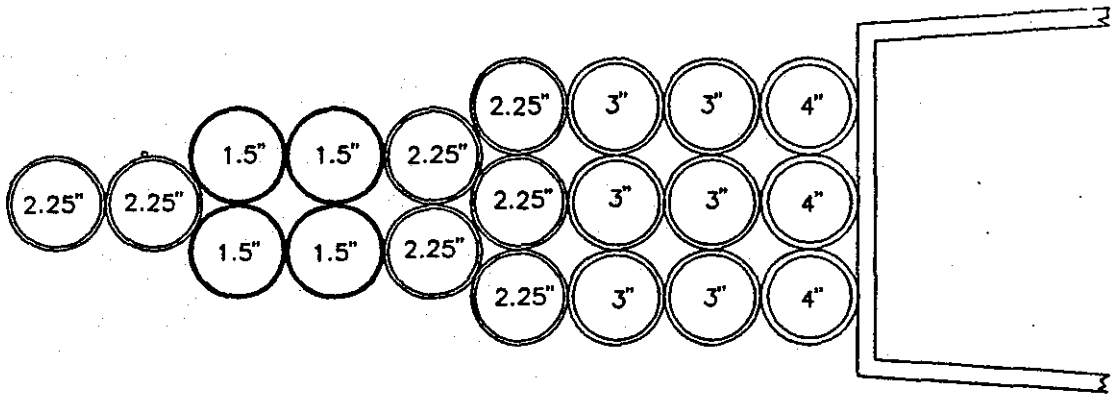

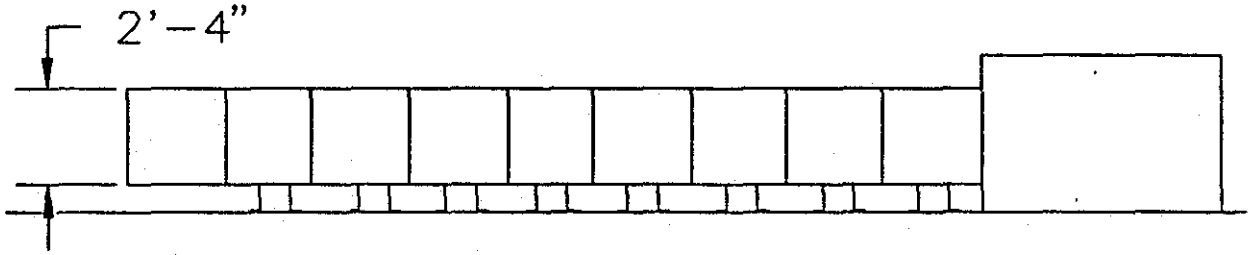

Material Type: Natural Rubber/20% EPDM blend

Cylinder Characteristics:

1.5" – 123 lb
2.25" – 190 lb
3.0" – 261 lb
4.0" – 360 lb

Total Rubber Weight: 4465 lb

Designed for temperature between −10°F and 115°F

Texas Transportation Institute	HIGH PERFORMANCE RUBBER CRASH CUSHION

FIGURE 23. High Performance Crash Cushion Design

CRASH CUSHION DESIGN

Prototype crash cushion designs were then developed based on the foregoing predictions of rubber cylinder performance. Two basic designs were developed, one for low speed applications capable of attenuating vehicles impacting at speeds up to 45 mph and another for freeway applications designed for impact speeds up to 60 mph. The designs were developed to meet NCHRP Report 230 (6) test standards. References 3 and 5 describe the basic design procedures employed. Predicted occupant impact velocities for the high performance system are shown in Table 10. Note that although the crash cushions are designed to perform safely at all temperatures between -10 °F and 115 °F, the systems would likely perform well for temperatures slightly below or above these extremes. The low speed design, shown in Figure 22, would require 18 cylinders and a total of 3787 lbs of rubber; and the high performance design shown in Figure 23, would require 20 cylinders and 4,468 lbs of rubber. Rubber cylinders are attached and supported in the same manner used in the clustered cell dynamic testing, as shown in Figure 17.

Note that these systems were designed based on the relatively proven technology of using unreinforced rubber cylinders for attenuating impacts. Although, as discussed previously, some bore reinforcement concepts were tested and shown to have the potential for significantly improving the efficiency of rubber crash cushion elements, time and monetary constraints prevented any further evaluation in this study.

Full-Scale Crash Tests

Delays in the manufacture of rubber cylinders for use in the prototype cushion prevented full-scale compliance testing of the two designs. Therefore, a reduced crash test program designed to demonstrate the overall feasibility of the concept was undertaken. This program involved testing the low speed prototype cushion, shown in Figure 24, for impacts with mini-size and full-size vehicles both for moderate and relatively high speeds. Crash tests results are described in detail below. Sequential photographs of the crash tests are shown in Appendix A. Accelerometer traces and rate gyro plots from the tests are shown in Appendices B and C, respectively.

FIGURE 24. Low Speed Prototype Crash Cushion

Test 2453-1

The first test was designed to determine the performance and durability of the cushion for a common impact condition with a full-size vehicle. A test vehicle weighed 4,500 lb and impacted the cushion head-on at 31.2 mph. The vehicle was smoothly decelerated over a distance of 13.6 ft, with no tendency to override or dive under the cushion. All measures of cushion performance were within recommended levels, as summarized in Figure 25. The test vehicle was virtually undamaged, as shown in Figure 26. No components of the cushion were damaged, and it was quickly restored to its original position with the restoration device described previously. Figure 27 shows the crash cushion after this test and after restoration to its original position.

Test 2453-2

The second test was to evaluate the performance of the prototype crash cushion for head-on impacts near its limit of performance. The test vehicle from test 2453-1 was reused for this test. The vehicle impacted the cushion head-on at 47.9 mph and was smoothly decelerated until all of the elements in the system were fully collapsed. The vehicle then experienced a short spike deceleration that brought it to a stop. As a result, the longitudinal occupant ridedown acceleration for this test was 17.6 g's, which is above the recommended limit of 15 g's but below the maximum allowable limit of 20 g's. All other measures of cushion performance were within recommended limits for this test. Analysis of accelerometer traces from this test indicated that the vehicle was very nearly stopped when the high decelerations occurred. The analysis showed further that the vehicle would have been stopped before completely collapsing the system if it had impacted at the design speed of 45 mph. Therefore, the safety performance of this system was determined to be relatively good. The test vehicle was moderately damaged as shown in Figure 28. The test is summarized in Figure 29.

A careful inspection of crash cushion components revealed significant cracks in several of the rubber cylinders. The cracks, shown in Figure 30, appeared to start at points of delamination between individual layers of rubber. Apparently there was inadequate bonding between the layers of rubber used to create the cylinder during the mandrell wrapping manufacturing process. The manufacturer of the components indicated that such problems can arise when the mandrell wrapping process is used to

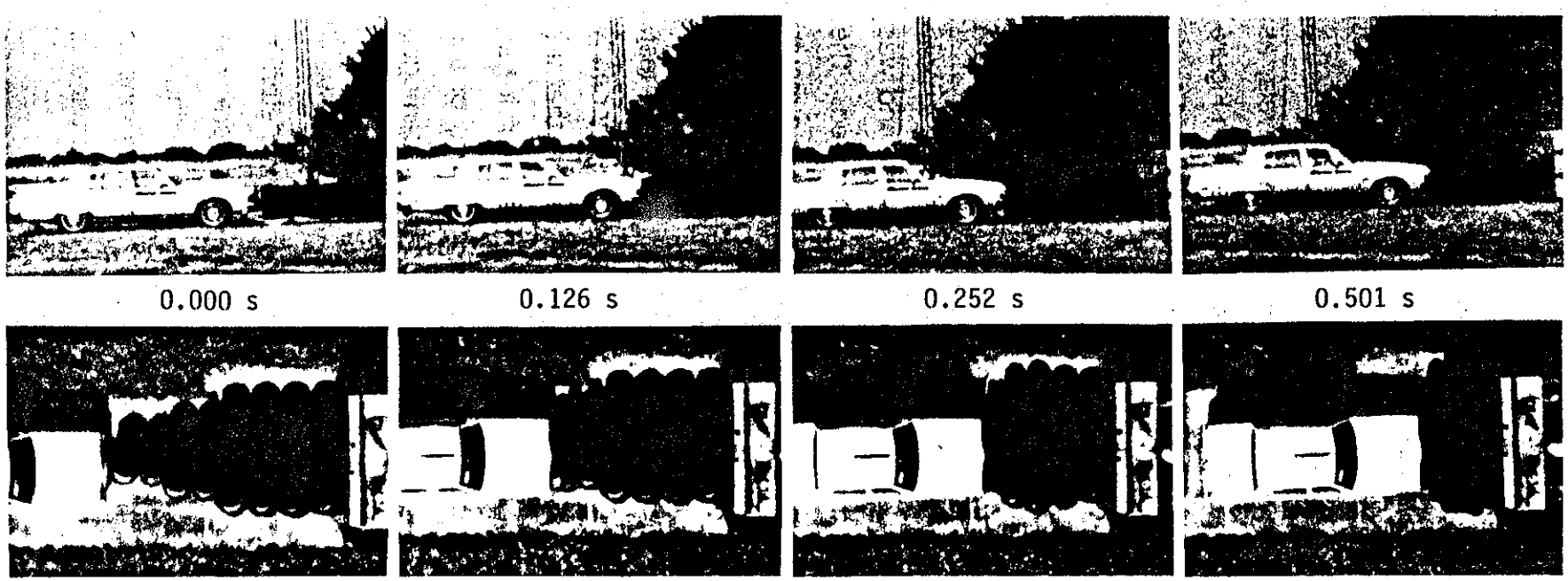

Test No.	2453-1
Date	08/24/88
Test Installation.	Clustered Rubber Cylinders
Length of Installation	20 ft (6 m)
Vehicle.	1981 Oldsmobile Regency
Vehicle Weight	
Test Inertia	4,500 lb (2,043 kg)
Vehicle Damage Classification	
TAD	12FD1
CAD	12FDLW1
Maximum Vehicle Crush	1.5 in (3.8 cm)
Max. Dyn. Deflection	13.6 ft (4.1 m)
Max. Perm. Deformation	1.4 ft (0.4 m)

Impact Speed.	31.2 mi/h (50.2 km/h)
Impact Angle.	0 deg
Time to Stop.	0.500 seconds
Vehicle Accelerations (Max. 0.050-sec Avg)	
Longitudinal.	-5.9 g
Lateral	-0.6 g
Occupant Impact Velocity	
Longitudinal.	20.6 ft/s (6.3 m/s)
Lateral	3.8 ft/s (1.2 m/s)
Occupant Ridedown Accelerations	
Longitudinal.	-6.1 g
Lateral	-0.5 g

FIGURE 25. Summary of Test 2453-1

FIGURE 26. Vehicle after Test 2453-1

FIGURE 27. Low Speed Crash Cushion After Test 2453 in Damaged and Restored Position

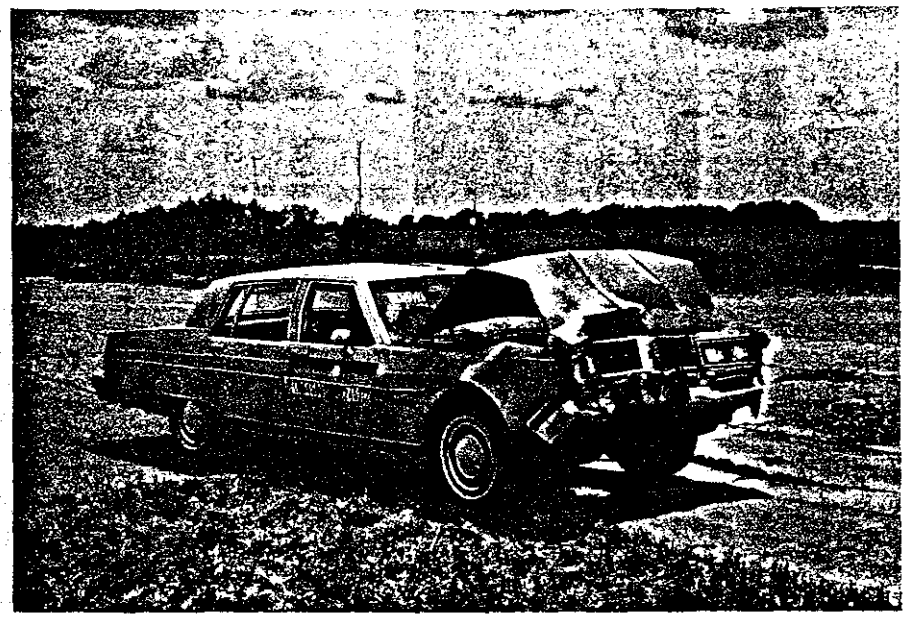

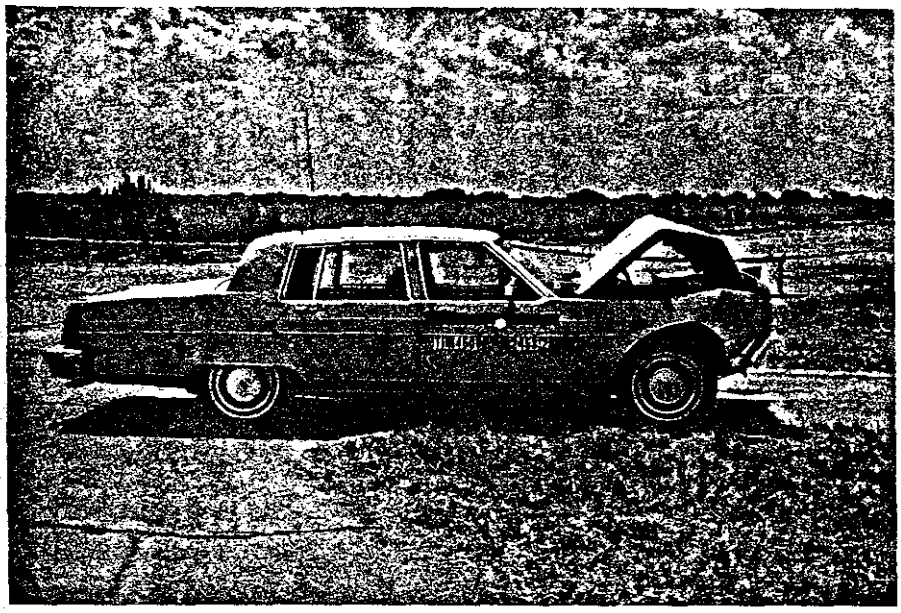

FIGURE 28. Vehicle After Test 2453-2

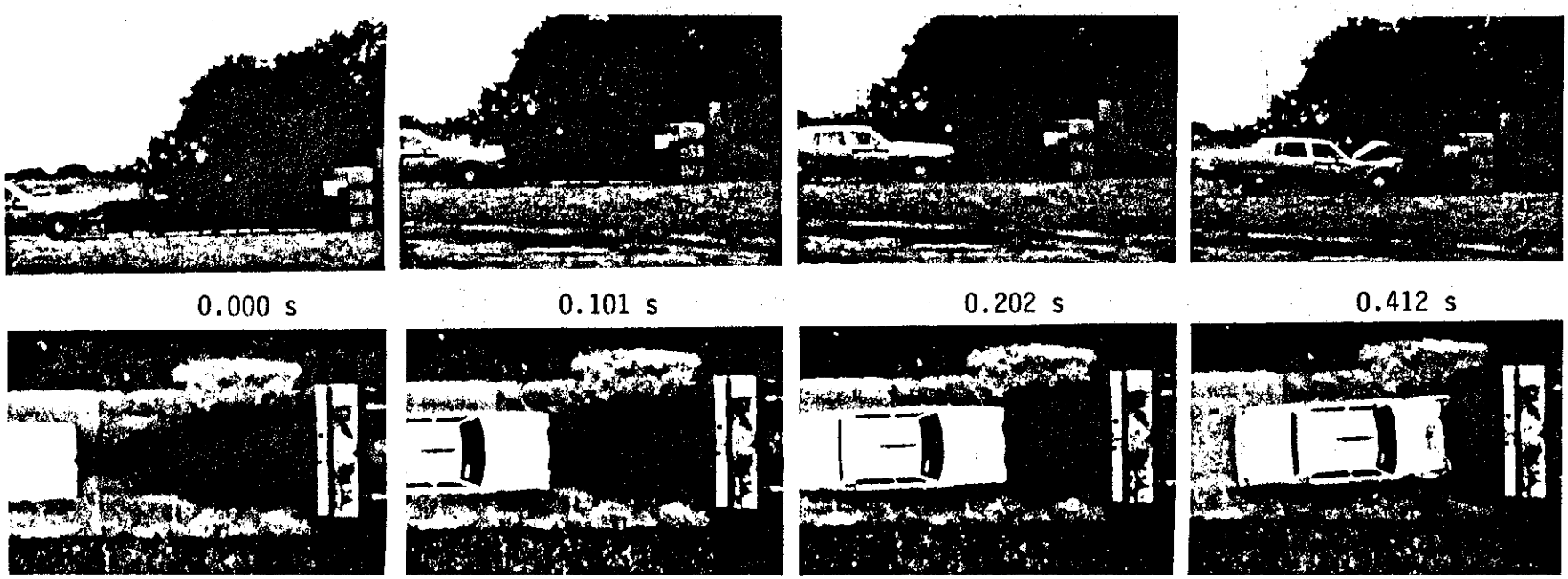

Test No.	2453-2
Date	08/24/88
Test Installation.	Clustered Rubber Cylinders
Length of Installation	20 ft (6 m)
Vehicle.	1981 Oldsmobile Regency
Vehicle Weight	
Test Inertia	4,500 lb (2,043 kg)
Vehicle Damage Classification	
TAD	12FD3
CAD	12FDEW2
Maximum Vehicle Crush	12.0 in (30.5 cm)
Max. Dyn. Deflection	14.0 ft (4.3 m)
Max. Perm. Deformation	5.3 ft (1.6 m)

Impact Speed.	47.9 mi/h (77.1 km/h)
Impact Angle.	0 deg
Time to Stop.	0.414 seconds
Vehicle Accelerations (Max. 0.050-sec Avg)	
Longitudinal.	-11.9 g
Lateral	-0.7 g
Occupant Impact Velocity	
Longitudinal.	27.6 ft/s (8.4 m/s)
Lateral	3.8 ft/s (1.2 m/s)
Occupant Ridedown Accelerations	
Longitudinal.	-17.6 g
Lateral	-0.6 g

FIGURE 29. Summary of Test 2453-2

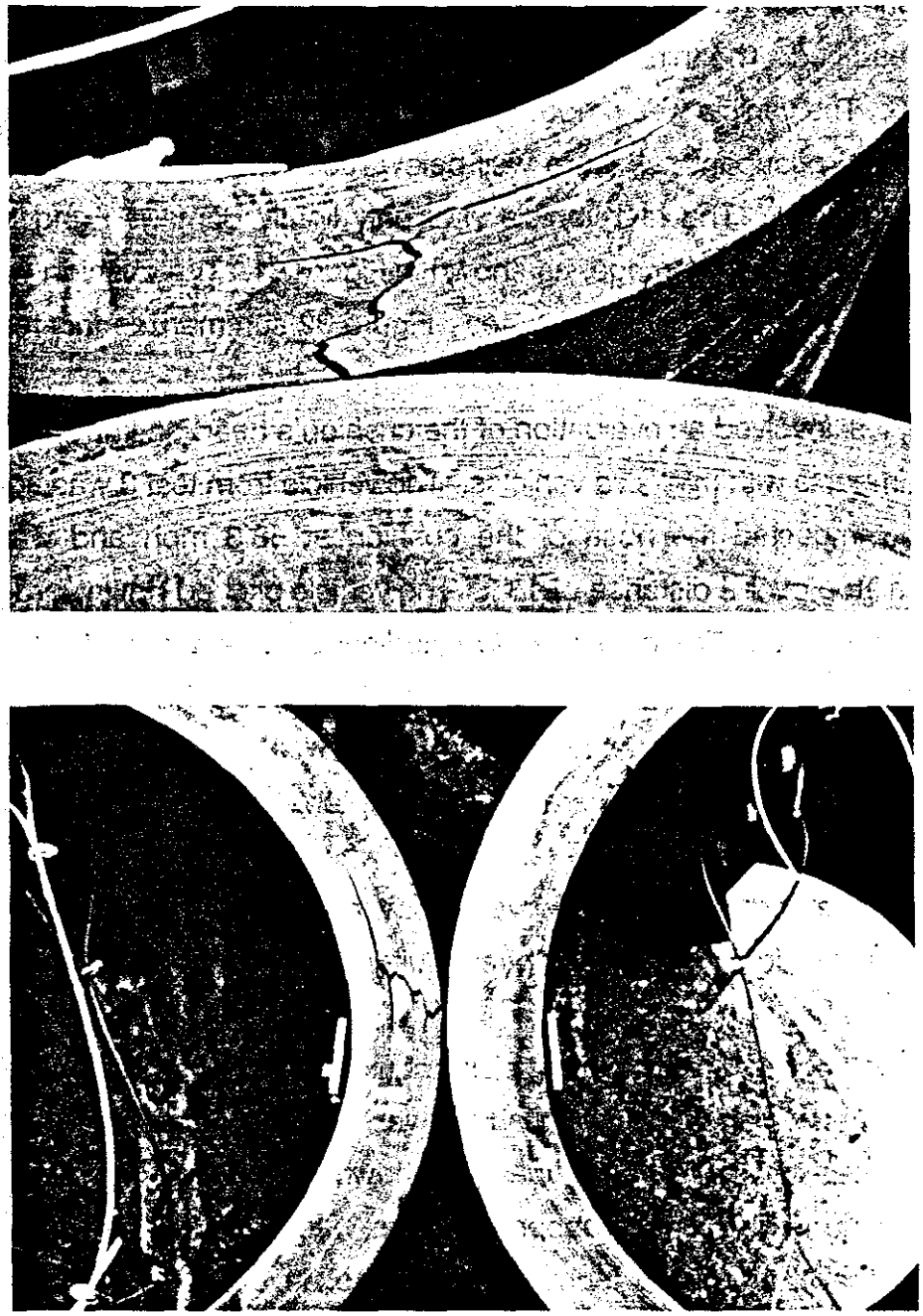

FIGURE 30. Damaged Cylinders After Test 2453-2

create large diameter and thick-walled components and that the problem can be totally eliminated by compression molding the rubber components.

Test 2453-3

The cushion was repaired by replacing several cracked cylinders and the test program was resumed. The third test involved an 1,800 lb vehicle impacting the cushion head-on at 24.6. The vehicle was smoothly decelerated to a stop over a distance of 7.6 ft. All measures of occupant risk were well below recommended limits established by NCHRP Report 230 (6). The test vehicle was only lightly damaged and the cushion exhibited no further signs of damage, as shown in Figure 31. The cushion was restored to its original position in less than 30 minutes. Figure 32 summarizes this test.

Test 2453-4

The final test involved an evaluation of the cushion's head-on impact performance for high speed impacts with mini-size vehicles. The vehicle from test 3 was again reused. The test vehicle impacted the nose of the cushion at 58.3 mph and was smoothly decelerated to a stop over a distance of 13 ft. The vehicle pitched downward and yawed slightly during the impact. The measured longitudinal occupant impact velocity of 32.6 ft/sec was slightly above the recommended limit of 30 ft/sec, but was well below the maximum allowable limit of 40 ft/sec recommended by NCRHP Report 230 (6). All other measures of cushion performance were within acceptable limits and, therefore, the test was considered quite successful. The test vehicle was only lightly damaged, as shown in Figure 33. However, cracks were observed in several more of the rubber cylinders and restoration of the cushion would have been quite costly. A summary of the test is presented in Figure 34.

Even though a number of rubber elements were damaged during some of the tests, the safety performance of the cushion was up to expectations. Test results compared quite well with predicted values as shown in Table 11. Thus, although a problem with the durability of the rubber cylinders was encountered, full-scale crash testing indicated that the analysis techniques used to develop the low speed cushion design led to a product that was capable of meeting established safety criteria (6). Further, problems associated with the cracking of rubber cylinder, energy-absorbing components are believed to be attributable to the manufacturing process.

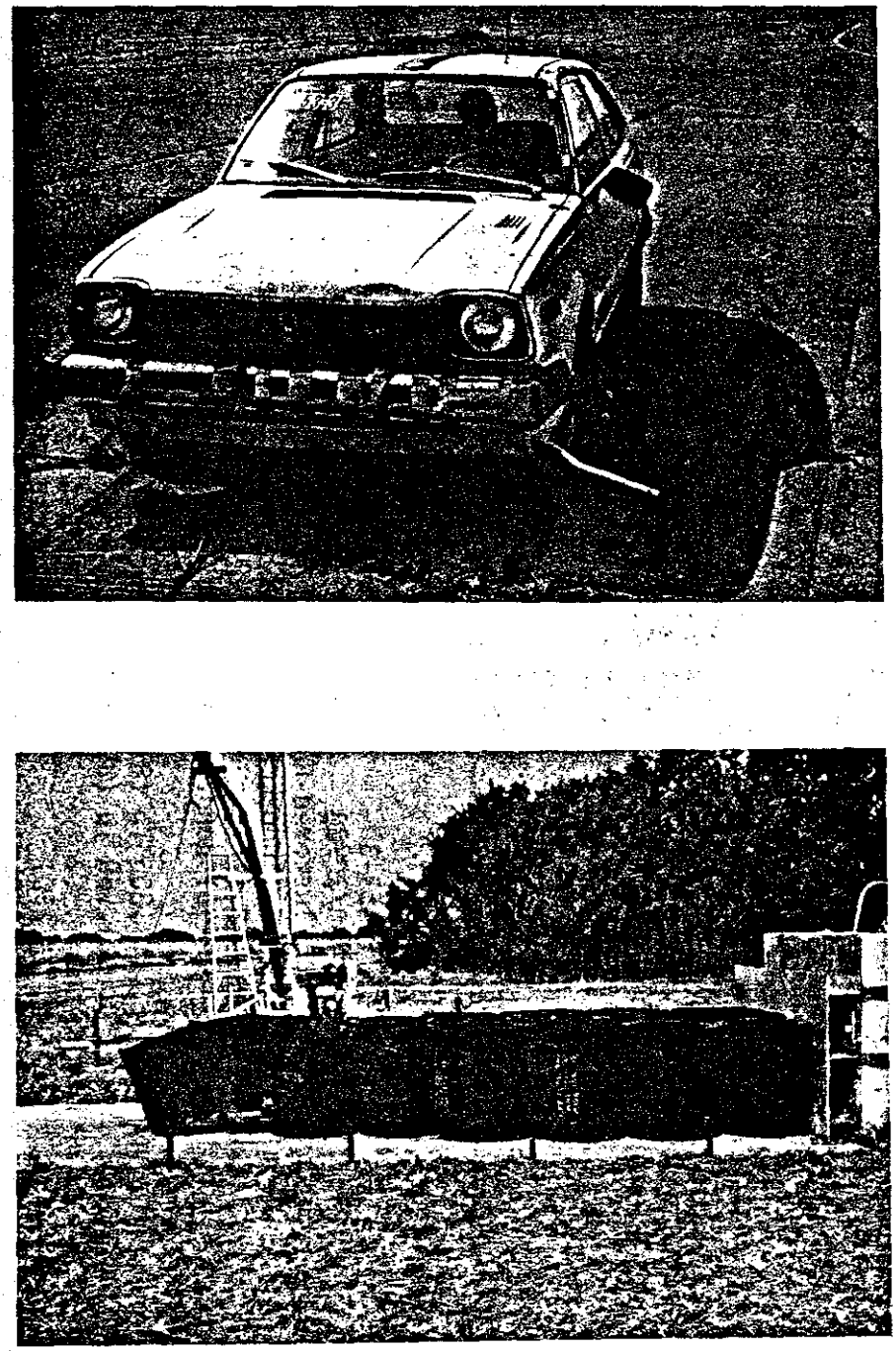

FIGURE 31. Test Vehicle and Cushion After Test 2453-3

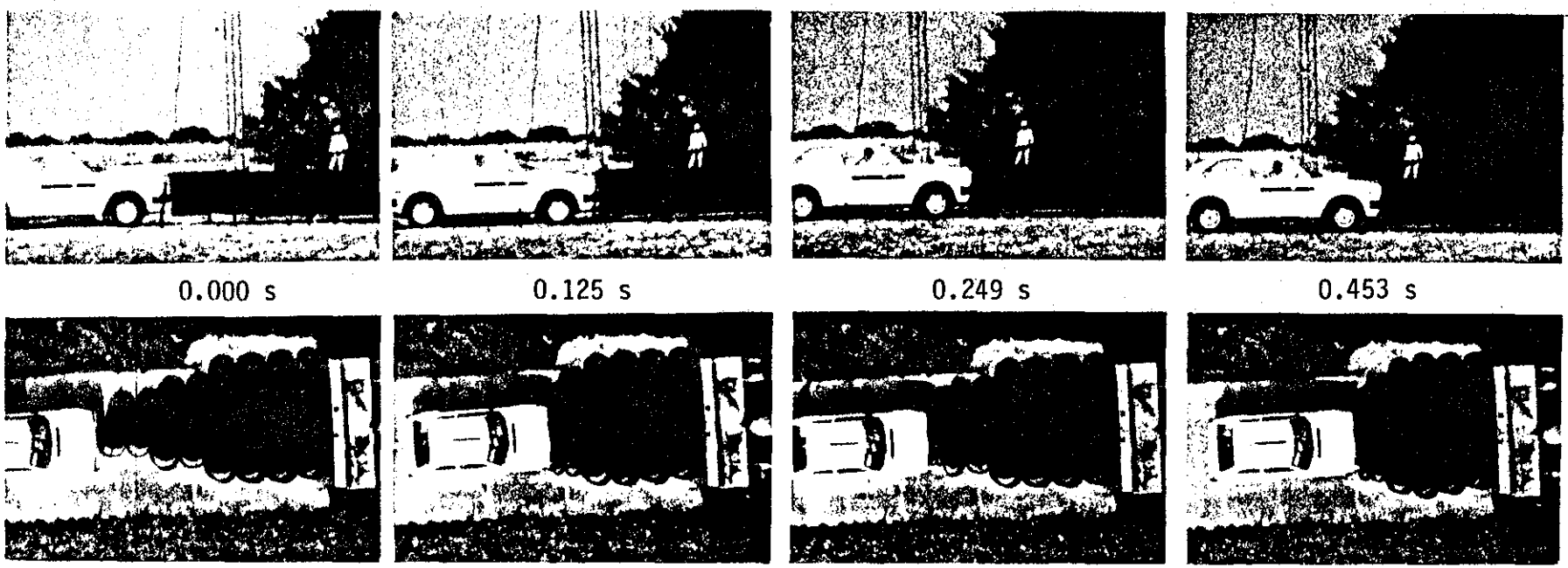

Test No.	2453-3
Date	08/30/88
Test Installation	Clustered Rubber Cylinders
Length of Installation	20 ft (6 m)
Vehicle	1981 Honda Civic
Vehicle Weight	
Test Inertia	1,800 lb (817 kg)
Gross Static	1,969 lb (894 kg)
Vehicle Damage Classification	
TAD	12FD1
CAD	12FDLW1
Maximum Vehicle Crush	2.5 in (6.4 cm)
Max. Dyn. Deflection	7.6 ft (2.3 m)
Max. Perm. Deformation	2.3 ft (0.7 m)
Impact Speed	24.6 mi/h (39.6 km/h)
Impact Angle	0 deg
Time to Stop	0.453 seconds
Vehicle Accelerations (Max. 0.050-sec Avg)	
Longitudinal	-5.1 g
Lateral	-0.5 g
Occupant Impact Velocity	
Longitudinal	19.3 ft/s (5.9 m/s)
Lateral	4.3 ft/s (1.3 m/s)
Occupant Ridedown Accelerations	
Longitudinal	-5.8 g
Lateral	-0.7 g

FIGURE 32. Summary of Test 2453-3

FIGURE 33. Test Vehicle and Cushion After Test 2453-4

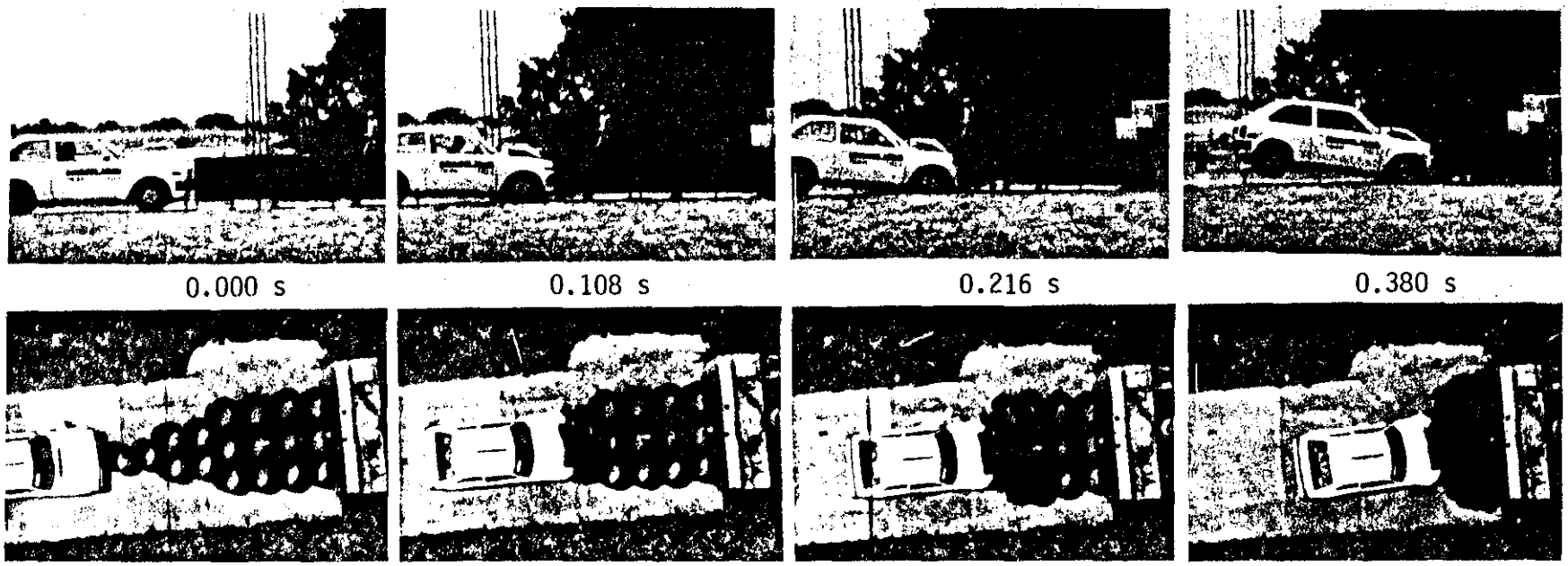

Test No.	2453-4
Date	08/30/88
Test Installation	Clustered Rubber Cylinders
Length of Installation	20 ft (6 m)
Vehicle	1981 Honda Civic
Vehicle Weight	
Test Inertia	1,800 lb (817 kg)
Gross Static	1,969 lb (894 kg)
Vehicle Damage Classification	
TAD	12FD3
CAD	12FDEW2
Maximum Vehicle Crush	10.0 in (25.4 cm)
Max. Dyn. Deflection	13.0 ft (4.0 m)
Max. Perm. Deformation	0.9 ft (0.3 m)
Impact Speed	58.3 mi/h (93.8 km/h)
Impact Angle	0 deg
Time to Stop	0.380 seconds
Vehicle Accelerations (Max. 0.050-sec Avg)	
Longitudinal	-11.5 g
Lateral	0.9 g
Occupant Impact Velocity	
Longitudinal	32.6 ft/s (9.9 m/s)
Lateral	1.2 ft/s (0.4 m/s)
Occupant Ridedown Accelerations	
Longitudinal	-10.8 g
Lateral	0.4 g

FIGURE 34. Summary of Test 2453-4

TABLE 11. MEASURED AND PREDICTED LOW SPEED CUSHION PERFORMANCE

VEHICLE WEIGHT (LB)	IMPACT VELOCITY (MPH)	LONGITUDINAL OCCUPANT IMPACT VELOCITY (FT/SEC)		STOPPING DISTANCE (FT)	
		PREDICTED	MEASURED	PREDICTED	MEASURED
1,800	24.6	16.8	19.3	7.7	7.6
1,800	45.0	27.7	N/A	11.6	N/A
1,800	58.3	30.8	32.6	12.3	13.0
4,500	31.2	19.3	20.6	12.2	13.6
4,500	45.0	27.3	N/A	15.8	N/A
4,500	47.9	28.4	27.6	16.2	16.7

ECONOMIC FEASIBILITY

Although research efforts described herein indicate that a low maintenance rubber crash cushion should be techniquely feasible, the system must offer some economic advantages if it is to become a cost-effective alternative to existing crash cushion designs. An economic evaluation of the high performance crash cushion design was therefore undertaken to detemine the overall feasibility of low-maintenance crash cushion systems. The steel drum crash cushion is more widely used across Texas than another conventional system and was selected as a basis for comparison against the rubber system.

Site requirements for these two systems are very similar--both should be installed on paved surfaces with rigid backstops. Therefore, cost estimates for each system do not include site preparation. Initial and maintenance costs for the steel drum crash cushion were estimated by surveying SDHPT district maintenance engineers. The initial cost of the steel drum system for freeway applications was estimated to be approximately $2,000, and repair records for several of these crash cushions deployed in Houston are shown in Table 12. A present worth analysis of this system based on an initial cost of $2,000, an annual repair cost of $5,325 (five impacts per year), a cushion life of 20 years, and a discount rate of 4 percent indicated that the present value of a steel drum system at one of the locations shown in Table 12 is approximately $74,000.

Initial and maintenance costs for the low maintenance rubber cushion were estimated as shown below:

Rubber cost = 4,470 lb @ $1.80/lb	= $8,046
Steel Components	= $2,000
Installation	= $1,000
Total	= $11,046

After impact of the rubber crash cushion, the cushion should only require restoration to its original position. The cushion required less than one hour for restoration after crash tests in which no rubber cylinders were damaged. The cost of a four-man repair crew for one hour at a freeway site should be less than $200. The total annual cost of a rubber system at one of the high impact locations described above would be approximately $1,000. The present worth of such a system based on a 20-year design life and a 4%

Table 12. Crash Cushion Repair Costs at High Impact Frequency Sites in Houston

Location	Times impacted in last 12 month period	Average Cost to repair
# 2 - West Loop 610, North bound at U.S. 59	6	$ 1,177.00
#13 - West Loop 610, South bound at Post Oak Blvd.	8	$ 1,095.00
#23 - U.S. 59, South bound at I.H. 45	5	$ 923.00
#52 - U.S. 59, North bound at Richmond Ave.	4	$ 1,014.00
Averages	5.75	$ 1,065.00

discount rate is approximately $25,000. Thus, the low maintenance rubber crash cushion would have a present cost less than 1/3 of that of the steel drum crash cushion at high impact frequency locations. A similar analysis can be conducted for lower impact frequencies to show that the rubber cushion design has a lower present cost than the steel drum system for any site with an average of 0.75 or more impacts per year. Note that although AASHTO recommends a discount rate of 4 percent to represent the real cost of capital for an economic analysis such as described herein (7), some agencies may use higher values. Higher discount rates would tend to reduce the benefits associated with the rubber crash cushion system. For example, a discount rate of 8 percent would raise the number of impacts required each year to justify the use of the low-maintenance rubber cushion to 1.05. Many sites in metropolitan areas have impact frequencies greater than these values. Therefore, the rubber crash cushion system has the potential for greatly reducing total crash cushion costs, and its development should be pursued further.

SUMMARY AND CONCLUSION

Numerous rubber compounds were evaluated through static and dynamic testing over a wide range of temperatures to identify compounds most suitable for use in a low-maintenance crash cushion. A natural rubber-20% EPDM blend was found to be the most cost-effective compound studied. Exhaustive scale model tests indicated that this material has the capacity to dissipate large amounts of energy during impact, has relatively low temperature sensitivity, and is extremely durable.

Scale model tests were also used to evaluate the relative merits of square and round cylinders for use as energy dissipation elements. Although square cylinders were found to be generally more efficient energy dissipators for head-on impacts, their sensitivity to impact direction and poor performance during clustered testing proved to be major disadvantages that made the circular cylinder more attractive for use in highway crash cushions. A limited scale model study indicated that flexible and rigid cylinder-bore stiffeners could improve the efficiency of circular energy dissipation elements by approximately 100 percent. Further evaluation of these methods for enhancing the performance of rubber energy dissipation elements is recommended.

Full-scale tests of rubber attenuation elements verified many of the findings of the scale model tests and results were used to design both a low speed and a high speed, low maintenance rubber crash cushion. Full-scale crash tests of the low speed cushion indicated that it could meet NCHRP Report 230 (6) safety appurtenance performance standards. The testing also revealed that the mandrell wrapping process used to manufacture prototype elements was not adequate for highway crash cushion applications. Many of the prototype elements had visible seams between each layer of the laminated rubber material. Cracks developed in several elements at these seams during high speed impact testing. These seams should not be present if the mandrell wrapping process had been adequate for the manufacture of such large elements. Similar full-scale testing of molded rubber cylinders did not exhibit the cracking phenomenon (3). Therefore, it is believed that compression molding of rubber attenuation elements will eliminate this undesirable behavior. A survey of rubber manufacturers indicated that the only dissadvantage associated with compression molding is the high cost of mold

construction. These manufacturers indicated that the intial cost of a mold for the full-scale rubber elements used in this study would be approximately $20,000.

A study of the economic feasibility of conventional low-maintenance crash cushions indicates that such systems could reduce total crash cushion costs by approximately 66 percent for high accident frequency locations. The analysis also indicated that the low-maintenance crash cushion would be the most cost-effective alternative for any site with impact fequency of 0.85 accidents per year. Element bore stiffeners have demonstrated the potential for significantly improving attenuator element efficiency, which would greatly reduce the initial cost of these crash cushions.

Although the low-maintenance crash cushion designs developed during this study could not be fully tested for compliance with national performance standards (6), this study has demonstrated the technical and economic feasibility of the concept. Therefore, further development of the low-maintenance crash cushion concept is recommended.

REFERENCES

1. Hirsch, T. J., and D. L. Ivey, "Vehicle Impact Attenuation by Modular Crash Cushion," Research Report 146-1, Texas Transportation Institute, Texas A&M University, June, 1969.

2. Fitch Inertial Barrier Systems, 44 School St., Boston, Mass.

3. Sicking, D. L., and H. E. Ross, Jr., "Roadside Concrete Barriers: Warrants and End Treatment," Research Report 346-1F, Texas Transportation Institute, Texas A&M University System, College Station, Texas, September, 1985.

4. Thompson, M. F., "Energy Dissipation Characteristics of Rubber Crash Cushion Elements," Masters Thesis, Texas A&M University, College Station, Texas, Dec. 1988.

5. Sicking, D. L., "Development of Low-Maintenance End Treatment for Concrete Barriers," Masters Thesis, Texas A&M University, College Station, Texas, May 1987.

6. Michie, J. D., "Recommended Procedures for the Safety Performance Evaluation of Highway Appurtenances," National Cooperative Highway Research Program Report 230, March 1981.

7. A Manual on User Benefit Analysis of Highway and Bus-Transit Improvements, American Association of State Highway and Transportation Officials, Washington, D. C., 1978.

APPENDIX A

SEQUENTIAL PHOTOGRAPHS

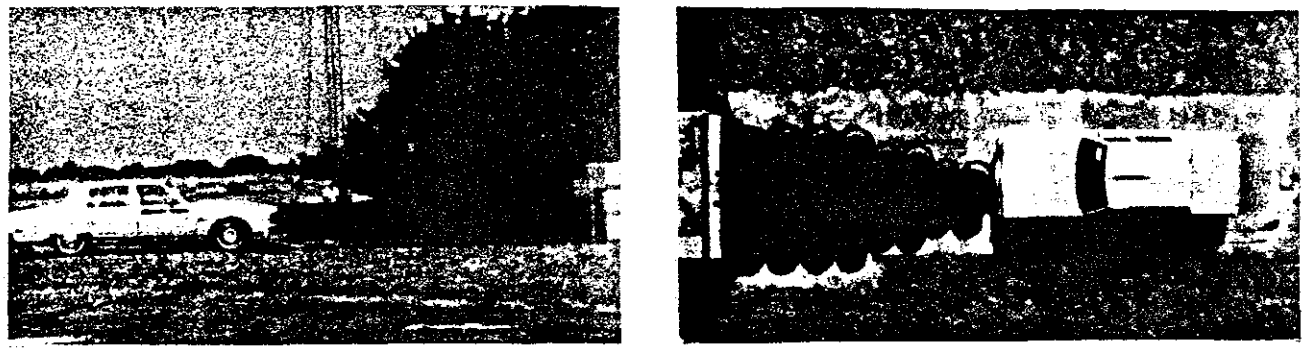

0.000 s

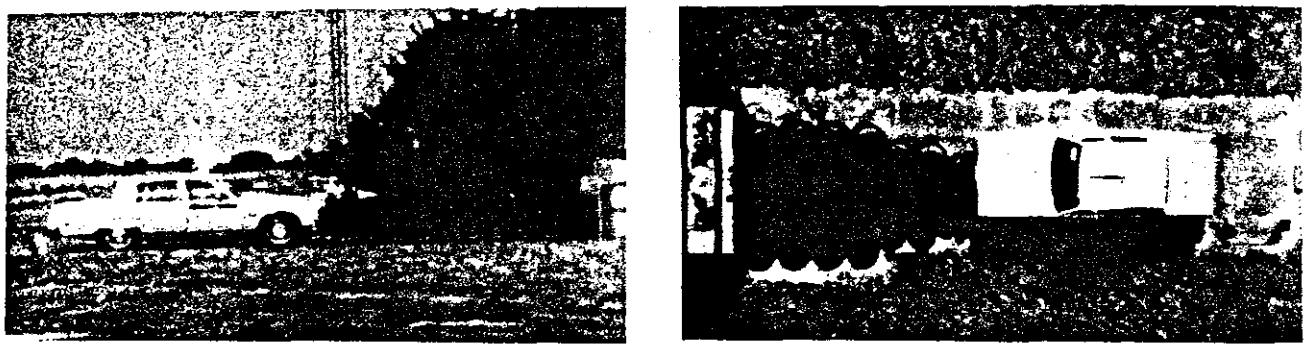

0.063 s

0.126 s

0.189 s

Figure A-1. Sequential photographs for test 2453-1

0.252 s

0.315 s

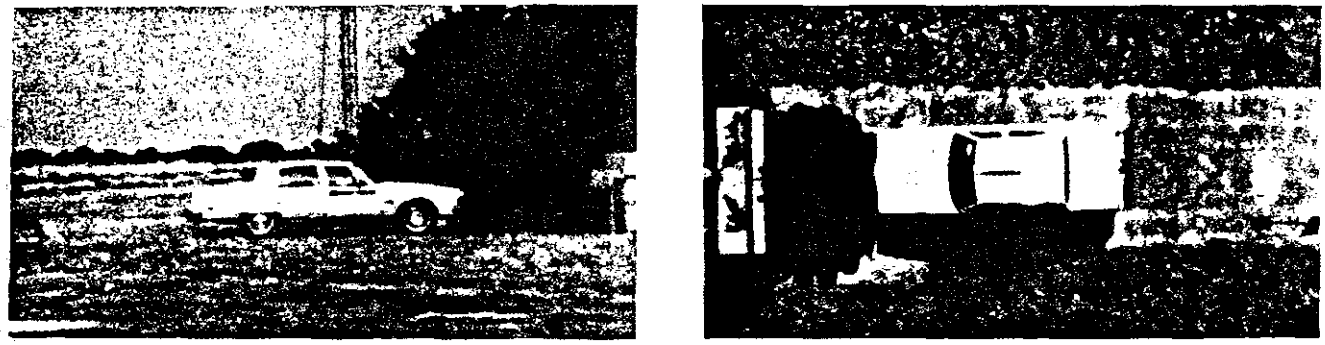

0.378 s

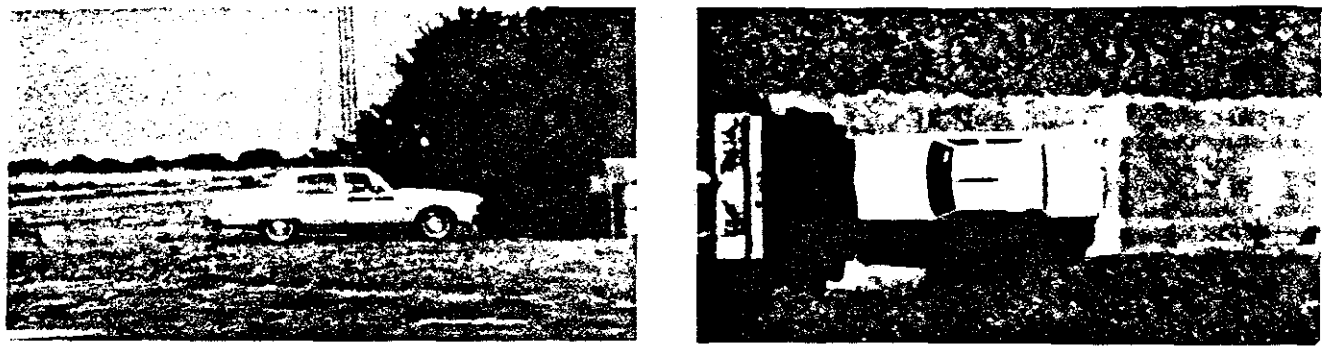

0.501 s

Figure A-1. Sequential photographs for test 2453-1 (Continued)

0.000 s

0.051 s

0.101 s

0.152 s

Figure A-2. Sequential photographs for test 2453-2

0.202 s

0.253 s

0.303 s

0.412 s

Figure A-2. Sequential photographs for test 2453-2 (Continued)

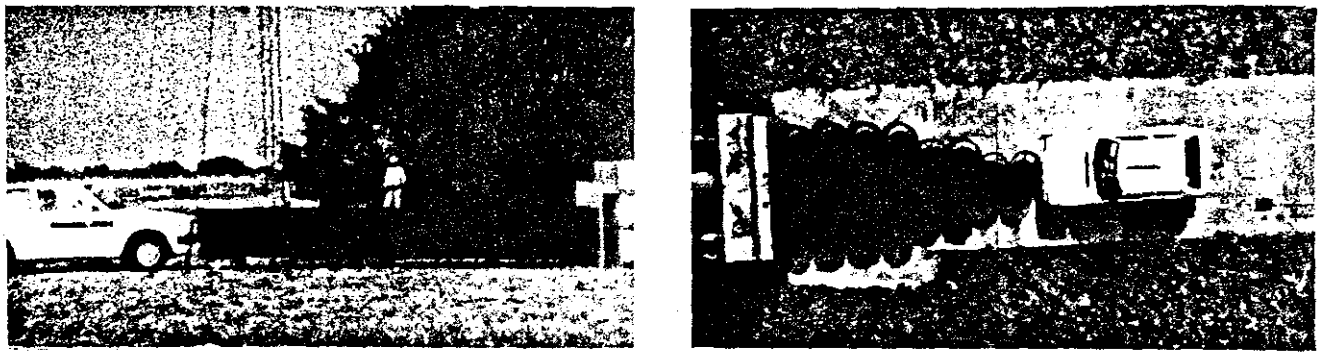

0.000 s

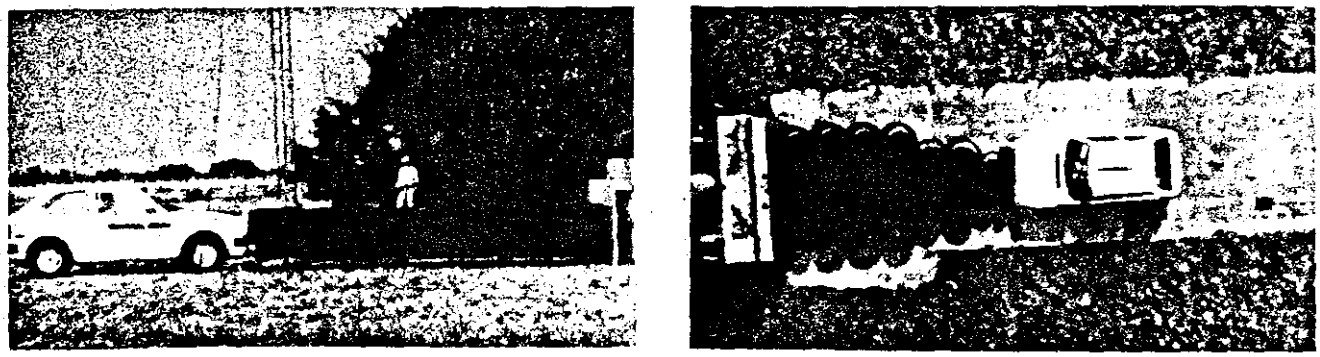

0.062 s

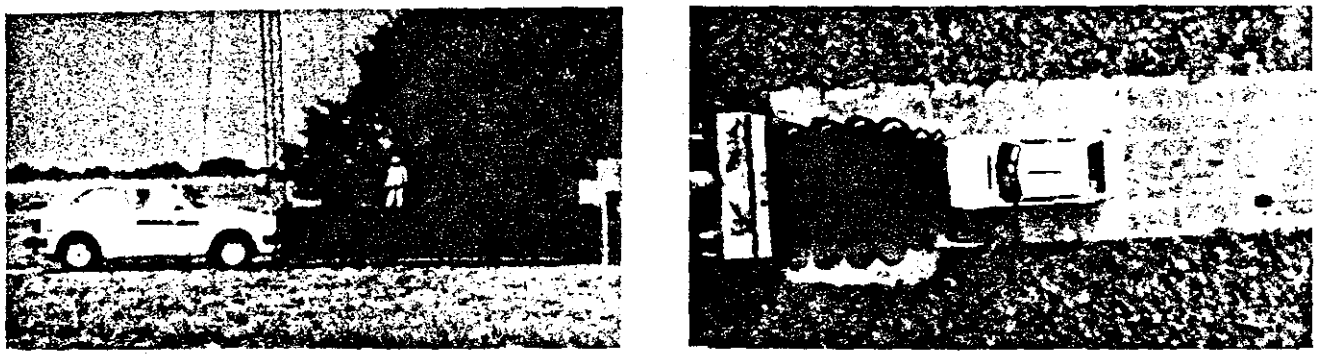

0.125 s

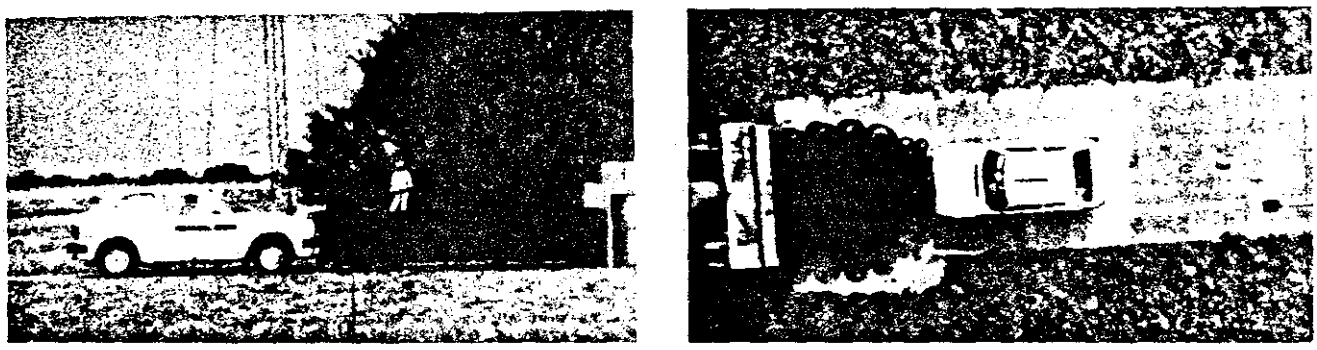

0.187 s

Figure A-3. Sequential photographs for test 2453-3

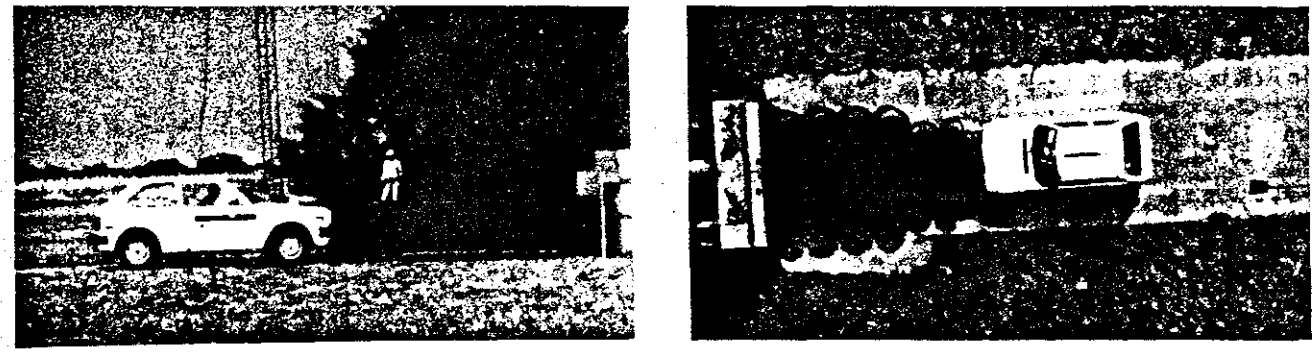

0.249 s

0.311 s

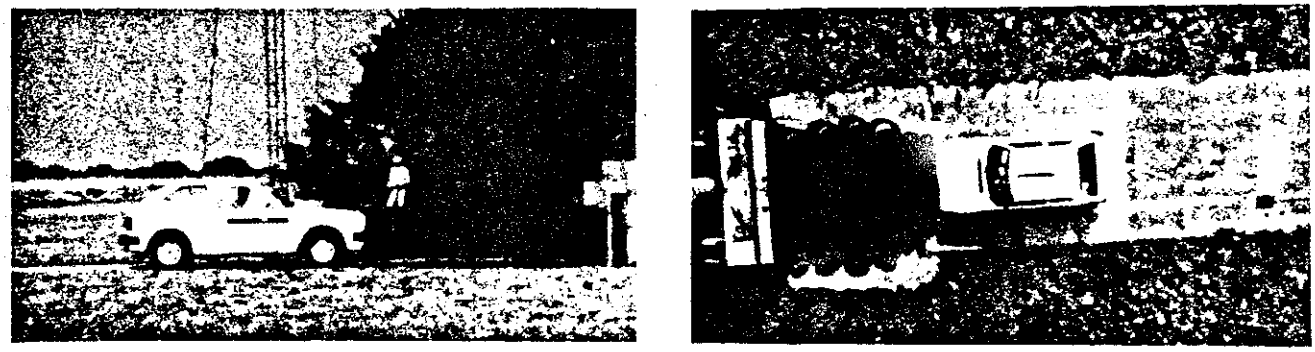

0.374 s

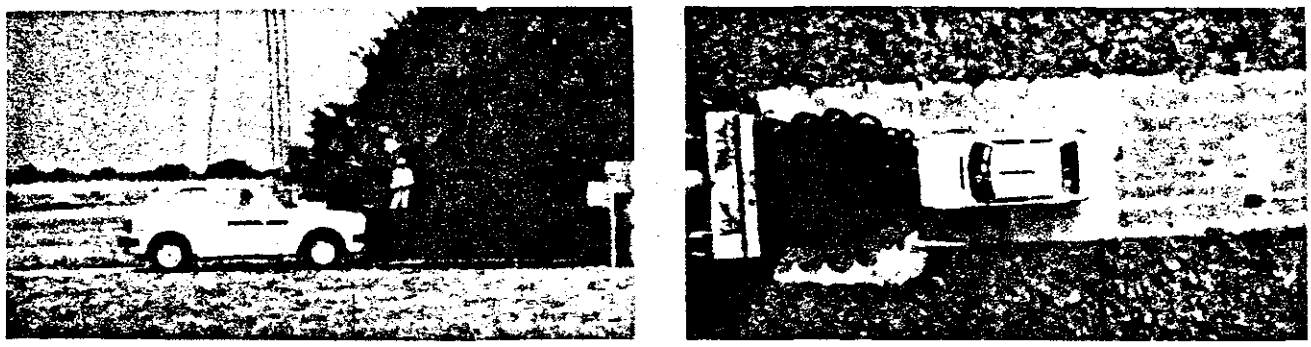

0.453 s

Figure A-3. Sequential photographs for test 2453-3 (Continued)

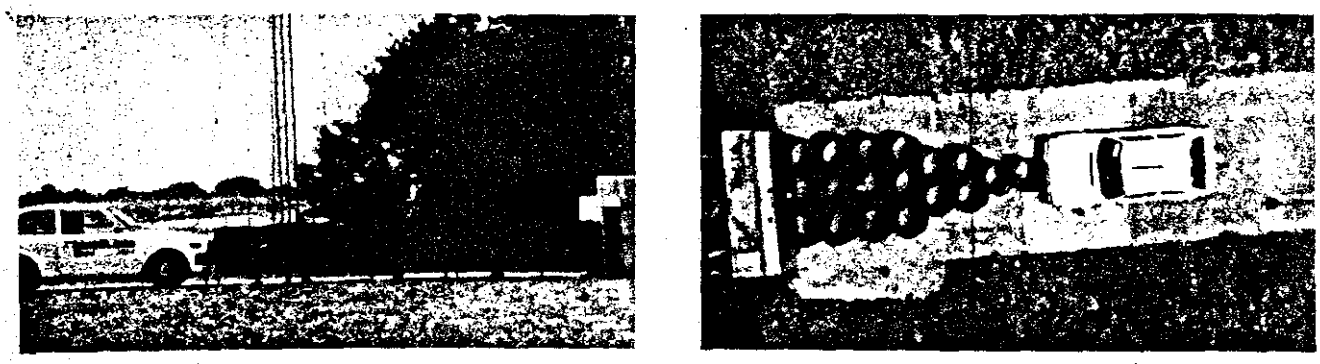

0.000 s

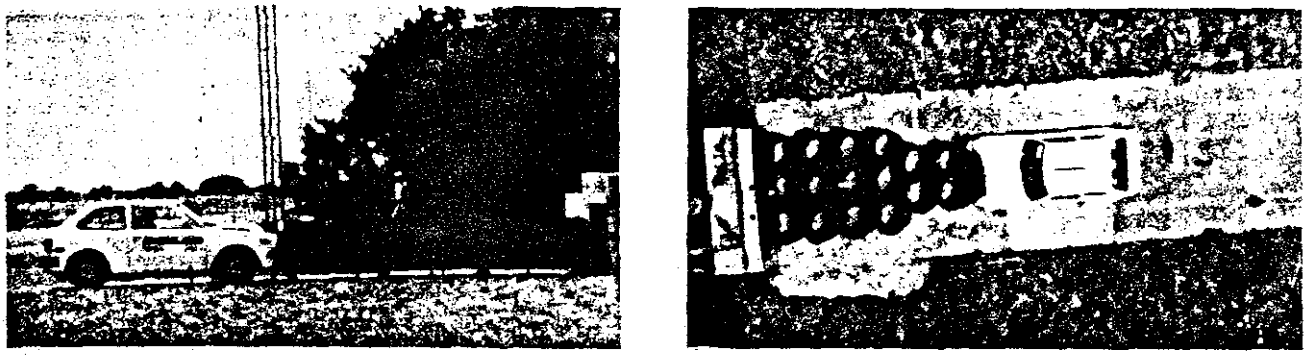

0.054 s

0.108 s

0.162 s

Figure A-4. Sequential photographs for test 2453-4

0.216 s

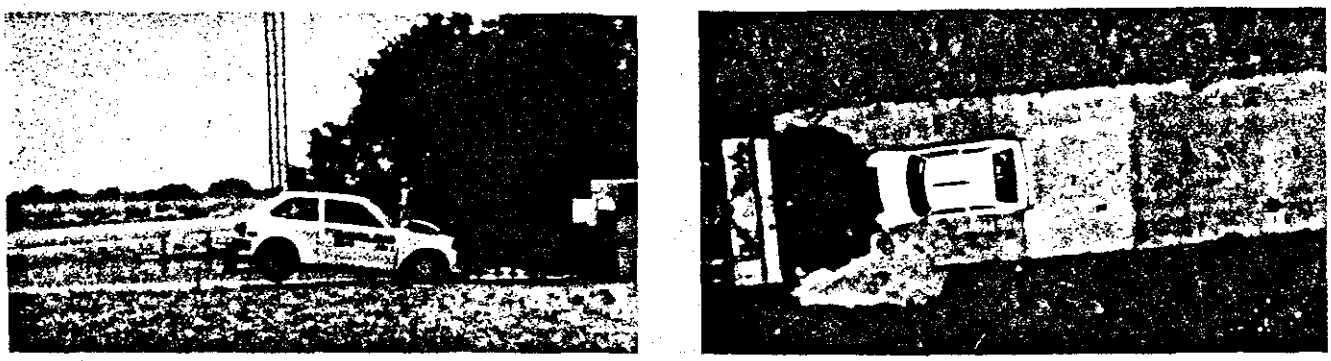

0.269 s

0.323 s

0.380 s

Figure A-4. Sequential photographs for test 2453-4 (Continued)

APPENDIX B

ACCELEROMETER TRACES

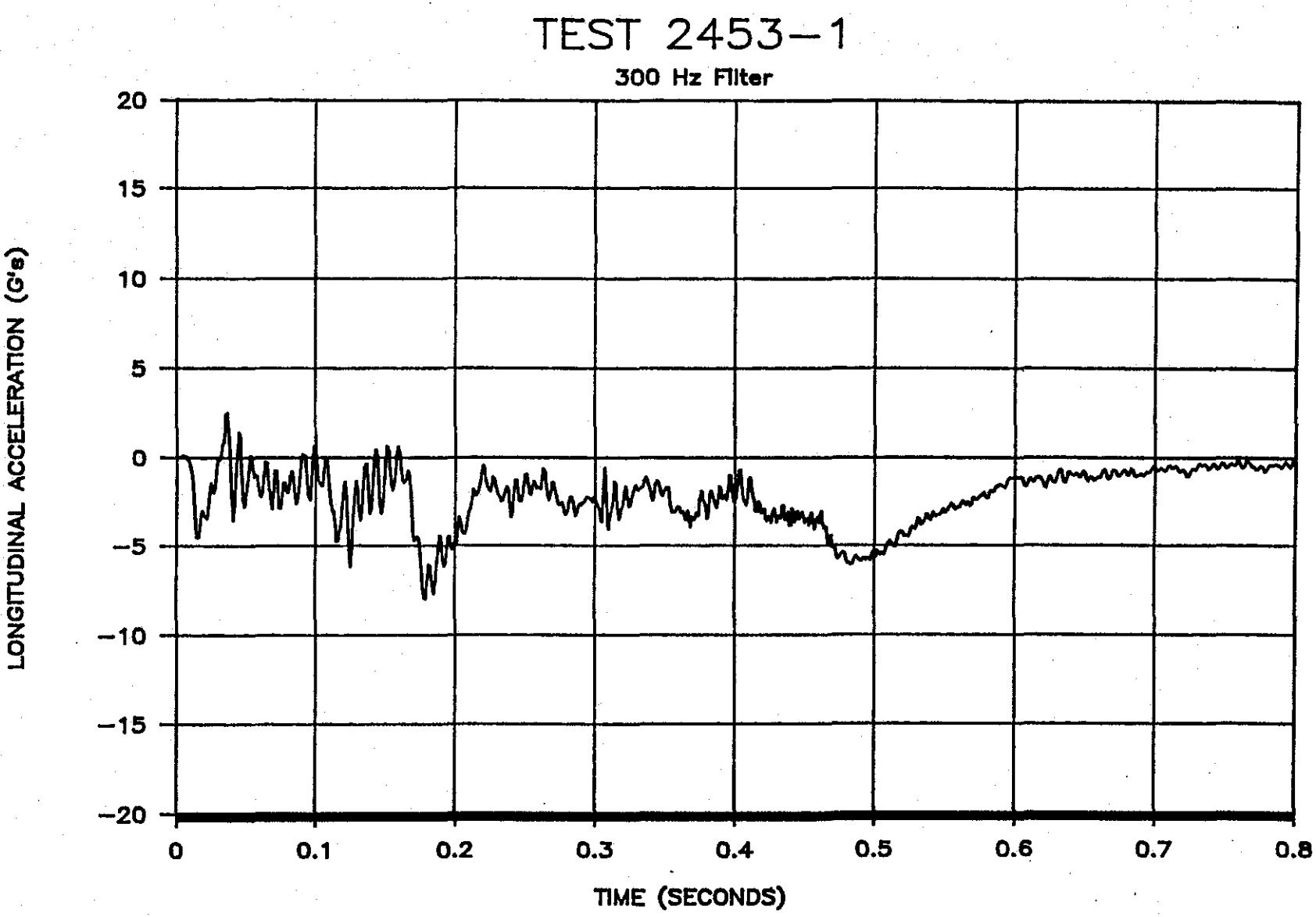

FIGURE B-1. LONGITUDINAL ACCELEROMETER TRACE FROM TEST 2453-1

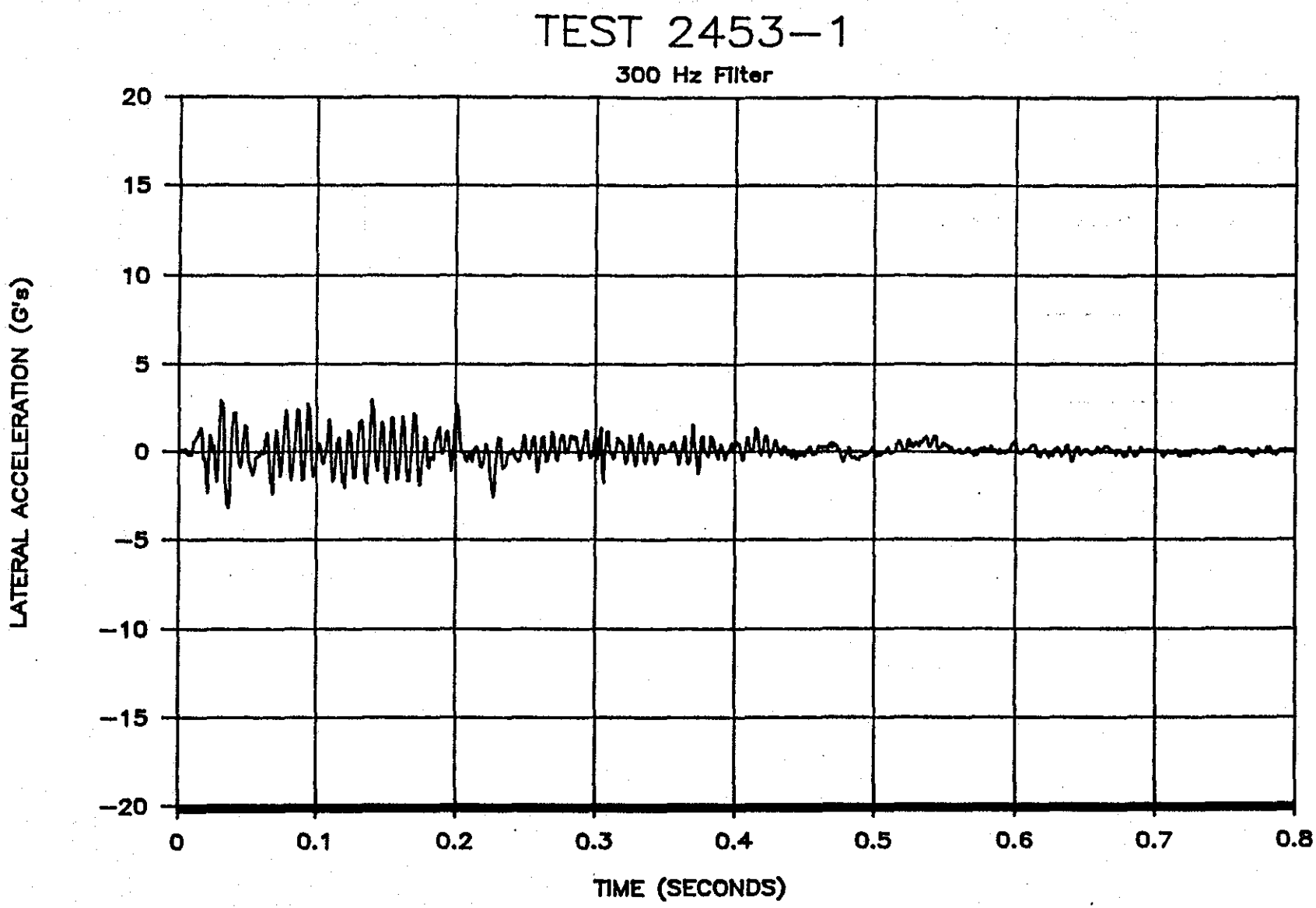

FIGURE B-2. LATERAL ACCELEROMETER TRACE FROM TEST 2453-1

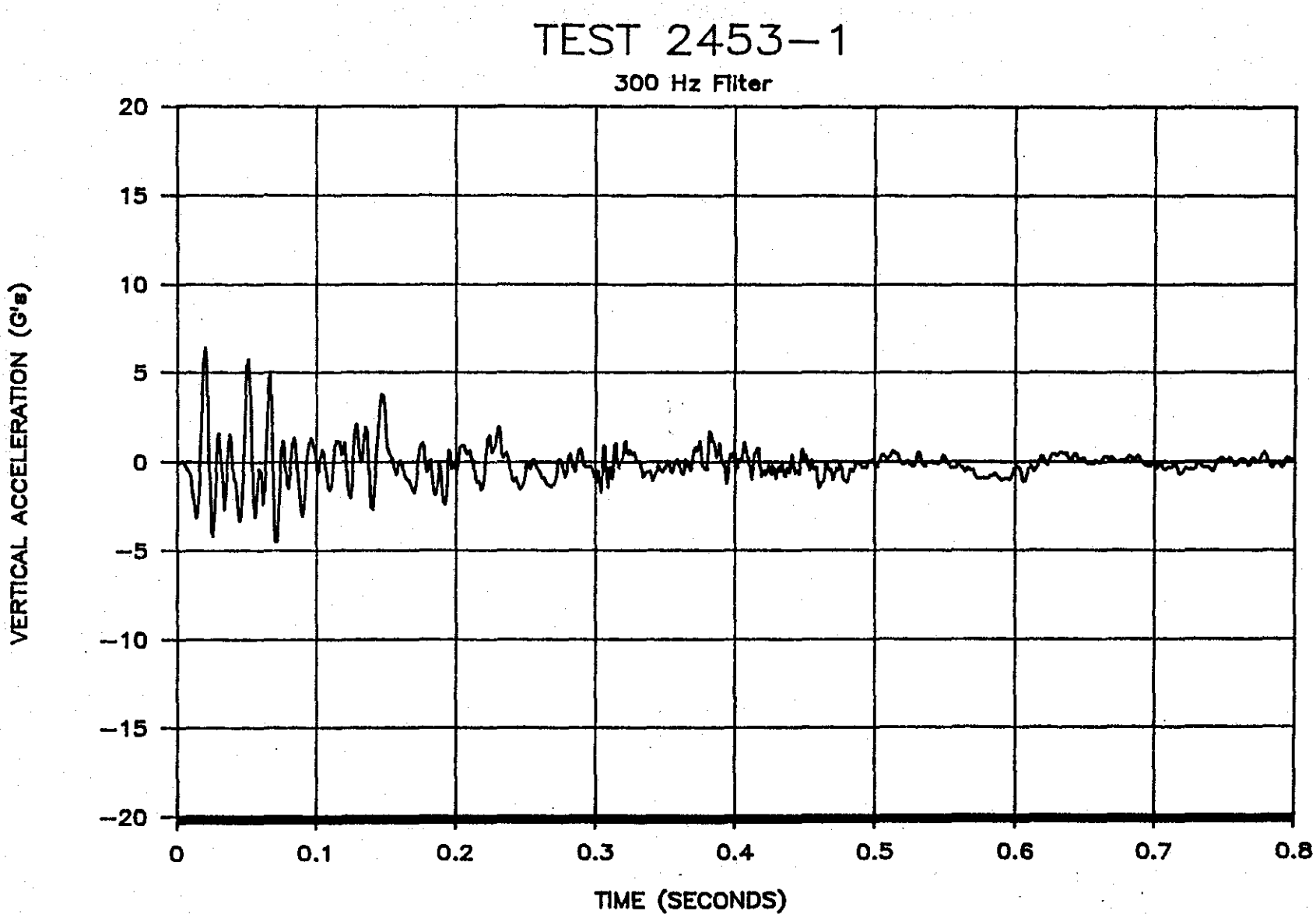

FIGURE B-3. VERTICAL ACCELEROMETER TRACE FROM TEST 2453-1

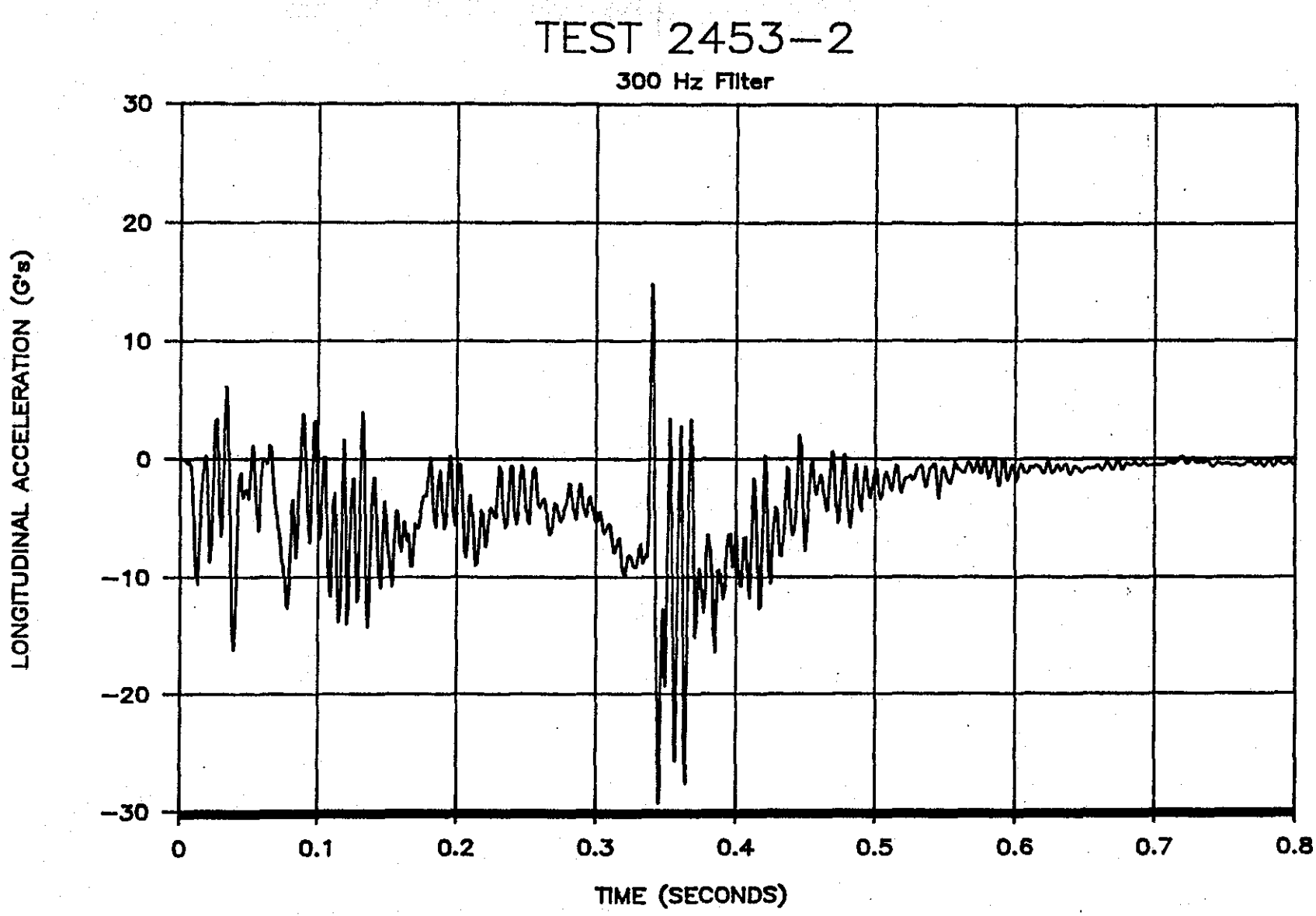

FIGURE B-4. LONGITUDINAL ACCELEROMETER TRACE FROM TEST 2453-2

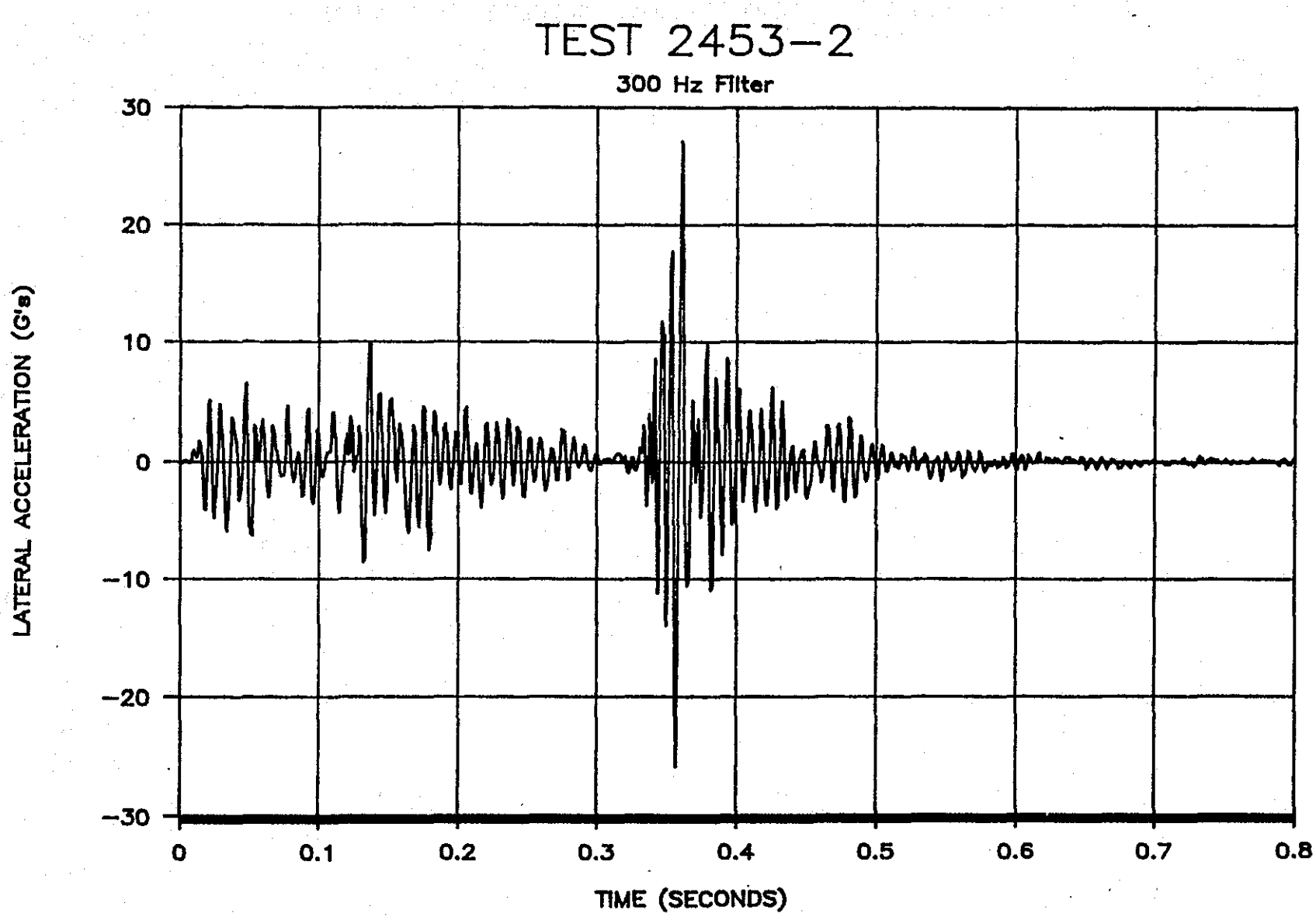

FIGURE B-5. LATERAL ACCELEROMETER TRACE FROM TEST 2453-2

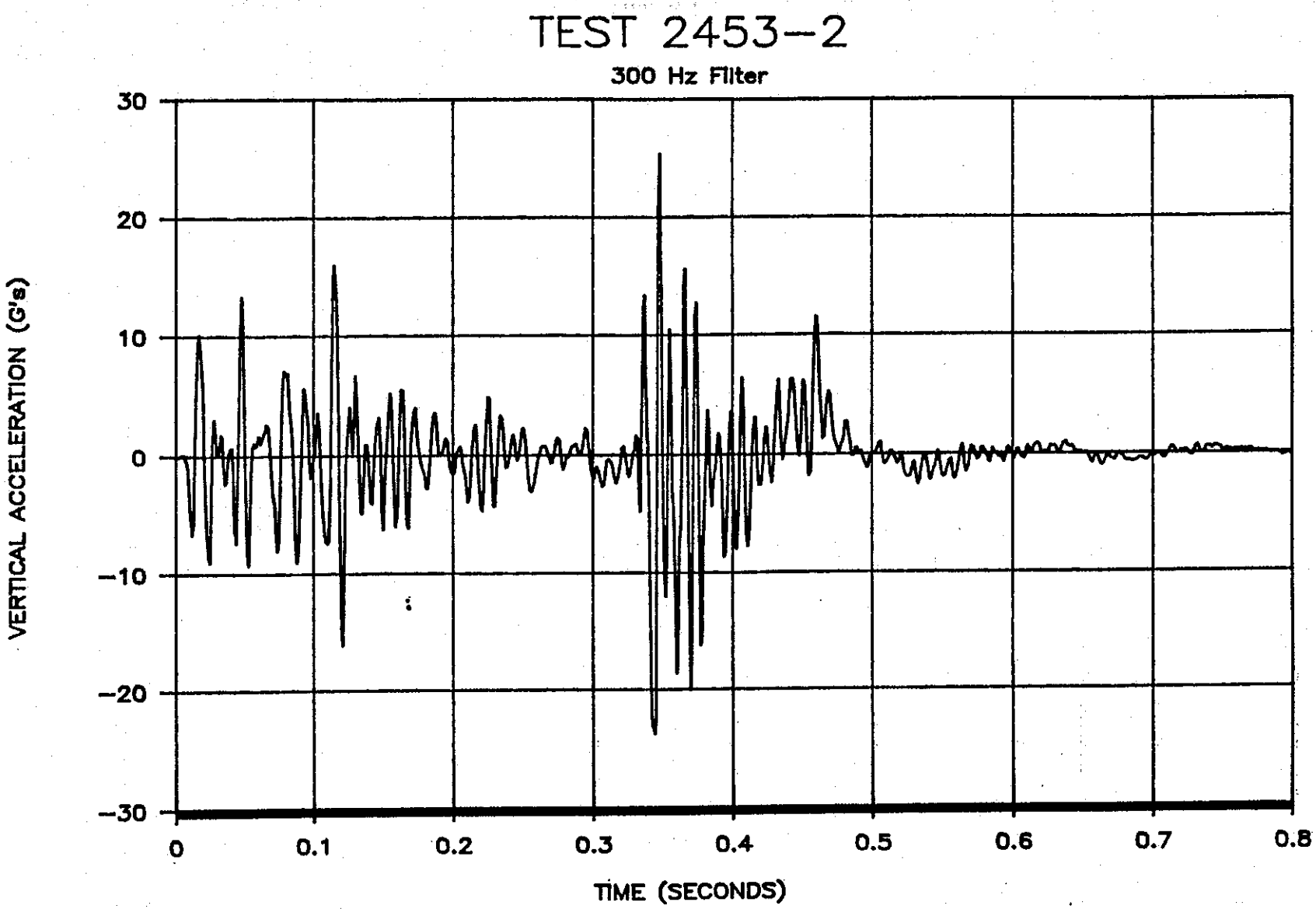

FIGURE B-6. VERTICAL ACCELEROMETER TRACE FROM TEST 2453-2

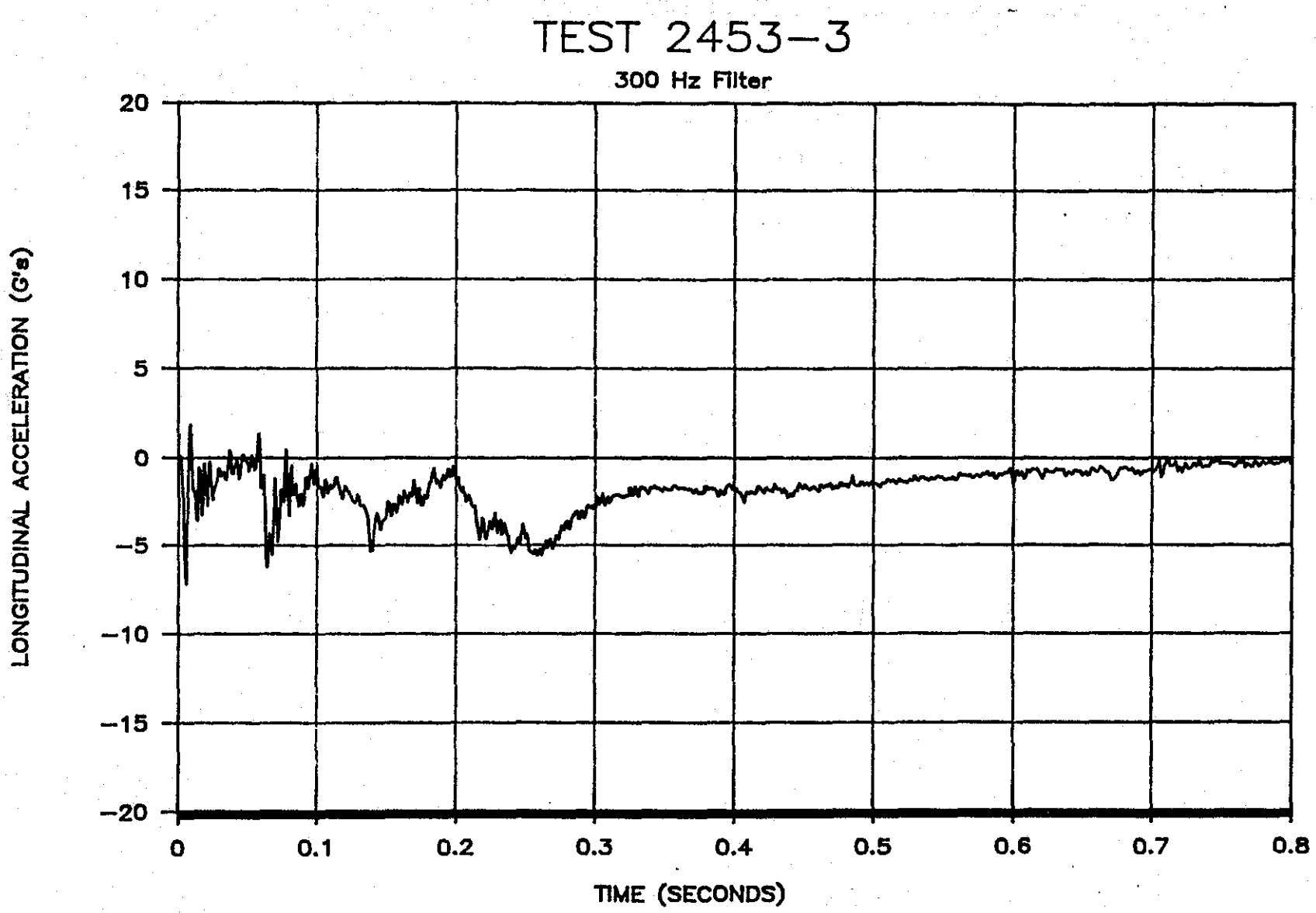

FIGURE B-7. LONGITUDINAL ACCELEROMETER TRACE FROM TEST 2453-3

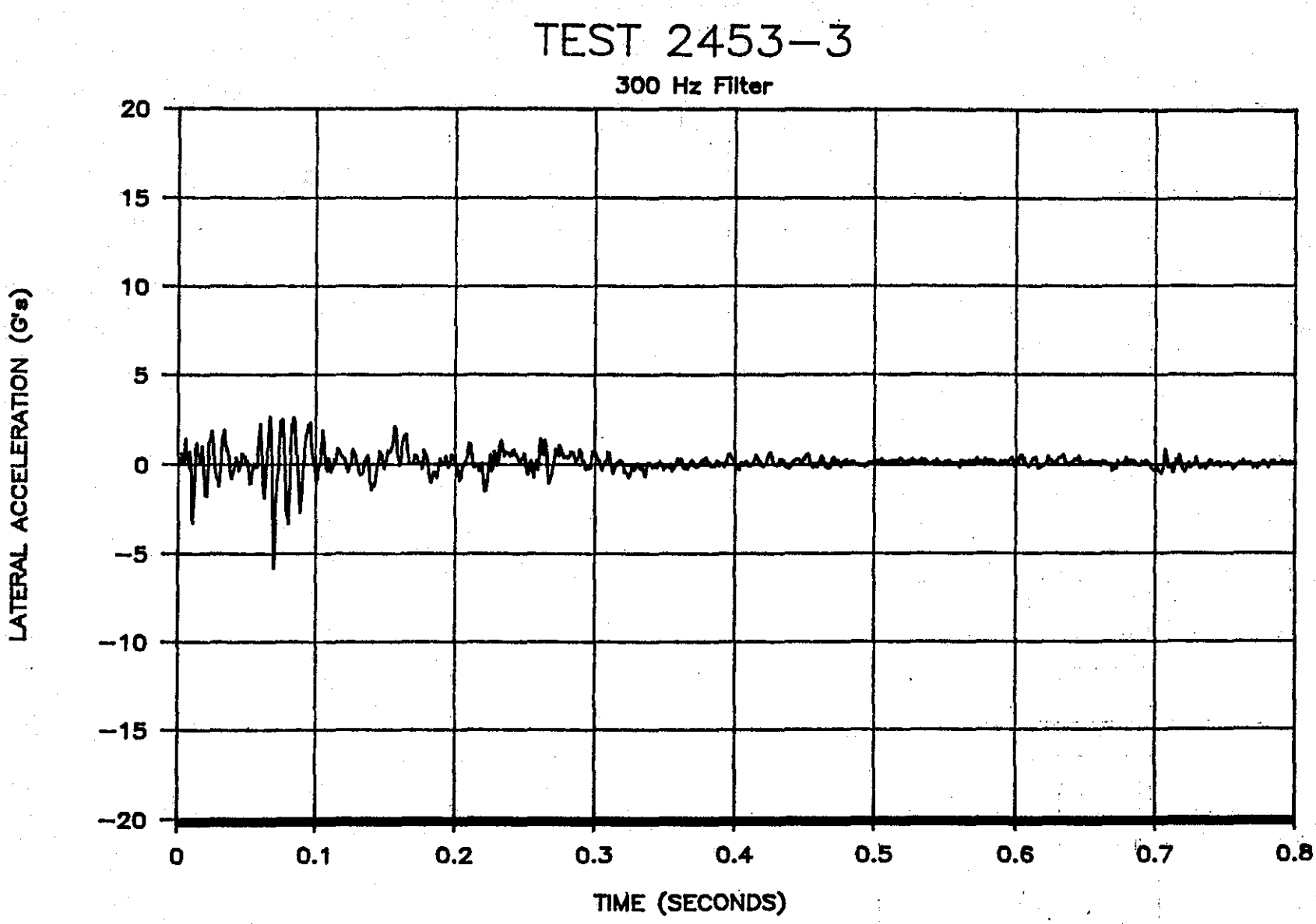

FIGURE B-8. LATERAL ACCELEROMETER TRACE FROM TEST 2453-3

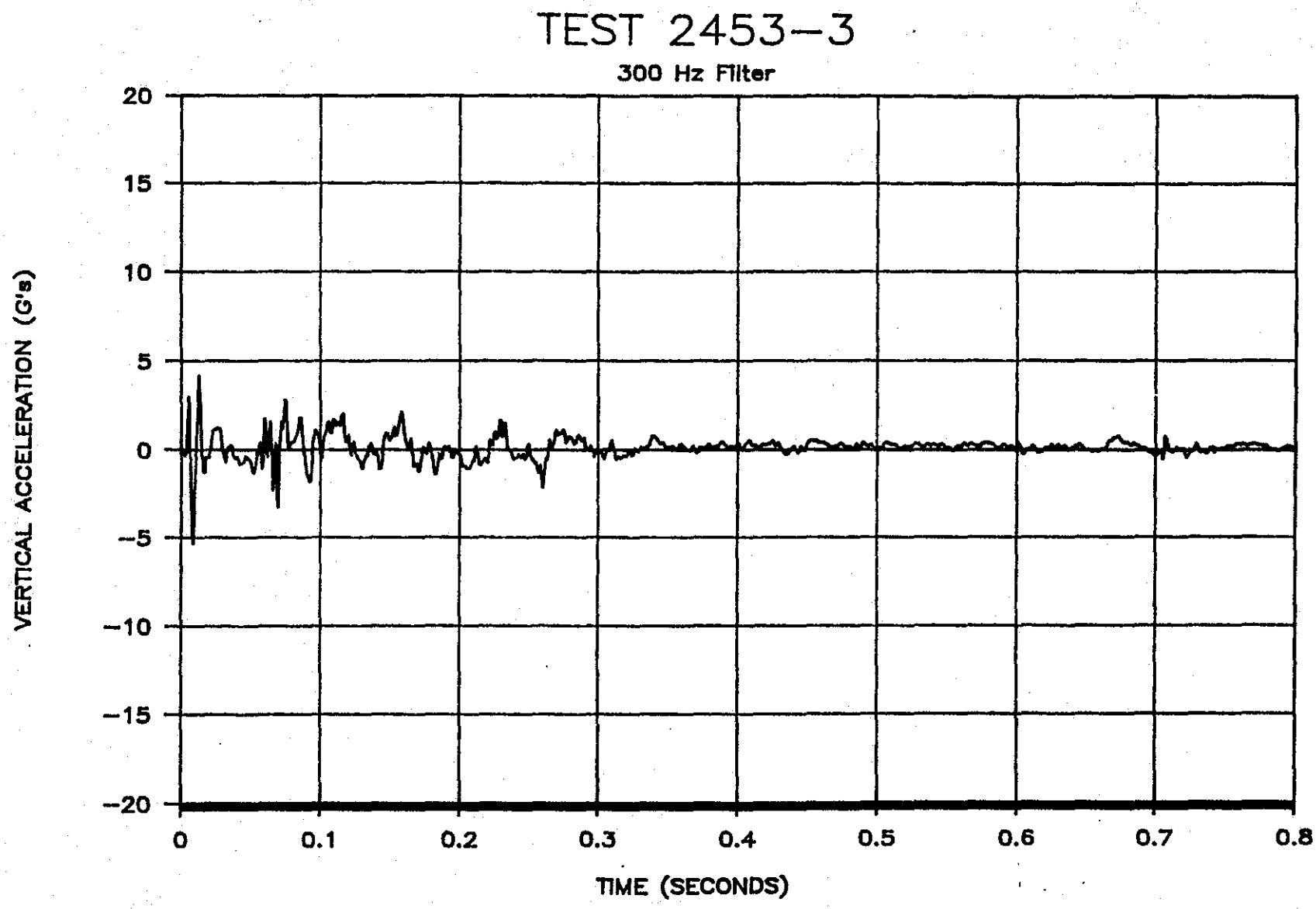

FIGURE B-9. VERTICAL ACCELEROMETER TRACE FROM 2453-3

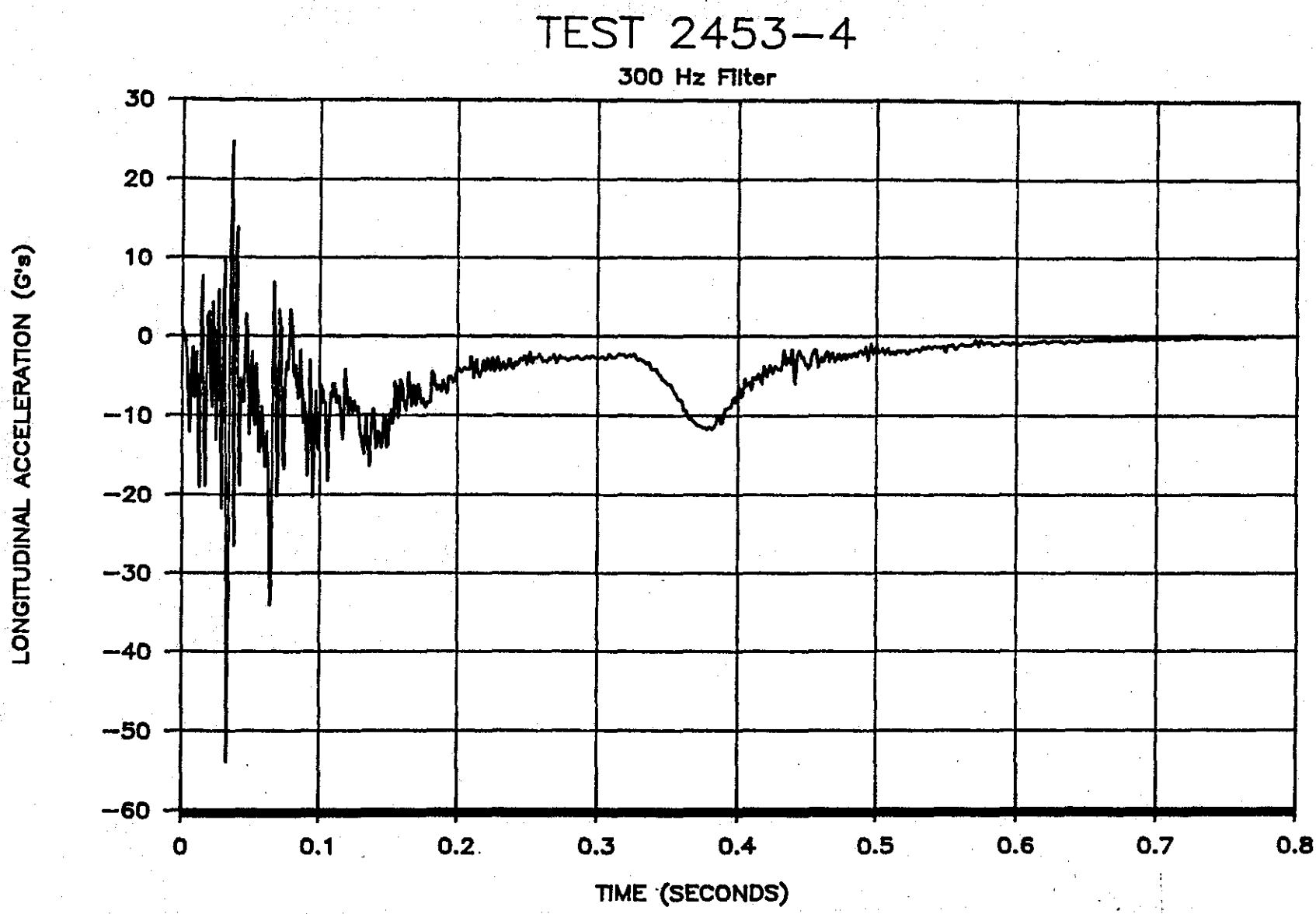

FIGURE B-10. LONGITUDINAL ACCELEROMETER TRACE FROM TEST 2453-4

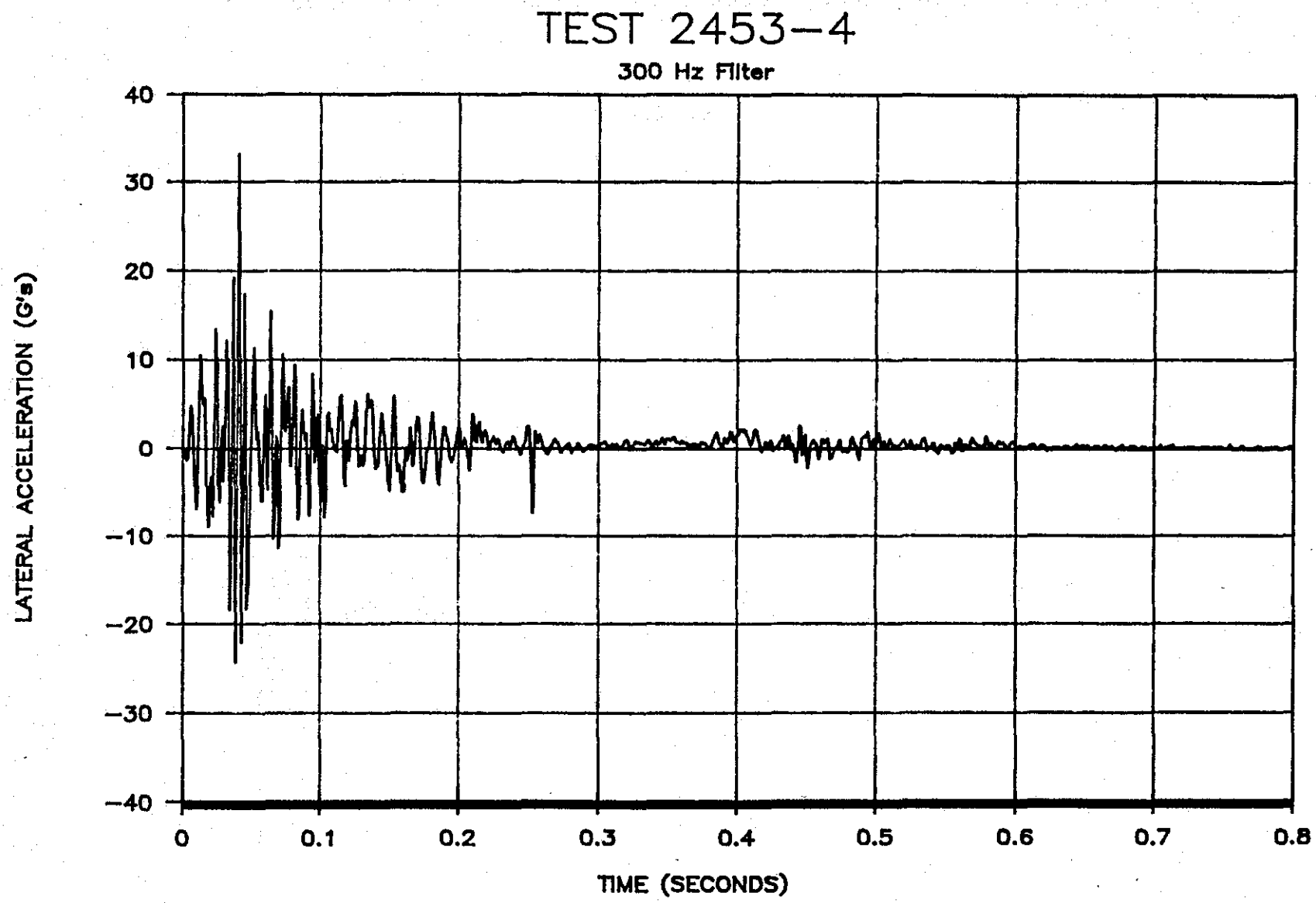

FIGURE B-11. LATERAL ACCELEROMETER TRACE FROM TEST 2453-4

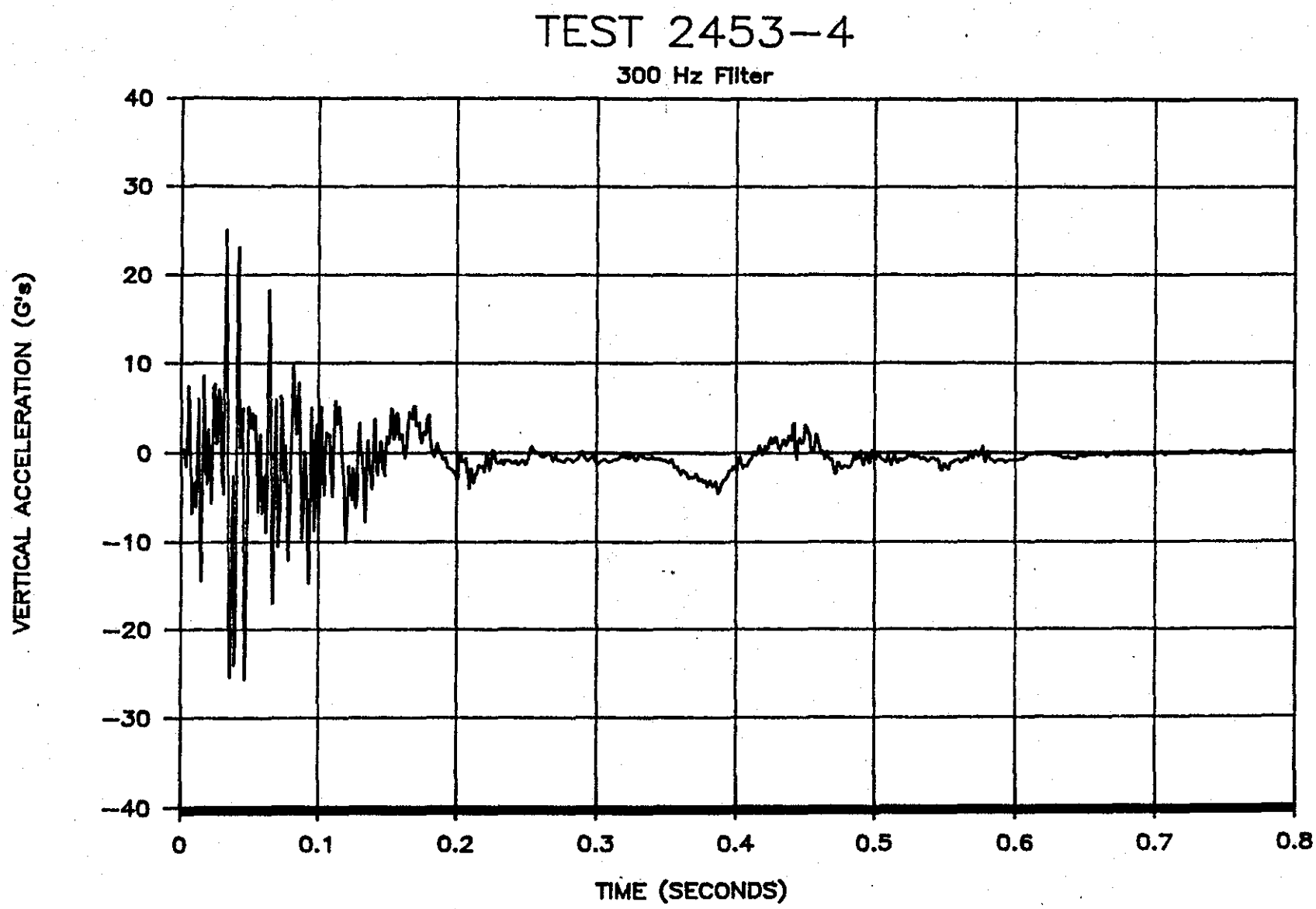

FIGURE B-12. VERTICAL ACCELEROMETER TRACE FROM TEST 2453-4

APPENDIX C

RATE GYRO PLOTS

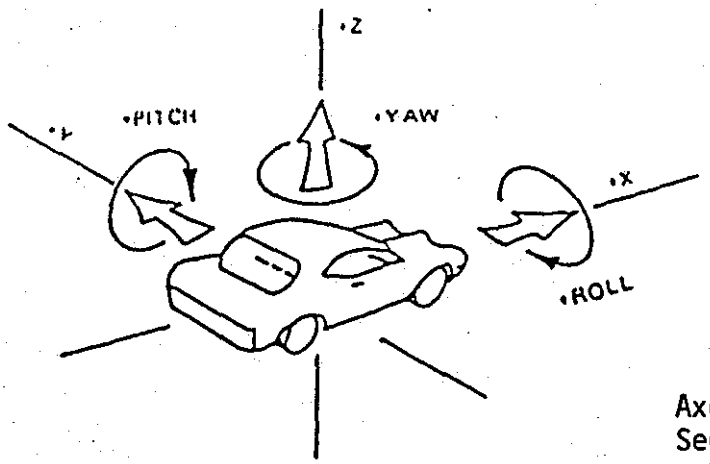

Axes are vehicle fixed.
Sequence for determining orientation is:

1. Yaw
2. Pitch
3. Roll

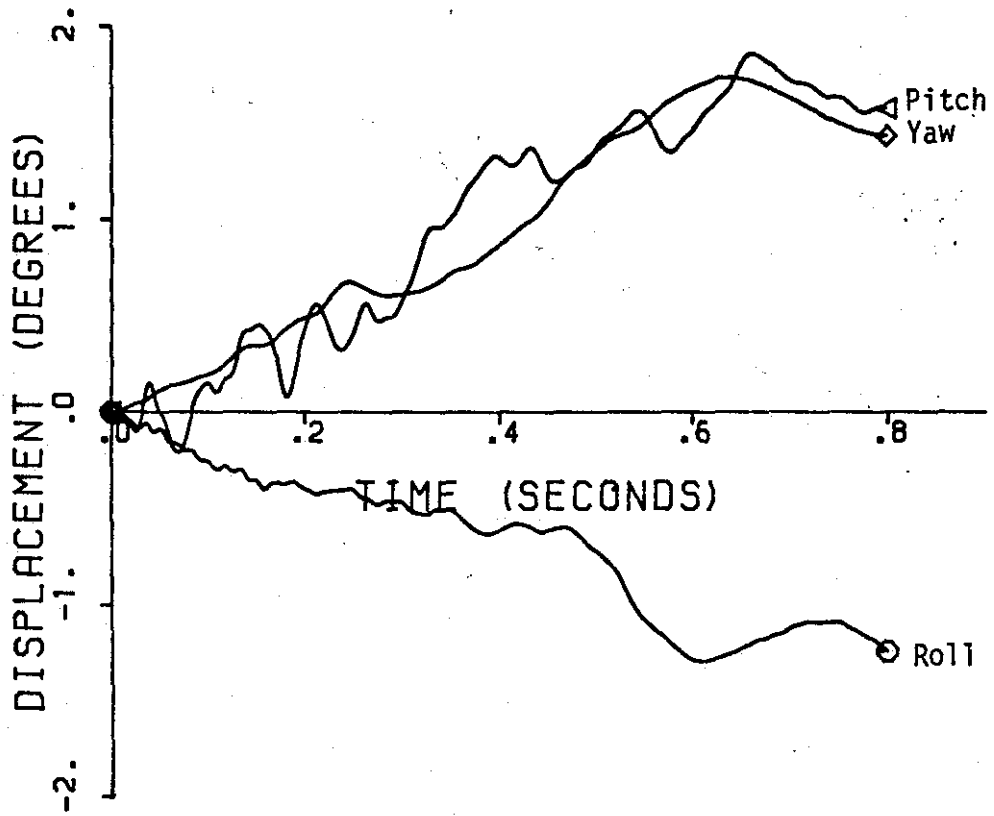

FIGURE C-1. VEHICLE ANGULAR DISPLACEMENTS FOR TEST 2453-1

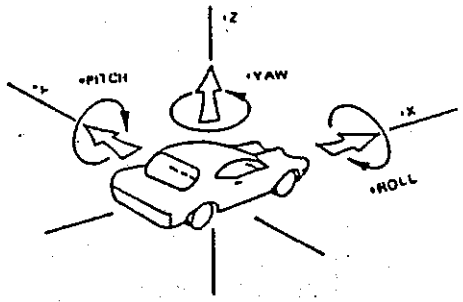

Axes are vehicle fixed.
Sequence for determining orientation is:

1. Yaw
2. Pitch
3. Roll

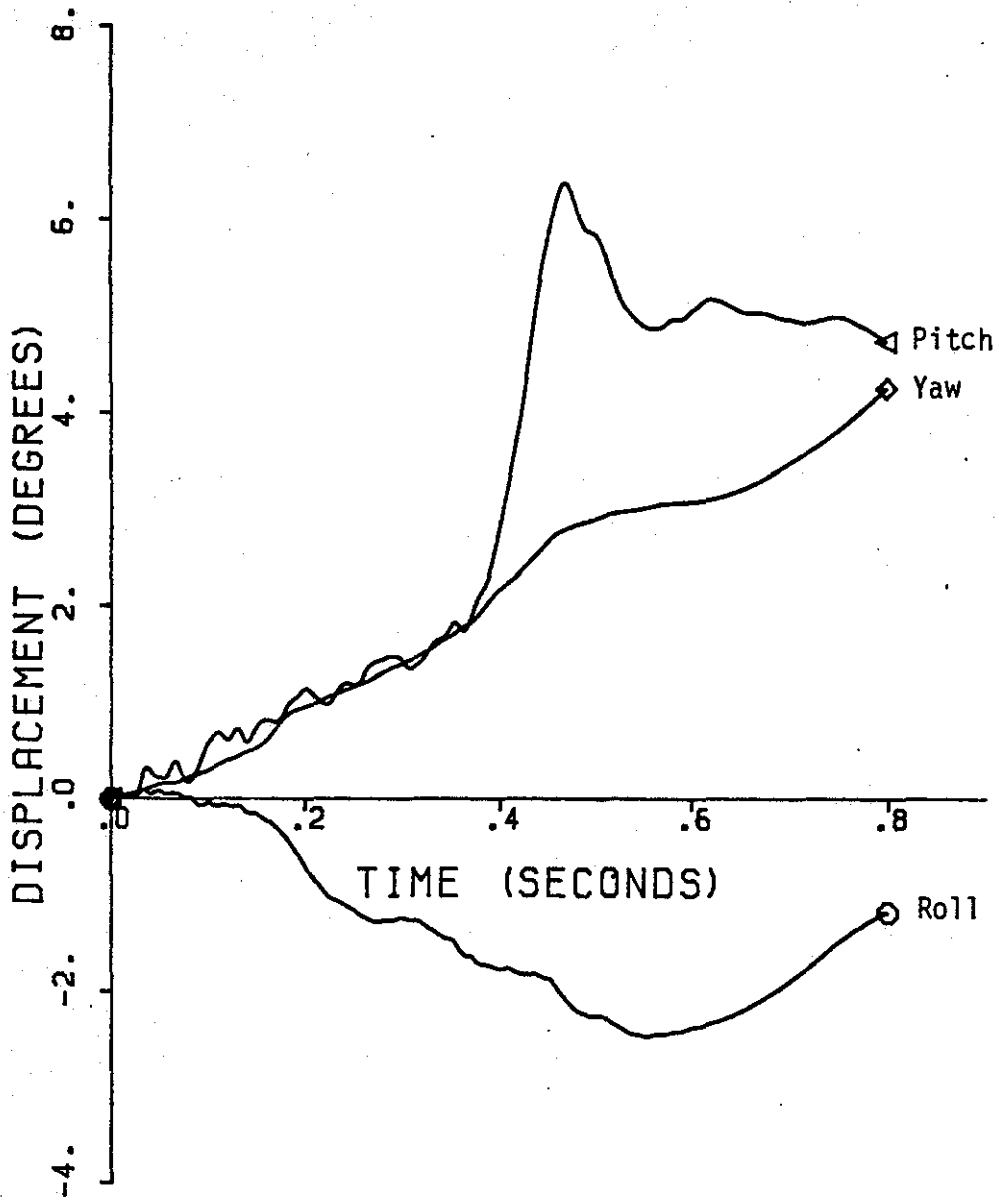

FIGURE C-2. VEHICLE ANGULAR DISPLACEMENTS FOR TEST 2453-2

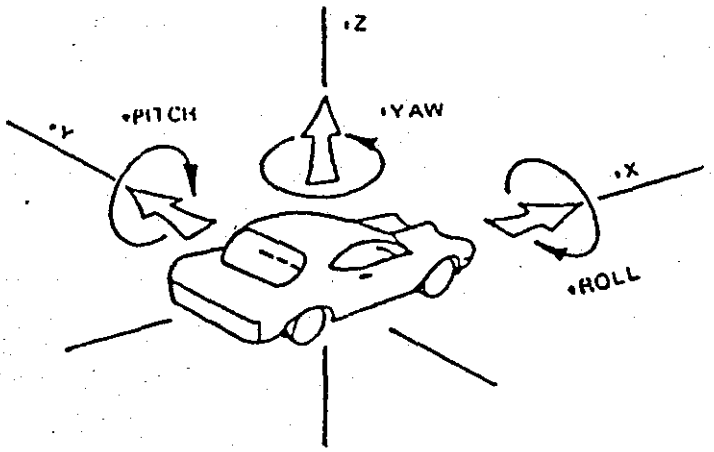

Axes are vehicle fixed. Sequence for determining orientation is:

1. Yaw
2. Pitch
3. Roll

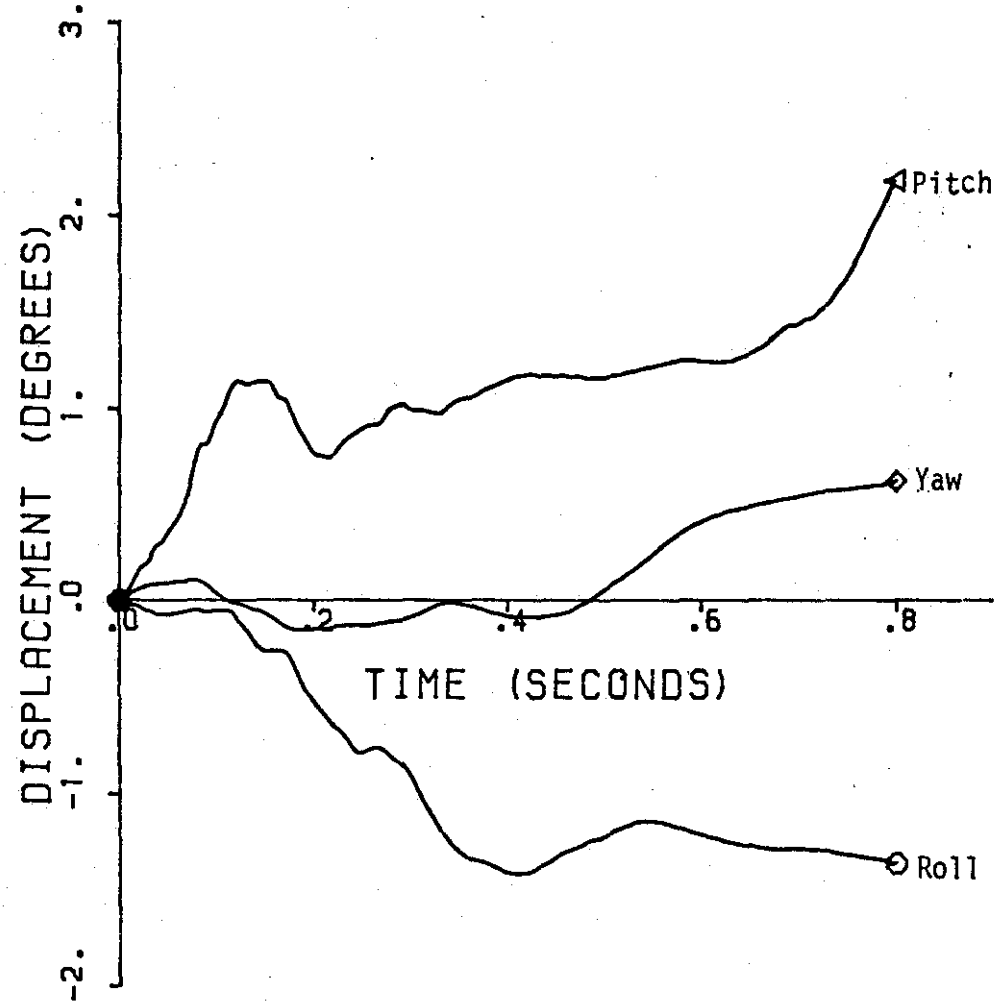

FIGURE C-3. VEHICLE ANGULAR DISPLACEMENTS FOR TEST 2453-3

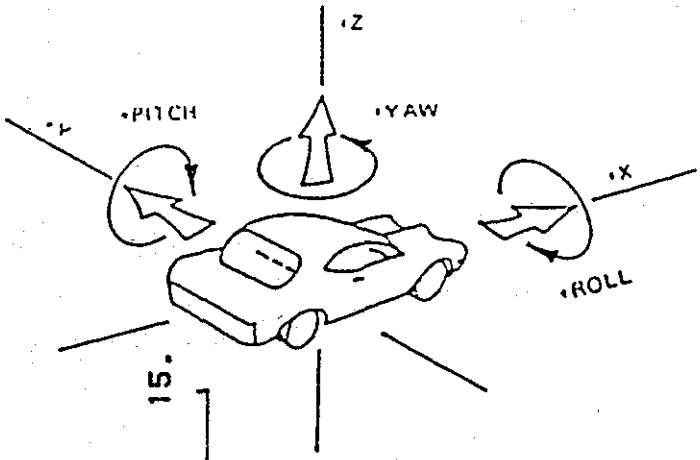

Axes are vehicle fixed.
Sequence for determining orientation is:

1. Yaw
2. Pitch
3. Roll

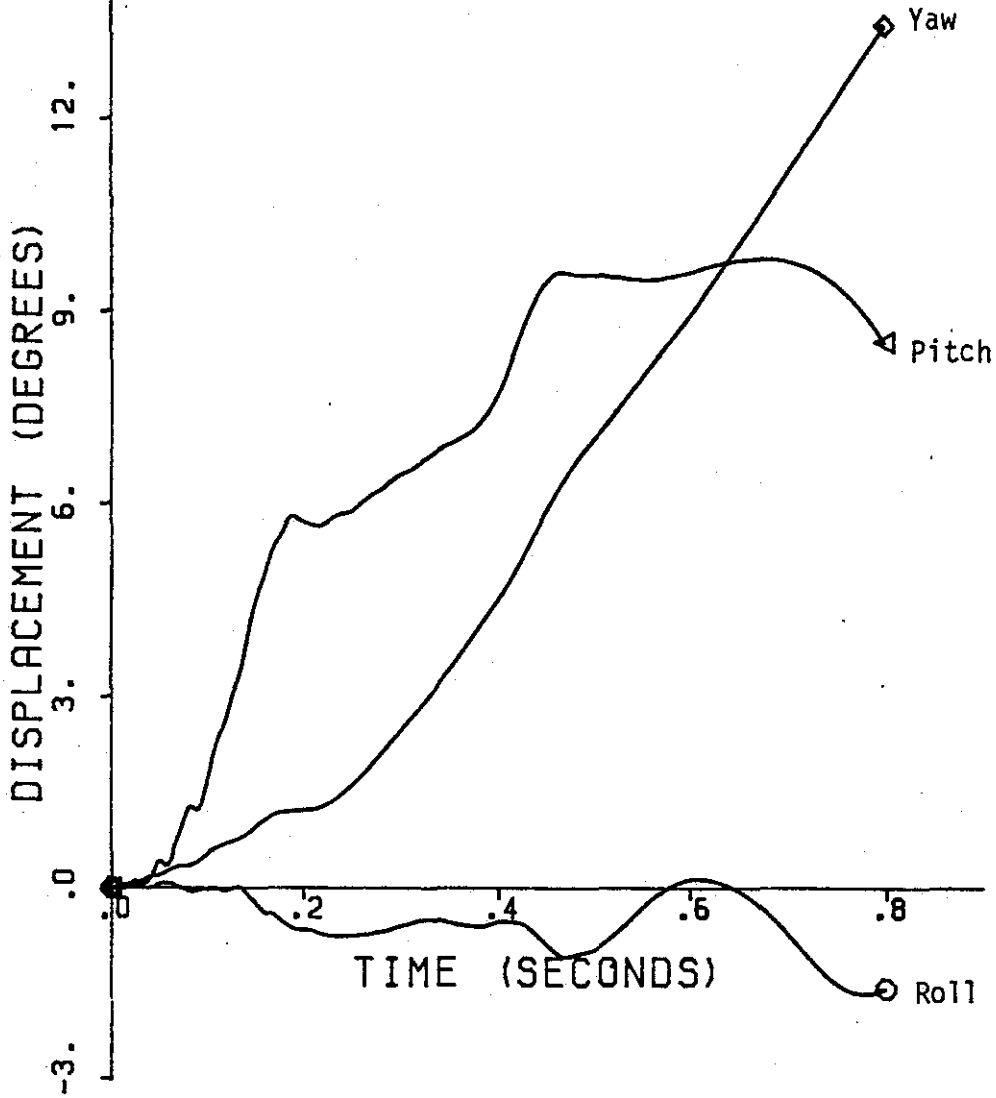

FIGURE C-4. VEHICLE ANGULAR DISPLACEMENTS FOR TEST 2453-4